Transverse energy analysis of relativistic heavy ion collisions through the use of identified particles spectra

A Thesis Presented for the

Master of Science

Degree

The University of Tennessee, Knoxville

Biswas Sharma

May 2018

Table of Contents

List of Tables

List of Figures

Chapter 1

Introduction

The Big Bang model is based on observational evidence, such as the cosmic microwave background radiation and the cosmological expansion, and suggests that at the beginning the universe must have been at a state of really high density and temperature. As the universe expanded, it went through several stages of cooling characterized by the formation of matters, with different compositions. The matter we mostly observe today exists at temperatures and densities much lower compared to those in the early universe.

The Large Hadron Collider (LHC) at CERN and the Relativistic Heavy Ion Collider (RHIC) at the Brookhaven National Laboratory have the ability to collide heavy nuclei, such as those of gold and uranium, at nearly the speed of light, reaching temperatures of trillions of degrees Celcius. These laboratories have provided evidence of the formation of an exotic state of matter, called the quark-gluon plasma (QGP). It only exists for a brief amount of time after such collisions and instantly freezes out into a plethora of new particles, which carry the signatures we can use to deduct QGP properties. Its properties suggest that it should be similar to the matter that existed within microseconds of the genesis of the universe[3].

One of the methods to probe the properties of this matter is by analyzing the conversion of the beam-direction energy at the time of collision into transverse energy after the collision. These measurements can be used to estimate the energy density of the QGP. This analysis is generally done by using data from the calorimeters (section 4.2.1) placed around the collision site. In this thesis, I use the data collected by tracking detectors (section 4.3.1), instead of the conventional calorimeters, to calculate the transverse energy.

This thesis is structured as follows. Chapter 2 touches on the theoretial background associated with the concept of the quark-gluon plasma. In chapter 3, I summarize the experimental concepts pertaining to relativistic heavy-ion collisions and the production and detection of QGP. Chapter 4 consists of the formalism of the measurement of transverse energy using calorimeters as well as tracking detectors. It also describes what has been done using calorimeters. Chapter 5 describes the data used to perform the analysis in this thesis and notes the relevant details of the analysis. In chapter 6, I present the results and compare them to the ones in literature obtained using a different method. Chapter 7 concludes the thesis and discusses its implications. Finally, in chapter 8, I present arguments on what can be done in the future using the results of and the software developed for this analysis.

Chapter 2

Theoretical Background

2.1 Quantum Chromodynamics

The strong force is one of the four fundamental interactions in physics. At large scales, it is also known as the residual strong force, and it is responsible for binding the nucleons together to give the nucleus its structure. At smaller scales, it is called the fundamental nuclear force, and it binds the fundamental units of subnuclear matter, the quarks, together to form the nucleons. The force carriers of the interaction are the mesons at the former scale and the gluons at the latter. The electrodynamic interaction between charged particles such as protons and electrons is described by quantum electrodynamics (QED) as mediated by photons; the strong interaction, albeit more complicated, is explained under the framework of quantum chromodynamics (QCD) [28, 40]. The quarks and gluons of QCD are collectively known as partons. Gluons are the gauge bosons of the Yang-Mills theory.

The Yang-Mills theory is a non-Abelian gauge theory. It has a Lagrangian with several degrees of freedom, some of which are redundant and need to be gauged. This is done by a mathematical treatment as prescribed under a gauge theory [8]. The gauge theory associated with the Yang-Mills theory is based on the SU(N) group. It is non-Abelian as represented by the non-commutative transformations. QCD is a gauge theory that describes the application of the SU(3) symmetry transformations on color charges, namely red, blue, and green. The electroweak theory, which describes the electromagnetic as well as nuclear weak interactions, can be formalized under the gauge group SU(2)×U(1). Together, they form the SU(3)×SU(2)×(U1) gauge theory called the standard model.

One of the ways QCD is different from QED is the confinement of partons. In QED, the fundamental particles are bound together by the Coulomb potential, which diminishes with distance between the charge-carrying particles, as demonstrated by the relation 2.1:

$$V_C \propto \frac{1}{r} \tag{2.1}$$

where V_C is the Coulomb potential, and r is the spatial separation between the particles. This means that bound QED particles can be isolated by increasing their spatial separation. The QCD potential, on the other hand, has an extra linear term in it, which means that the potential increases linearly with distance at large distances, and so an infinite amount of energy is required to separate quarks [11]. Hence, we never observe isolated quarks and they are said to be confined, not just bound, to form composite structures called hadrons [36]. A quark and an anti-quark forms a meson and three quarks forms a baryon. In addition to having a color charge, a quark also carries a flavor. There are six different quarks based on the flavors they carry: up, down, top, bottom, beauty, and strange.

2.2 Phase Transitions

In everyday life, we observe matter existing in four distinct phases: solid, liquid, gas, and plasma. Changes in physical conditions can lead to a transition from one of these phases to another, exemplified by the commonly observed conversion of ice to water. Distinctions among the various phases can be represented in a chart called the phase diagram.

The phase diagram consists of thermodynamic observables such as temperature and density on its axes. Curves in the phase diagram represent boundries of physical conditions separating one phase from another: crossing a boundary represents an abrupt transition from one phase to another. This abruptness is mathematically characterized by the discontinuity in the change of the derivative of the free energy – a thermodynamic variable – with respect to the physical quantities in the axes. Such an abrupt transition is called a first-order phase transition. Along the boundary represented by the curve, there can be a point beyond which the phase transition is continuous instead of being abrupt, and the distinction between two phases is not clear. This point is called a critical point, and the phase transition that takes place beyond this point is called a crossover.

One of the main focuses of current experimental and theoretical nuclear physics research is the study of the phase diagram of strongly interacting matter at a range of temperatures and baryon chemical potentials. In experiments involving the collisions of heavy ions at high and low energies, different regions of the phase diagram can be probed by varying the collision energy [4]. For instance, the high-baryon chemical potential regime corresponds to lower beam energies and higher temperatures correspond to higher beam energies. The results of these experiments and model calculations can be used to study the possibilities and signatures of transitions in the QCD phase diagram.

A schematic representing the QCD phase diagram as a function of the temperature (T) and quark chemical potential (μ) is shown in Figure 2.1 [10]. A crossover is predicted at low baryon chemical potentials (close to baryon-antibaryon symmetry) and high temperatures reminiscent of the early universe. Methods to study this region of the phase space will be explored in this thesis. At low temperatures and high net baryon densities, loose predictions have been made regarding the existence of exotic phases of high density matter, and programs, such as the Compressed Baryonic Matter experiment at the Facility for Antiproton and Ion Research in Germany, are being designed to study this region of the phase diagram [24].

2.3 Quark-Gluon Plasma

The confinement of quarks into the hadronic phase of QCD matter, as described in section 2.1, has its limitations. At very high densities, when the wave function of a single hadron overlaps with the spatial regions covered by multiple such hadrons, it is impossible to classify which pair or triplet of quarks belongs to which meson or baryon. As long as a particular quark is close enough to the other quarks in the volume, it is deconfined in such a way that it can freely move anywhere in the volume [36]. QCD predicts such phase transition, at

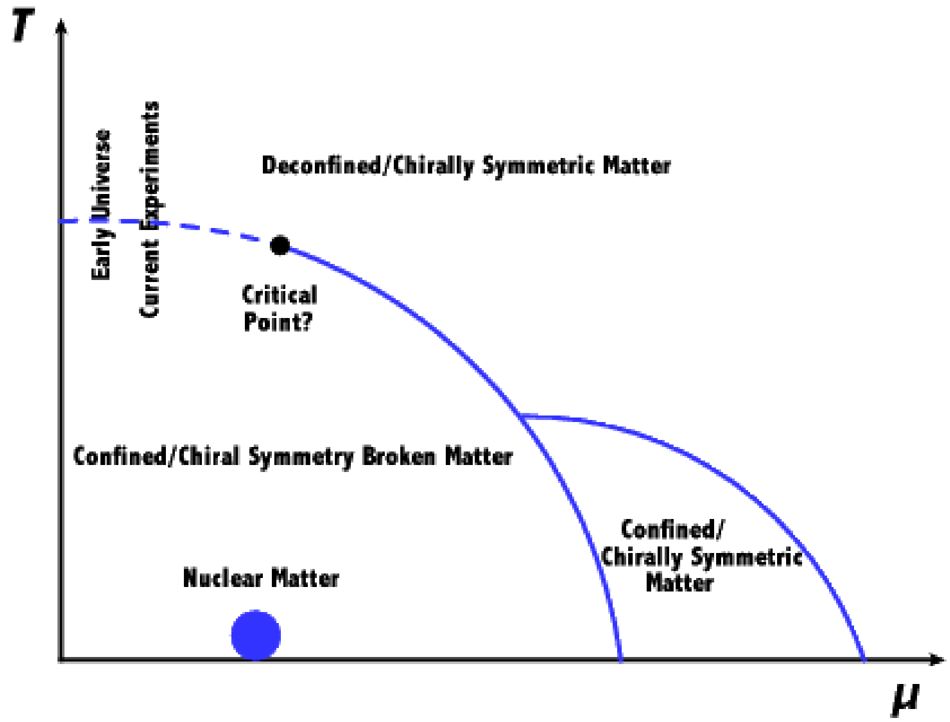

Figure 2.1: Schematic of the QCD phase diagram [10].

energy densities above 0.2-1 GeV/fm^3 [1] and around a critical temperature of about 160 MeV [21], of strongly interacting matter to a phase with quarks and gluons in thermal and chemical equilibrium representing the relevant degrees of freedom. This deconfined state of quarks and gluons is termed the quark-gluon plasma (QGP) in analogy to the quantum electrodynamical plasma phase of matter. The QGP has been found to behave like an almost perfect fluid [16]

Chapter 3

Relativistic Heavy Ion Collisions

The experimental evidence for the QGP comes from the collisions of heavy nuclei. Some of its signatures are described in section 3.5. Physicists proposed the existence of such matter since as far back as 1984, when nuclei were accelerated and collided with stationary targets [23]. They were able to agree on a conclusive discovery of this matter during the 2000s, after colliding accelerated nuclei with other such nuclei or smaller species (protons, deuterons) at unprecedented energies and with improved detection schemes [42]. With further increases in collision energies and enhancements in detector technology, modern accelerator facilities provided additional evidence and estimates of some of the properties as well as the dynamics of the evolution of the QGP. The following sections describe two such facilities, the physics of the collisions, and what happens after the collisions.

3.1 RHIC and LHC

The Relativistic Heavy Ion Collider (RHIC) is located in Upton, New York in the premises of the Brookhaven National Laboratory (BNL). Its construction started in 1991 and was completed in 1999. Figure 3.1 shows the layout, at the time of construction, of the collider along with the Alternating Gradient Synchrotron (AGS) complex and the locations of the original four detectors: Solenoidal Tracker At RHIC (STAR), Pioneering High Energy Nuclear Interaction eXperiment (PHENIX), Phobos, and BRAHMS (Broad RAnge Hadron Magnetic Spectrometers). Phobos, BRAHMS, and PHENIX were decommissioned after the completion of their science objectives, but STAR is still operational. The AGS was part of BNL before the construction of the RHIC, and its capabilities were augmented with the construction of the AGS Booster in 1991.

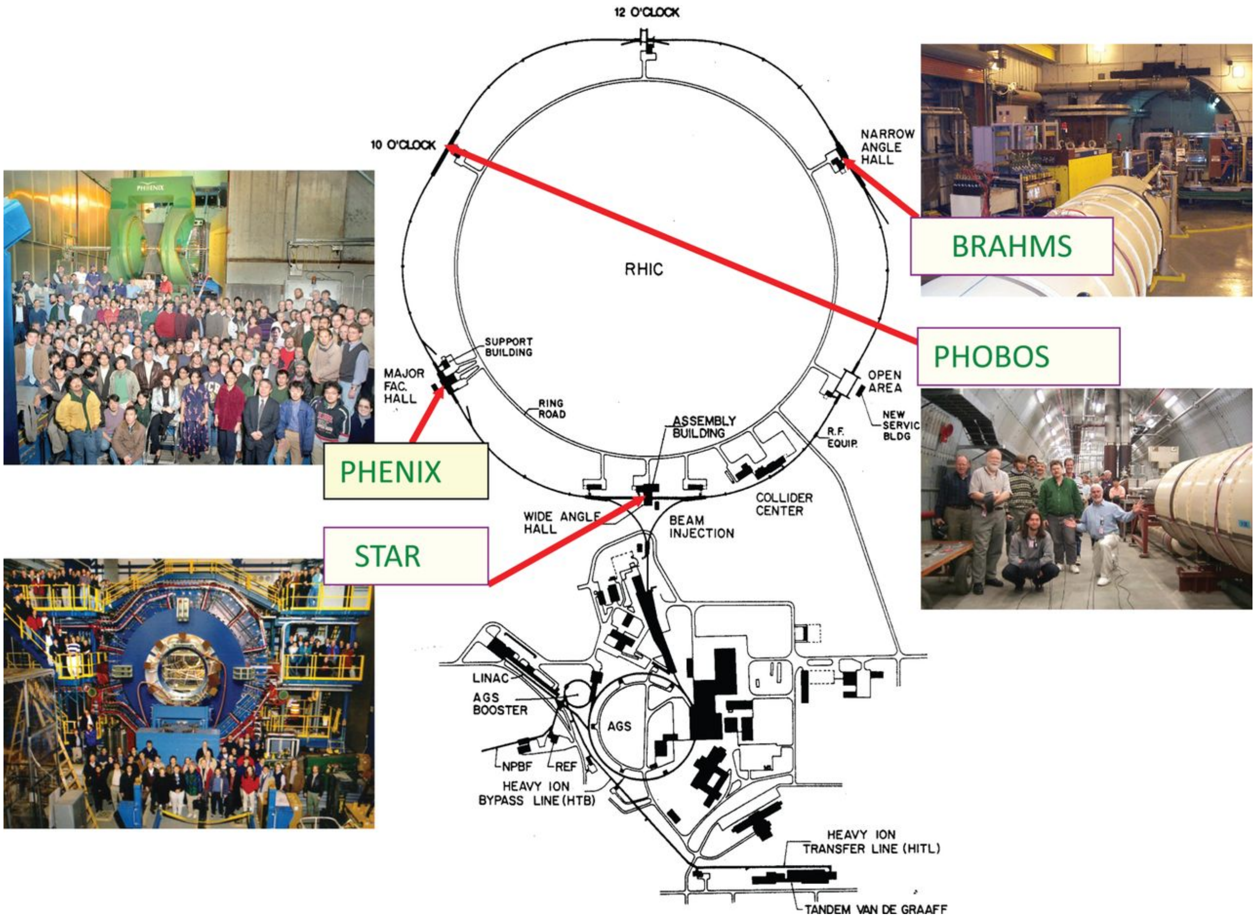

Figure 3.1: Initial layout of the RHIC [32].

Heavy ion beams in RHIC are created in a series of steps before collision. In case of gold ions, a pulsed sputter source produces negatively charged ions, which are stripped of some of their electrons with a foil on the positive end of the high-voltage Tandem Van de Graff. The ions are now positively charged and are accelerated to 1MeV/u toward the negative terminal of the Tandem. Upon exiting it, some more stripping takes place. The bending magnets then selectively deliver +32 charge states of the ions to the Booster Synchrotron, which accelerates them to 95MeV/u and strips them to a +77 charge state before injecting them to the AGS. The AGS accelerates them to 10.8 GeV/u and strips them of the remaining two electrons at the exit. The gold ions are then injected through the AGS-to-RHIC Beam Transfer Line to the two RHIC rings. These rings carry beams moving in opposite directions and intersect at six symmetric locations in the 3.8 km circumference. The original four detectors are located in four of these six locations where the beams undergo head-on collisions.

The Large Hadron Collider (LHC) is located underground (between 45m and 170m) beneath the France-Switzerland border near the city of Geneva. The two rings of the collider were constructed between 1998 and 2008 by the European Organization for Nuclear Research (CERN) in the 26.7 km circular tunnel originally housing CERN's Large Electron-Positron collider. Analogous to the RHIC, the LHC gets its beams prepared by a series of machines in the CERN accelerator complex. The collisions occur at the locations of the four big LHC experiments: Compact Muon Solenoid (CMS), A Toroidal LHC ApparatuS (ATLAS), Large Hadron Collider beauty (LHCb) experiment, and A Large Ion Collider Experiment (ALICE). ALICE is dedicated to the study of heavy-ion collisions [20].

3.2 Collision Energy and Geometry

What happens in the aftermath of a collision depends on how much energy is available at the time of the collision as well as the geometry of the collision. The collision energy is determined by the collider configuration. The geometry of the collision is deduced as the collision *centrality*, as described later in this section, through the estimation of the charged particle multiplicities (N_{ch}) resulting from the collisions.

In collision experiments, it is convenient to use a reference frame in which the net momentum of the pair of colliding species is zero. This frame is called the center-of-mass frame. In this frame, the total energy of the species in the two beams is a function of the number of nucleons and the center-of-mass energy per nucleon. The collision energy is reported as the center-of-mass energy per nucleon pair, $\sqrt{s_{NN}}$.

RHIC has the unique capability of colliding species at a range of energies spanning almost two orders of magnitude. Table 3.1 lists the collision energies produced so far at RHIC for various collision systems. The LHC boasts the highest amount of collision energy for any collider on earth. It collided species (p+p, p+A, Pb+Pb) at a center of mass energy up to

2.76 TeV per nucleon pair at the end of 2010. At the end of 2015, 5.02 TeV Pb+Pb and 13 TeV p+p collisions were successfully completed [22].

Collision system	$\sqrt{s_{NN}}(GeV)$
p+p	200, 500
d+Au	200
Cu+Cu	62, 200
Au+Au	9, 20, 62, 130, 200

Table 3.1: Colliding species and associated collision energies at RHIC [30].

In general, any collision between two nuclei is not perfectly head-on. Some collisions are close to being head-on and are called central collisions. Some are glancing and are called peripheral collisions. By convention, 0% is the centrality of a perfectly head-on collision and 100% is that of the least head-on, i.e., the most peripheral collision. More central collisions generally produce more particles [18].

The centrality is estimated through a model-based correlation between N_{ch} and the impact parameter, defined as the distance between the centers of the two nuclei at the time of their maximum overlap. The Monte Carlo based model, for instance, assumes that all nucleons travel in straight lines along the beam direction [**?**] and that they collide if they overlap [**?**]. N_{ch} is assumed to scale with the number of participants and the number of binary collisions. The distribution of this quantity is then fit to the data and the fraction of the overlap is estimated from the observed N_{ch} value. 5% of all collisions with the highest N_{ch} values, for example, are then referred to as being 0-5% central [18].

Figure 3.2 illustrates the aftermath of a mid-central collision, i.e, a collision in which about half of the volume of each of the nuclei intersects the other.

The collision of two nuclei can be modeled as collisions of the constituents that make up the nuclei. The nucleons that take part in the collisions and are called participants. The rest of the nucleons are known as spectators. Figure 3.3 illustrates the distribution of participants and spectators in two colliding nuclei.

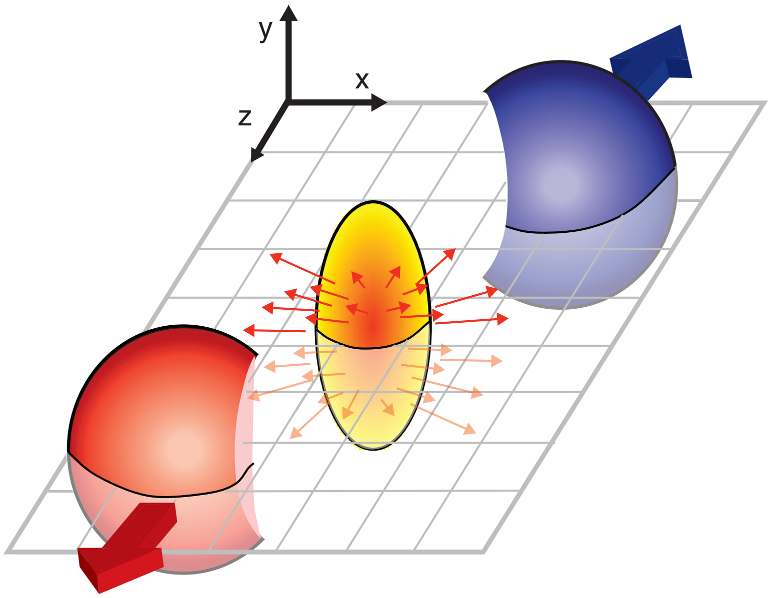

Figure 3.2: An illustration of a mid-central collision of two nuclei traveling in the z direction. The X-axis is parallel to the line joining the centers of the two nuclei at the time of collision [18].

3.3 QGP Evolution

The evolution of the QGP is shown in a lightcone diagram in figure 3.4 [18]. The initial state of the colliding nuclei is not precisely known and is the topic of research for upcoming experiments. During the collision, the participants scatter off of each other while the spectators keep traveling almost unperturbed in their original direction. The immediate aftermath of a central collision of heavy ions at RHIC and LHC energies is the formation of a hot fireball. This fireball evolves in time to form a liquid-like medium of quarks and gluons. This medium attains a local equilibrium and remains in such a state, depending on the collision energy, for about 1-10 fm/c. This equilibrium is broken as the liquid QGP evolves by expanding and cooling to attain a density and temperature at which the medium undergos hadronization followed by a chemical freeze-out to form a hadron gas. The particle ratios are fixed after the chemical freeze-out. Collisions between the constituents of this gas become scant as it evolves with further expansion and cooling, and the hadrons undergo a thermal freeze-out to attain their final energies and momenta [18].

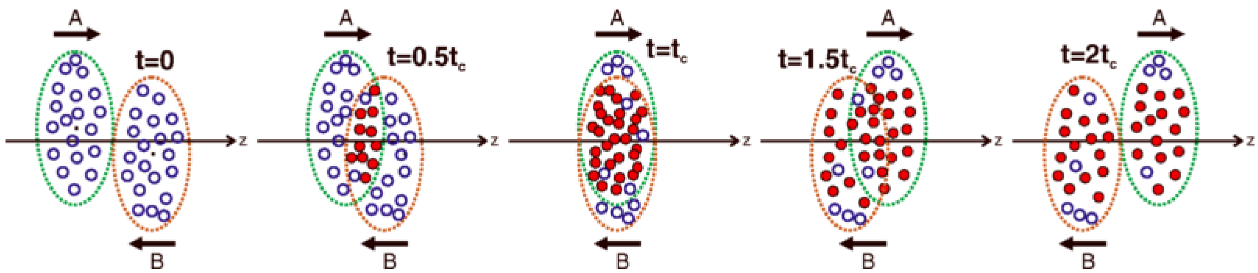

Figure 3.3: An illustration of a collision consisting of participants (solid red) and spectators (open blue) within the colliding nuclei labeled A and B. t_c denotes the time of maximum overlap of the two nuclei. The apparent narrowing of the volumes of the nuclei in the z-direction is due to Lorentz contraction [47].

3.4 Detection of Collision Products

Detectors are placed around the collision site to perform measurements on the final state particles emitting from the thermal freeze-out of the medium. These measurements typically include the reconstruction of the particle tracks, estimation of the the types of particles, and the momenta and energies they carry.

Generally, a tracking detector surrounds the collision site, and there are particle identifiers followed by calorimeters around it. A magnetic field is applied parallel to the beam direction around the collision site. Due to this orientation of the magnetic field, the spectators traveling parallel to it move roughly undeflected and the final state charged particles with components of velocity transverse to the beam axis get deflected around the beam axis with radius given by

$$r = \frac{p_T}{qB}, \tag{3.1}$$

where p_T is the transverse momentum of the particle, q is its electric charge, and B is the applied magnetic field. Two kinds of detectors most relevant to this thesis, tracking detectors and calorimeters, are described in chapter 4.

3.5 Detection of QGP Signatures

The existence and properties of the QGP in the aftermath of high-energy heavy-ion collisions can be probed using different techniques relevant to several theoretical characteristics of the

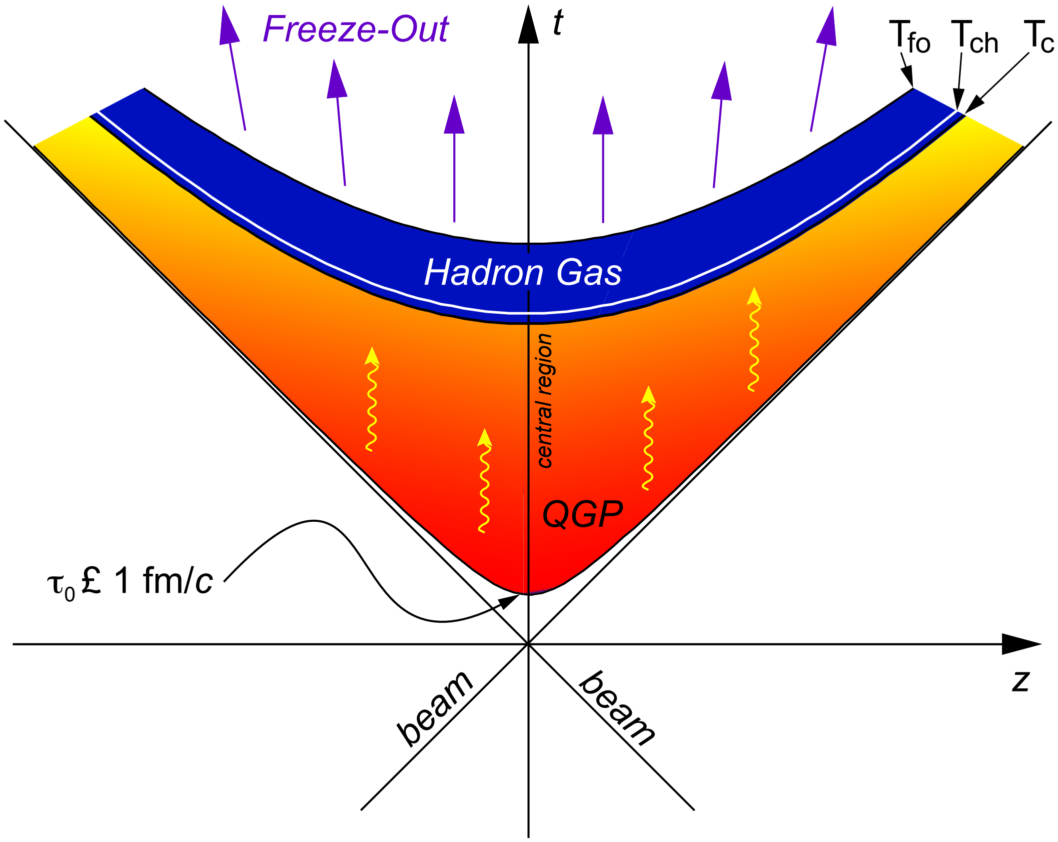

Figure 3.4: Evolution of the QGP represented in a lightcone diagram. τ_0 denotes the formation time of the QGP. T_c is the critical temperature of the transition from the QGP to the hadron gas phase. T_{ch} and T_{fo} stand for the temperatures at, respectively, chemical freeze-out and thermal freeze-out [18].

medium. No signature can alone be used to claim the production of the QGP, and some of the probes, which should be interpreted together, are described below.

3.5.1 Bjorken Energy Density

In 1983, J.D. Bjorken[14] prescribed a formula to use the final state particles to estimate the initial energy density, ϵ_0, in a nucleus-nucleus collision. With slight changes in the original formula, the energy density is estimated by:

$$\epsilon_0 = \frac{1}{\tau_0 A_T} \langle \frac{dE_T}{dy} \rangle, \tag{3.2}$$

where τ_0 is the formation time of the QGP, A_T is the transverse area of the intersection of the two nuclei, and $\langle\frac{dE_T}{dy}\rangle$ is the mean transverse energy per unit rapidity. τ_0 is model-dependent and is normally estimated to be $1fm/c$. A_T depends on the centrality of the collision and can be estimated using the Glauber model discussed earlier. $\langle\frac{dE_T}{dy}\rangle$ is found from the measurement of the transverse energy carried by the final state particles from the collision and is the central theme of this thesis. Details about it are in the following chapters. The estimate of the initial energy density from the Bjorken formula is an underestimate of the maximum energy density because the measured dE_T/dy is an average over the system as it undergoes expansion and cooling. It can be compared with the QCD prediction of the critical energy density [1] to check if the results from a collision imply the achievement of the critical physical condition required for the phase transition [27].

3.5.2 Elliptic Flow

The evolution of the medium produced in relativistic heavy ion collisions can be well described under the framework of relativistic hydrodynamics [38, 43]. This description indicates the presence of a collective flow of a locally thermalized liquid. The angular distribution of the momenta of the final state particles emitted out of the collectively flowing system can be decomposed into a Fourier expansion in its azimuthal components. The second harmonic coefficient, $\nu_2(y, p_T)$, of this decomposition characterizes what is known as the elliptic flow [26]. The magnitude of the elliptic flow from a non-central collision represents the anisotropy in azimuthal momentum space of the thermalized post-collision system [41]. The elliptic flow of the medium, as a function of the momentum or the kinetic energy in the transverse direction, points towards quarks, rather than hadrons, being the relevant degrees of freedom in the QGP. Figure 3.5 shows v_2 as a function of the transverse momentum and the transverse kinetic energy for identified particles. The spectra scale consistently at lower values of both p_T and KE_T. However, they branch out as mesons and baryons at higher values: $p_T \gtrsim 2GeV/candKE_T \gtrsim 1GeV$. Figure 3.6, on the other hand, is similar to figure 3.5, with the exception that both the axes have quantities that are normalized by the number of quarks, n_q. In this case, the KE_T spectra strongly exhibits a scaling which is more comprehensively consistent with the number of quarks than in case of figure 3.5. This universal quark-number scaling can be interpreted as the degrees of freedom of the system being quark-like [5].

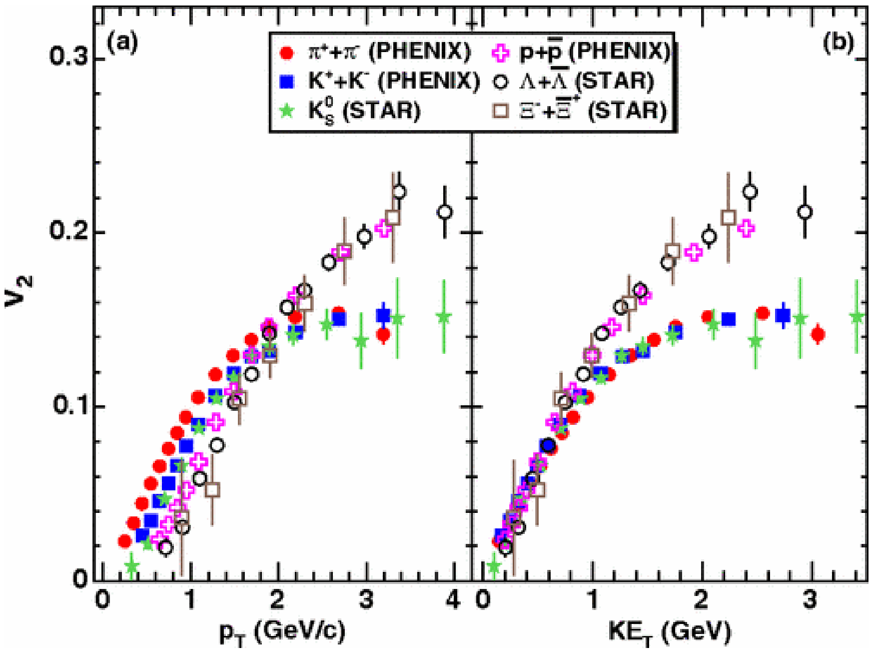

Figure 3.5: Minimum-bias Au+Au ($\sqrt{s_{NN}} = 200GeV$) elliptic flow spectra for identified particles: (a) v_2 vs p_T and (b) v_2 vs KE_T [5].

3.5.3 Prompt and Thermal Photons

Most of the photons observed after relativistic heavy ion collisions are the results of the decay of the neutral pion into two gammas. When these photons are subtracted from the observations, the remaining photons are called direct photons [33]. These direct photons are produced within the fireball via different mechanisms as discussed below.

In the QGP, a quark and an antiquark can annihilate to produce a photon and a gluon. It is also possible for the pair to annihilate and produce two photons, but the probability of this process is smaller than the former by about two orders of magnitude. Furthermore, a quark (or an antiquark) can interact with a gluon to produce an antiquark (or a quark) and a photon, a process analogous to Compton scattering in QED. The photons produced from the hard scattering processes between the partons are called prompt photons, and their multiplicity scales with the number of binary collisions. Photons can also be produced due to scatterings of partons within the thermalized medium, and these photons are called

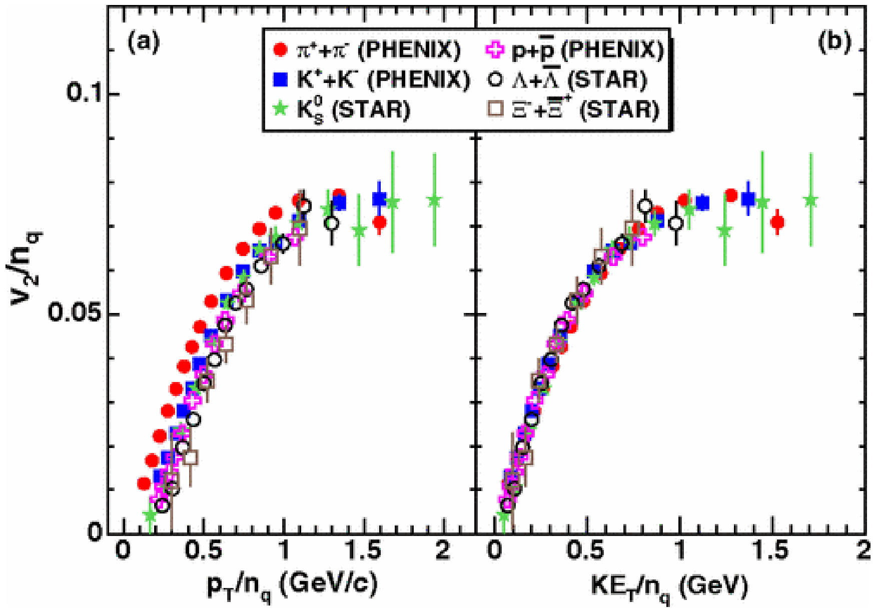

Figure 3.6: Minimum-bias Au+Au ($\sqrt{s_{NN}} = 200GeV$) elliptic flow spectra for identified particles: (a) $\frac{v_2}{n_q}$ vs $\frac{p_T}{n_q}$ and (b) $\frac{v_2}{n_q}$ vs $\frac{KE_T}{n_q}$ [5].

thermal photons. The nature of the p_T distribution is different in this case as the emission process mimics blackbody radiation. This difference helps distinguish these photons from the direct photons produced by partonic interactions. Just like the leptons described in the previous section, the photons produced in the QGP can only interact with the medium electromagnetically. Therefore, they undergo minimal scattering before being detected, and hence can be used to probe the thermodynamical state of the medium at the time of their creation [49, 33, 48].

3.5.4 Strangeness Enhancement

The interacting nuclei carry no net strangeness before colliding, and so an observation of strange and multi-strange particles after the collision can be used to probe the properties of the post-collision medium [19]. Strangeness can also be produced in hadron-hadron collisions. However, it is enhanced in nucleus-nucleus collisions [12]. This is interesting because it possibly indicates a restoration of chiral symmetry, which is a topic of ongoing research: in the zero baryon chemical potential limit, lattice QCD calculations reveal a transition of QCD matter between a phase with broken and one with restored chiral symmetry [15].

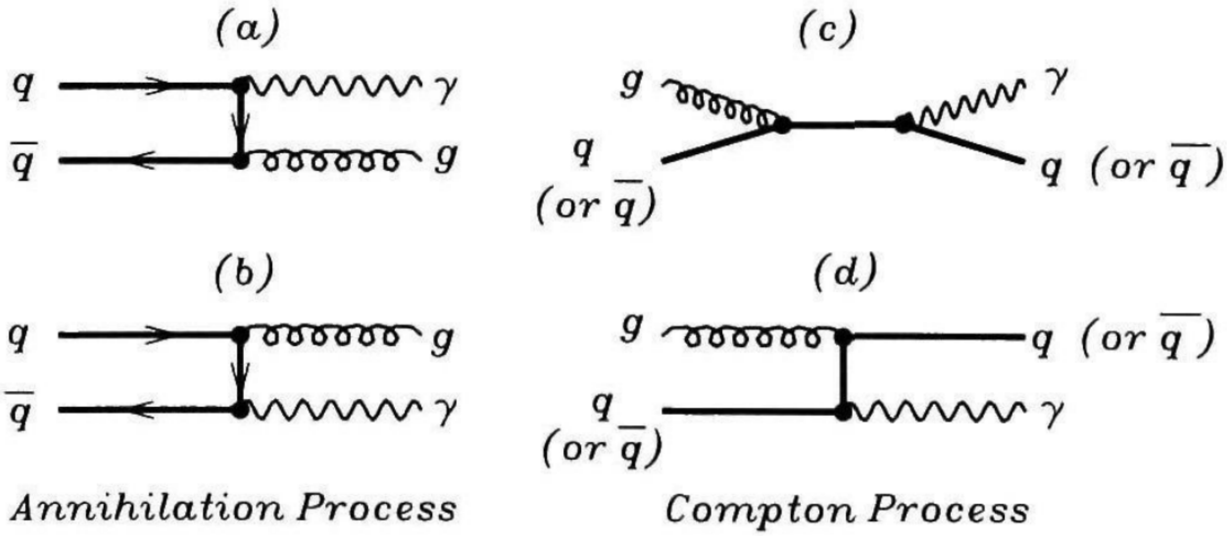

Figure 3.7: Feynman diagram representing the production of photons from quarks and gluons. (a) and (b) represent annihilation processes, whereas (c) and (d) represent Compton processes [49].

Chiral symmetry restoration has the implication of all the flavors of quarks losing their masses [37]. Hence, when chiral symmetry is restored, it is more feasible to produce strange quarks, for instance, which have higher masses than the light quarks, up and down, in a state of broken chiral symmetry. Chiral symmetry restoration is not the only possible reason for the production of many strange quarks. It is also feasible to produce strange quarks as long as the temperature of the system is above the strange flavor mass scale, and so it carries effects of the system temperature. This is exemplified by the ratio of the production of the strange kaons to that of the non-strange pions, which are the most abundant hadrons produced from nucleus-nucleus collisions: kaon yield increases more rapidly than pion yield does as the temperature increases[49].

3.5.5 Jet Quenching

A scattering event in which the participants transfer a large amount of their original momenta is called hard scattering. The products of the scatterings are called jets. In heavy-ion collisions, most hard scatterings are the results of two partons from the opposite nuclei scattering off each other. These partons can lose their momenta by strongly interacting with a medium made of deconfined quarks and gluons. Therefore, the properties of the jets, as carried by the final state hadrons, should be different for collisions that produce the QGP as compared to those that do not, and hence they can be used as signatures and probes of QGP. Figure 3.8 illustrates the quenching of jets that have to travel long distances in the medium.

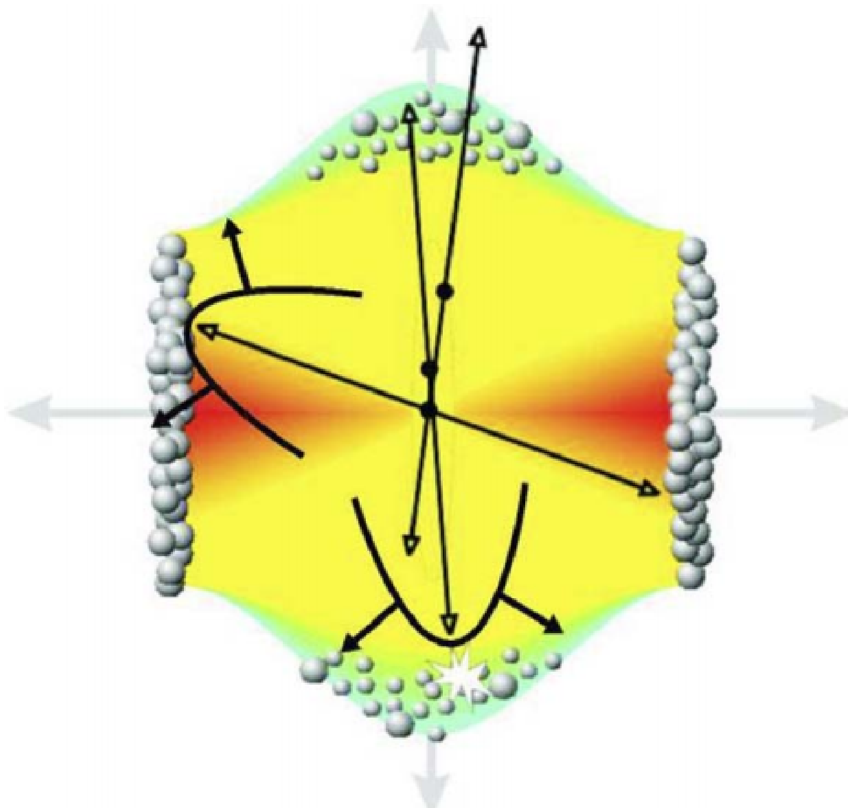

Figure 3.8: Illustration of jet quenching. Two jets are produced from each of the hard scatterings occuring at the locations of the solid dots. Jets originating closer to the initial surface are more probable to propagate outside the medium, as shown. Jets opposite to them interact with the medium, losing their energy and resulting in bow front shock waves [44].

3.6 The Beam Energy Scan Program

The RHIC, in 2010, started a multi-phase Beam Energy Scan (BES) program to study the QCD phase diagram. Between 2010 and 2011, during the exploratory phase I of the BES program, the collider provided Au+Au collisions at 7.7, 11.5 (not completed in PHENIX), 19.6, 27, and 39 GeV. Together with the data formerly collected by the RHIC at higher collision energies, BES phase I data can scan the interval from 450 MeV to 20 MeV in μ_B space [31, 29]. One of the things that can be studied with the data associated with this region of the phase space is the possibility of a "turn-off of new phenomena already established at higher RHIC energies"[31]. Results corresponding to the high-μ_B region might provide evidence of a first order phase transition, and possibly the critical point [29].

The manifestation of such phenomena might be in terms of the fluctuations or other properties of the post-collision system. One can, for instance, study the scaling of the energy density after the collision with the longidutional energy at the time of the collision, $\sqrt{s_{NN}}$, for which one needs to measure the transverse energy. This can be done in multiple ways using a detector like STAR or PHENIX that is made up of sub-systems such as the Time Of Flight (TOF) detectors, Time Projection Chambers (TPCs)/Time Expansion Chambers, and calorimeters. The next chapter describes the measurement of transverse energy using BES data from PHENIX calorimeters. Also, the next chapter and the ones after it contain the procedures and the results of the analysis of the BES data from STAR using the identified particle spectra.

Chapter 4

Measurement of Transverse Energy

This chapter indroduces the definitions of transverse energy, ways to measure it using different detectors, and particular examples for the detectors at the RHIC.

4.1 Definition of Transverse Energy

The transverse energy, E_T, from a collision can be defined as the sum of the transverse masses, m_T, of all the particles produced in the collision, i.e.,

$$E_T \equiv \sum_i m_{T,i} \tag{4.1}$$

with

$$m_T \equiv \sqrt{p_T^2 + m^2} \tag{4.2}$$

where m is the rest mass of the particle and p_T is its transverse momentum. Using this definition to calculate the E_T requires perfect identification of all the particles. It has not been possible to do so in experiments, and so a more feasible, operational definition of E_T is used. A commonly accepted definition in the case of calorimetric measurements is [6, 16]:

$$E_T = \sum_i E_i \sin\theta_i, \tag{4.3}$$

$$\frac{dE_T}{d\eta} = \sin\theta \frac{dE}{d\eta}, \tag{4.4}$$

where the index i runs over all the particles going into a fixed solid angle for each event, θ is the polar angle, i.e, the angle with respect to the beam axis, η is the pseudorapidity defined as

$$\eta \equiv -\ln\tan\frac{\theta}{2}, \tag{4.5}$$

and E_i is the energy deposited in the calorimeter by the i^{th} particle. E_i is considered to be, by convention [7], the following

$$E_i = \begin{cases} E_i^{tot} - m_0 & \text{for baryons} \\ E_i^{tot} + m_0 & \text{for anti-baryons} \\ E_i^{tot} & \text{otherwise} \end{cases} \tag{4.6}$$

where E_i^{tot} is the total energy of the i^{th} particle defined canonically as

$$E^{tot} \equiv \sqrt{p^2 + m_0^2} \tag{4.7}$$

and m_0 is the particle's rest mass.

E_i given by equation 4.6 is what would be observed by a calorimeter. In order to account for the portion of the emitted transverse energy not detected or overestimated by the calorimeters, corrections are made based on simulations.

4.2 E_T Measurement with Calorimeters

4.2.1 Calorimeter

A calorimeter in a particle or nuclear physics experiment is a device used to measure the energy carried by a particle by analyzing the signal generated by the shower of particles produced by the interaction of the incoming particle with the material of the device [34]. In theory, a single calorimeter can be made to measure the energy deposited by different kinds of particles. However, it makes more sense to have two different kinds of calorimeters: one optimized to measure the energy deposited by particles like electrons (or positrons) and photons, called an electromagnetic calorimeter (EMCal), and the other optimized to measure the energy deposited by hadronic particles, called a hadronic calorimeter (HCal). This is because of the difference in the particle showers that these two categories of particles generate. Electrons and photons mostly lose their energies in the calorimeter material via bremsstrahlung, Compton scattering and pair production. They generate particle showers made of electrons and photons which cannot travel much farther into the medium before losing all their energies in a series of interactions producing an avalanche of sequential showers. However, hadrons can interact inelastically with the nucleus generating a shower of hadrons. These secondary hadrons have much larger masses than the secondary electrons in the shower generated by the electrons and photons. This means they are not deflected nearly as much by the electric forces in the material and travel much farther into the calorimeter. For this reason, EMCals are comparably smaller in depth and are placed before the HCals in a detector assembly.

4.2.2 E_T from PHENIX Calorimetry

Adare et al. [4] uses electromagnetic calorimetry in PHENIX to analyze the transverse energy corresponding to several different pairs of species colliding at a range of energies. It uses the raw transverse energy measured by the EMCal, E_{TEMC}, to obtain the total E_T by making corrections in three different steps.

They first scale the data by a constant factor, 4.188, calculated to account for the fiducial acceptance in azimuth and pseudorapidity. The second factor is calculated to adjust for the effects of the calorimeter towers that are disabled. The third factor, k, is the ratio of E_T and E_{TEMC} and is computed as follows:

$$k = k_{response} \times k_{inflow} \times k_{losses} \tag{4.8}$$

where $k_{response}$ corresponds to hadronic particles only depositing a fraction of their total energy while passing through the EMCal, k_{inflow} is attributable to the energy deposited by particles coming from outside the EMCal's fiducial aperture, and k_{losses} accounts for the energy not registered in the EMCal due to energy thresholds, edge effects, and more importantly due to the particles that make it into the fiducial aperture but decay into products outside the aperture.

$k_{response}$ is estimated using simulations of event generation and particle detection. With 3/4 of the incident energy measured by the EMCal in the simulation, $k_{response} = 1/(3/4) =$ 1.33. 24% of the energy measured by the EMCal is found to be associated with the 'inflow' particles, and so k_{inflow} = 1-0.24 = 0.76. 22% of the energy is lost due to aforementioned reasons (10% + 6% + 6%), and so k_{losses} = 1/(1-0.22) = 1.282. From equation 4.8, then, k = 1.30, and this factor was found to vary for all the data sets by less than 1%.

The systematic uncertainties due to several contributions (listed in Table II in [4]) are added in quadrature to obtain the total systematic uncertainties in $dE_T/d\eta$. The uncertainty is low for the correction related to the acceptance (2%) as compared to that for the k factor: 3% for losses and inflow and 4.5%-4.7% for the energy response.

4.3 E_T Measurement with Tracking Detectors

Transverse energy analysis can be done using tracking detectors as well if they are able to produce measurements of other physical quantities that implicitly contain information about the transverse energy. Specifically, the charged particle multiplicity distributions with respect to the transverse momenta can be used, with assumptions involving particle ratios (section 5.2.2) and mean p_T, to calculate the particle's transverse energy. Since the corrections related to the tracking detectors are very different from those related to the calorimeters, results from the two different methods can be used to test the assumptions involved in each.

4.3.1 Tracking and Particle Identification

The tracking detectors in experiments such as the STAR (Solenoidal Tracker At RHIC) experiment and ALICE (A Large Ion Collider Experiment) at CERN include Time Projection Chambers (TPCs) and Time-of-Flight (TOF) detectors that can be used to measure the p_T spectra, yields, and particle ratios of the identified charged hadrons [35, 2]. The TPCs provide measurements of particle trajectories that can be used to determine the momenta for low-momentum particles. They also provice measurements of their specific energy loss, $\frac{dE}{dx}$, which can be used in combination with the momenta to identify particles using the Bethe-Bloch formula [13]. The particle identification (PID) capabilities of STAR are discussed in section 4.3.3. TOF detectors cover the high-momentum part of the measurements. In ALICE, the combination of the measurements of the TPC with those of the Inner Tracking System (ITS) effectively adds the tracking length, thereby improving the resolution of the measured p_T spectrum. Details about the PID and momentum determination capabilities of the detectors in ALICE can be found in [17].

The p_T spectra, reported as $\frac{d^2N}{dydp_T}$ as a function of p_T, can be used to calculate $\frac{dE_T}{d\eta}$ as formulated in the following section.

4.3.2 Calculation of $\frac{dE_T}{d\eta}$ from p_T spectra

In relativistic heavy ion collisions, rapidity (y) is defined as follows:

$$y \equiv \frac{1}{2} \ln \frac{E + p_z}{E - p_z}, \tag{4.9}$$

where E is given by equation 4.7 and p_z is the component of the momentum parallel to the beam axis. Pseudorapidity, η, is just y with $m_0 = 0$, which leads to equation 4.5. Taking the exponential of both sides of the equation 4.5 and using Euler's formula, we get:

$$\sin\theta = \frac{1}{\cosh\eta}. \tag{4.10}$$

Hence,

$$\begin{aligned} p &= \frac{p_T}{\sin\theta} \\ &= p_T \cosh\eta, \end{aligned}$$

and so we have

$$E_T = E \sin\theta = \frac{\sqrt{p_T^2 \cosh^2\eta + m_0^2}}{\cosh\eta} \tag{4.11}$$

The Jacobian for the transformation from y-space to η-space is derived to be:

$$\frac{\partial y}{\partial \eta} = \frac{p_T \cosh \eta}{\sqrt{m_0^2 + p_T^2 \cosh^2 \eta}} \tag{4.12}$$

From equations 4.11 and 4.12, we can see that the product of E_T with the Jacobian is equal to p_T. That leads to a formulation of $\frac{dE_T}{d\eta}$ as a function of only η and p_T:

$$\frac{dE_T}{d\eta} = \frac{1}{2a} \int_0^{10GeV/c} \int_{-a}^{a} p_T \frac{d^2 N}{dy dp_T} \, d\eta \, dp_T \tag{4.13}$$

where a and $-a$ are the bounds for η. The estimate for the upper limit of p_T makes sense in accordance with the mean p_T of the spectra being comfortably an order of magnitude less than 10 GeV/c as discussed in chapter 5. More details on the kinematic variables y and η are in appendix A.

4.3.3 Tracking Detectors in STAR

In the STAR experiment, the TPC is the primary tracking detector. It is 4.2 m long and it cylindrically encloses the accelerator beam pipe from its outside, with an inner diameter of 1 m and an outer diameter of 4 m [30]. It covers a pseudorapidity range of $|y| < 1.8$ in all of azimuth for charged particles. It can identify particles with momenta over 100 MeV/c up to about 1 GeV/c as well as measure their momenta from 100 MeV/c to 30 GeV/c [9]. Figure 4.1 shows the PID capability of the STAR TPC for very high-multiplicity events [25]. Separation of pions from protons is demonstrated up to a little more than 1 GeV/c. At higher momenta, separating particles is more difficult because their energy loss has lower dependence on the rest mass [9]. The TOF system in STAR, with a time resolution of $\lessapprox$ 100 ps, aids PID at higher momenta. However, at intermediate p_T, between $\approx$ 2.0 and 4.0 GeV/c, the TPC by itself cannot distinguish between pions and protons and the TOF by itself cannot separate pions from kaons. This problem is resolved by utilizing the fact that the dependence of the particle velocity on p_T – in case of the TPC – is different from that of the energy loss on p_T in case of the TPC; combining the results from the two, hence, makes PID feasible in this p_T range [39].

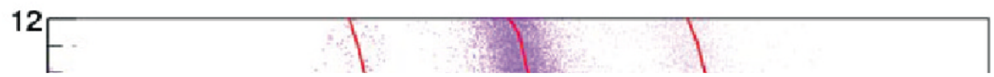

Figure 4.1: Energy loss distribution in the STAR TPC for primary and secondary particles [9].

Chapter 5

Data Analysis

This thesis details the method of transverse energy analysis through the use of p_T spectra from the STAR BES data. As described in section 4.3.3, the TPCs and TOF detectors in STAR can identify particles as well as their trajectories and ultimately measure their multiplicity distributions with respect to the momenta. The availabe distributions were extrapolated to calculate the transverse energies and charged particle multiplicities. Details follow.

5.0.1 STAR p_T spectra

Adamczyk et al. [2] reports the results for the p_T spectra for six different identified hadrons, π^+, π^-, K^+, K^-, p, and $\bar{p}$, from the STAR experiment. The spectra come from $\sqrt{s_{NN}} =$ 7.7, 11.5, and 39 GeV Au+Au collisions data taken in the year 2010, and from $\sqrt{s_{NN}} =$ 19.6 and 27 GeV Au+Au collisions data taken in 2011, both as part of the BES Program. Figure 5.1 [2] shows the spectra corresponding to 39 GeV collisions categorized into seven different collision centralitiy classes. Additionaly, preliminary spectra were available from the STAR experiment for idenfitied lambdas and anti-lambdas [?]. All of these spectra were used to calculate the total transverse energy per event per particle species. This result was then used to estimate the total transverse energy due to all the collision products. The corrections applied by Adamczyk et al. [2] to the raw data to obtain the spectra and the reported systematic uncertainties in their results are discussed below (under construction) ....

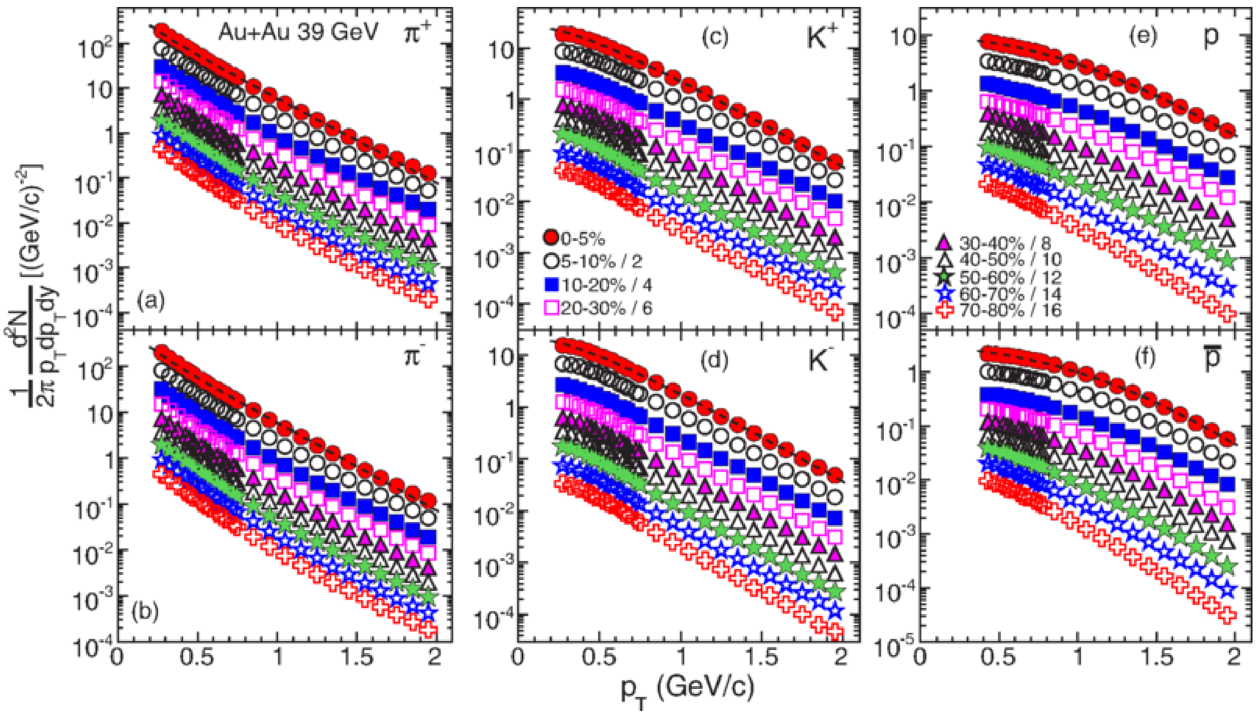

Figure 5.1: Transverse momentum spectra for π^+, π^-, K^+, K^-, p, and $\bar{p}$ at midrapidity ($|y| < 0.1$) from 39 GeV Au+Au collisions at RHIC. The fitting curves on the 0-5% central collision spectra for pions, kaons, and protons/anti-protons represent, respectively, the Bose-Einstein, m_T-exponential, and double-exponential functions [2].

5.1 Extrapolation of Spectra

The available spectra were limited to a range of transverse momenta from around 0.25 GeV/c to around 2 GeV/c (for pions). At higher momenta, with model-dependent values, the p_T spectra may be dominated by hard-scattering processes. To account for the transverse energy corresponding to the momenta for which there were no available data, an extrapolation had to be used. The model used for the extrapolation and the associated statistics are discussed below.

5.1.1 Boltzmann-Gibbs Blast Wave

The blast wave is a common model used in the analysis of particle momentum distributions [45, 46, 2]. The specific model used in this thesis is the Boltzmann-Gibbs blast wave (BGBW). This model assumes local thermal equilibrium at the kinetic freeze-out temperature for the applicability of a Boltzmann distribution. It also assumes a radially increasing velocity that attains a maximum value at the surface of the expanding fireball [46]. The BGBW is represented by the equation:

$$BGBW, \tag{5.1}$$

where r is the radial distance from the collision vertex, m is the particle mass, T is the thermal freeze-out temperature, β is the flow velocity, ρ is the flow profile, n is the flow velocity profile exponent, $K_1(x)$ and $I_0(x)$ are the modified Bessel functions given by...........................

5.1.2 Fitting Spectra to BGBW

Figure 5.2 presents an example of a BGBW fit on one of the individual particle spectra with χ^2/ndf as well as other statistics and the associated uncertainties. The fitting is done in the ROOT software framework which is widely used in high energy physics data analysis. T, β, and n are treated as free parameters, while m is fixed. The results of the fits for each of the spectra are tabulated in appendix B

5.2 Calculations from the Spectra

The available multiplicity distribution for the p_T range, $p_{T,low}$ to $p_{T,high}$, of a spectrum divided the total spectrum into three different regions: (i) region where the experimental data is available, i.e., $p_{T,low}$ to $p_{T,high}$, (ii) extrapolation region from p_T = 0 GeV/c to p_T = $p_{T,low}$, and (iii) extrapolation region from p_T = $p_{T,high}$ to p_T = 10 GeV/c, The total transverse energy and particle multiplicity for each of the spectra was calculated by adding said quantities corresponding to three different in the distribution.

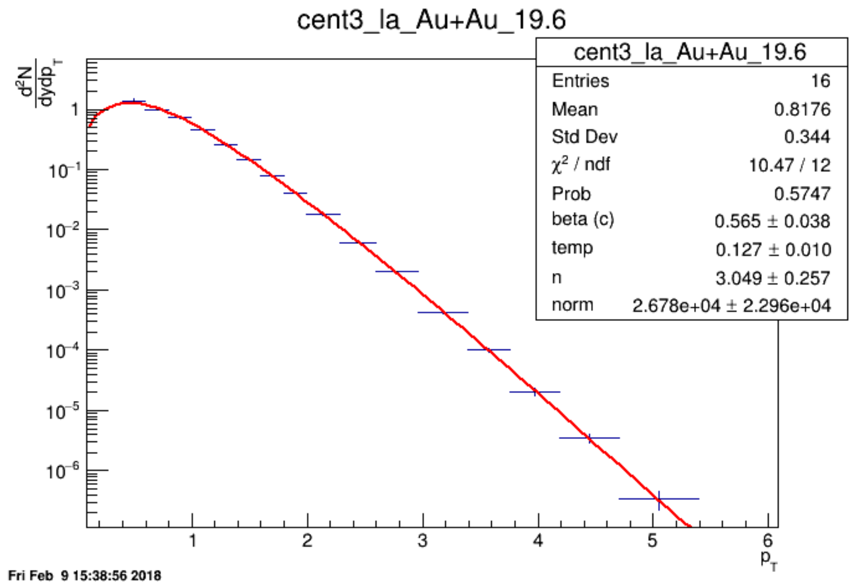

Figure 5.2: Red curve shows the Boltzmann-Gibbs blast wave functional fit on the preliminary transverse momentum spectrum for lambda particles identified by the STAR detector for 19.6 GeV Au+Au collisions (10-15% central). Parameters extracted from the chi-square goodness-of-fit test, as well as other statistics, are shown in the box on the top right.

5.2.1 Calculation of $\frac{dE_T}{dy}$, $\frac{dE_T}{d\eta}$, $\frac{dN_{ch}}{dy}$, and $\frac{dN_{ch}}{d\eta}$

The method described in section 4.3.2 +++++++++++++ talk about the jacobian from the appendix/previous chapter for conversion from y to eta was used to calculate ....

.....corresponding to region (i) was calculated by adding the areas of the rectangles corresponding to each p_T bin.

5.2.2 Corrections, Uncertainties, and Estimation of Total E_T

It is reasonable to assume that, at high energies, there should be roughly the same multiplicity of all the isospin states of a final state particle. This assumption was partially tested by comparing the E_T values calculated for the identified charged particles with those independently calculated for their anti-particles for the same values of collision energy and centrality. The comparisons revealed the E_T values of the particles being almost exactly equal to those of the antiparticles.

Table 5.1 lists the isospin states associated with the pion, the kaon, the proton, and the lambda particles. The total E_T for all the particles would then be:

Particle	Isospin multiplets
pion	π^+, π^0, π^-
kaon	$K^+, K^0, K^-, \bar{K}^0$
proton	$p, n, \bar{p}, \bar{n}$
lambda	$\Lambda, \bar{\Lambda}$

Table 5.1: Isospin states of different identified particles.

$$E_T = \frac{3}{2}(E_T^{\pi^+} + E_T^{\pi^-}) + 2(E_T^{K^+} + E_T^{K^-}) + 2(E_T^{p} + E_T^{\bar{p}}) + E_T^{\Lambda} + E_T^{\bar{\Lambda}} \tag{5.2}$$

................text content...................

5.2.3 Lambdas Centralitiy Adjustments and E_T Interpolations

The centrality bins corresponding to the lambdas spectra were slightly different from those corresponding to the rest of the particles........

5.3 Uncertainties

.........The systematic uncertainties are assumed to be 100% correlated point-to-point and uncorrelated between particles........ ?

Chapter 6

Results

Present results and comparisons to Adare et al.....

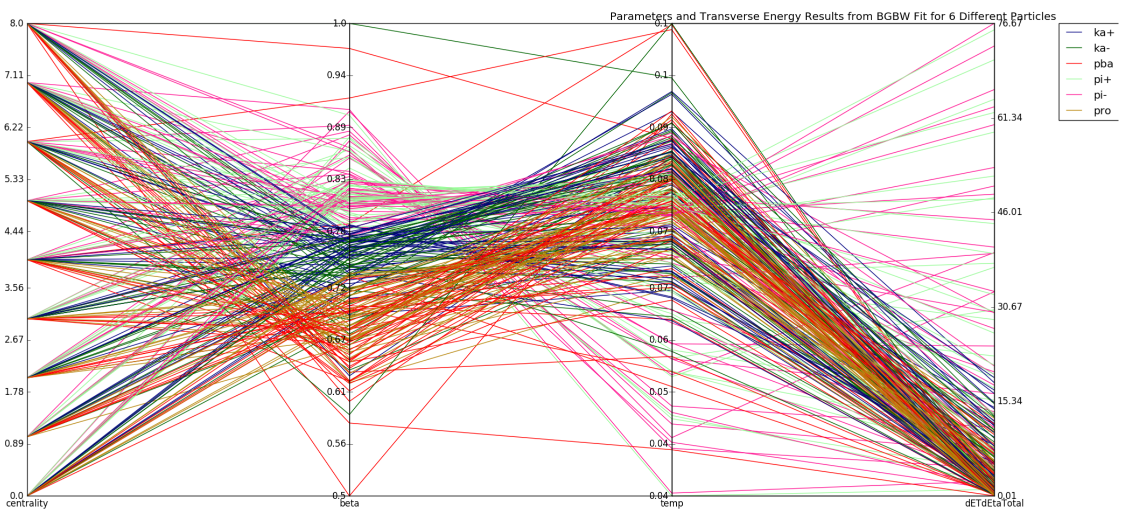

Figure 6.1: Parallel coordinates plot for 270 diffrent spectra relating 6 different identified particles (color-coded) to their respective collision centrality classes, good-fit parameters, and the transverse energy calculated using said parameters.

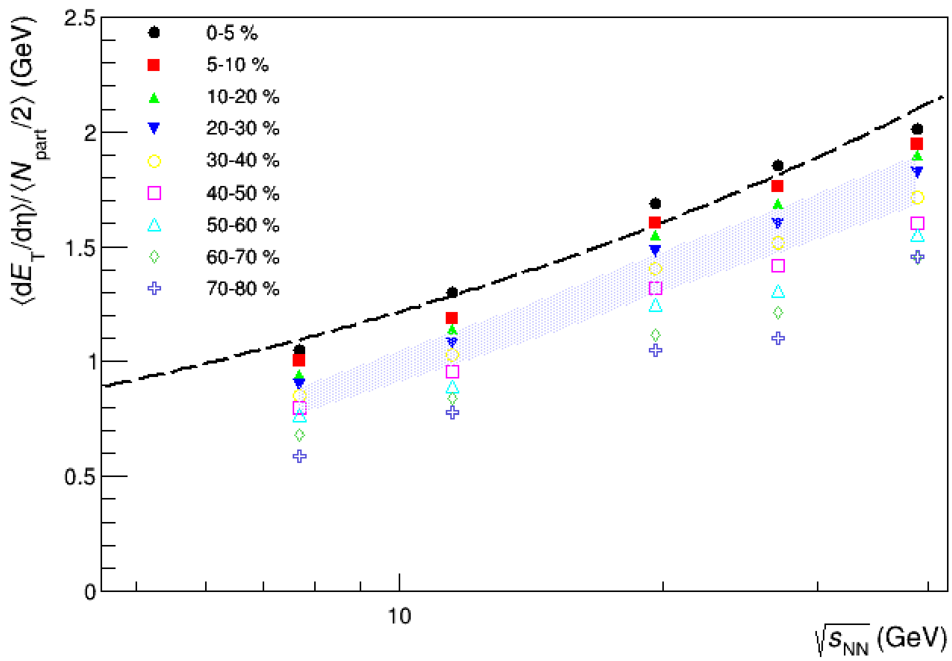

Figure 6.2: $(dE_T/d\eta)/0.5N_{part}$ at midrapidity as a function of $\sqrt{s_{NN}}$ for different centralities. The dashed line represents a power-law fit to the 0-5% central data in the form $y = ax^{2b}$, where x and y are the placeholders for the quantities in the plot axes. $\chi^2/n.d.f$ for the fit was 1.806, and the good-fit parameters were $a = 0.4838 \pm 0.0429$ and $b = 0.2005 \pm 0.01466$. The shaded area represents the uncertainty bounds for the 0-5% central PHENIX data from [4].

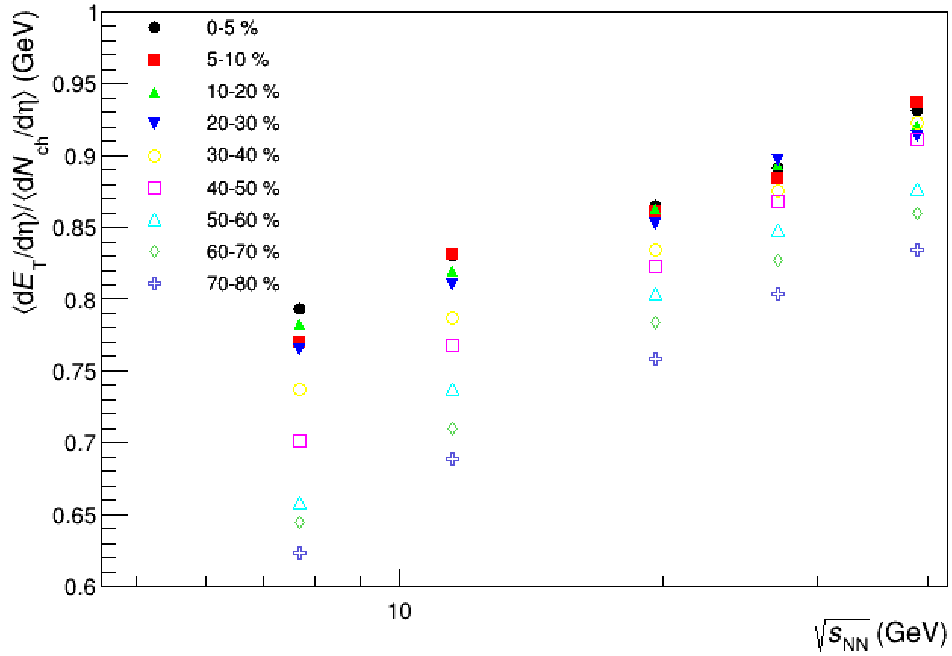

Figure 6.3: $(dE_T/d\eta)/(dN_{ch}/d\eta)$ at midrapidity as a function of $\sqrt{s_{NN}}$ for different centralities.

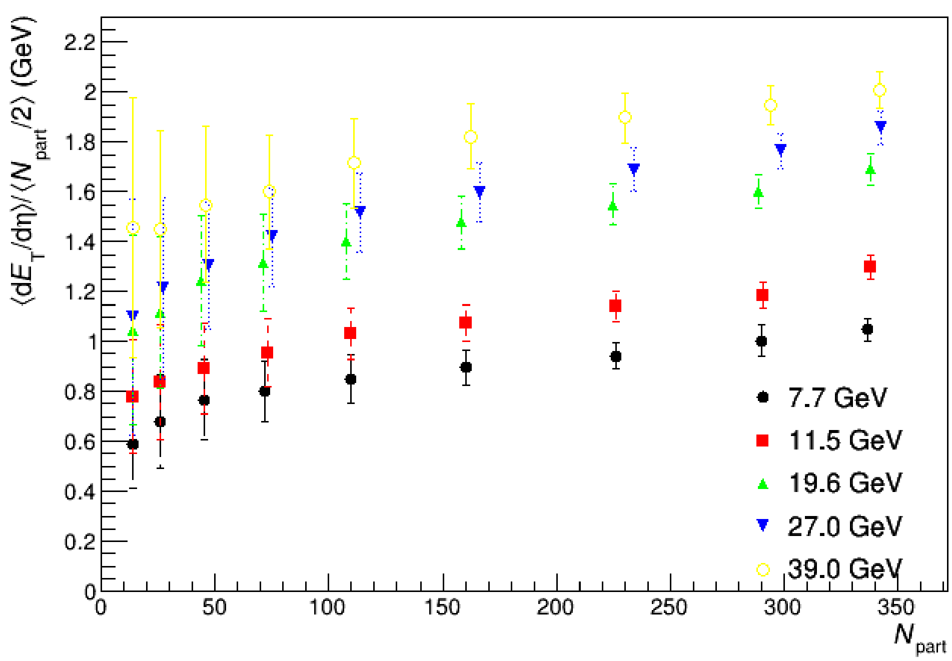

Figure 6.4: $(dE_T/d\eta)/0.5N_{part}$ at midrapidity as a function of N_{part} for different collision energies.

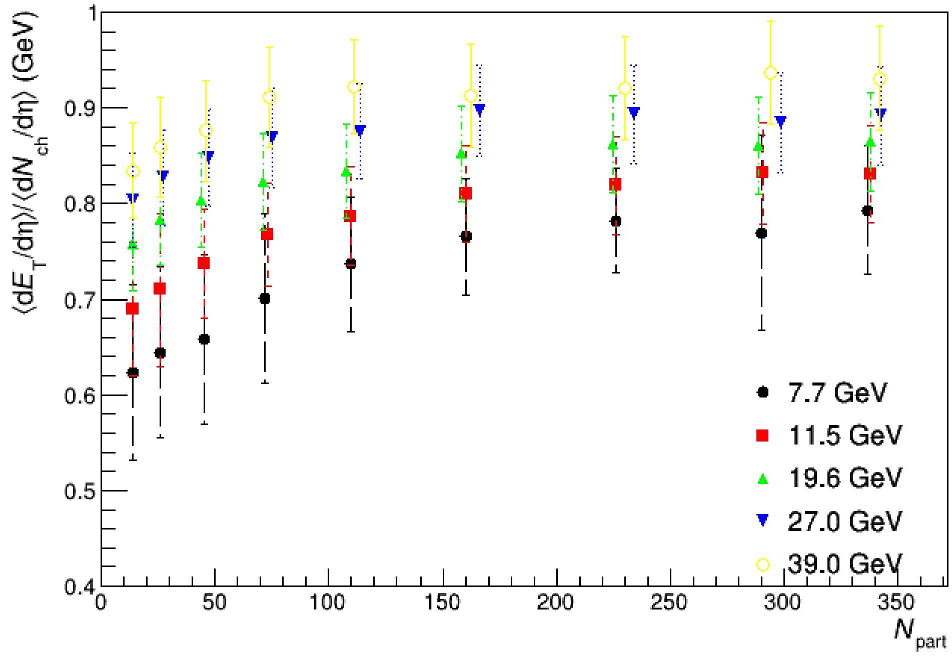

Figure 6.5: $(dE_T/d\eta)/(dN_{ch}/d\eta)$ at midrapidity as a function of N_{part} for different collision energies.

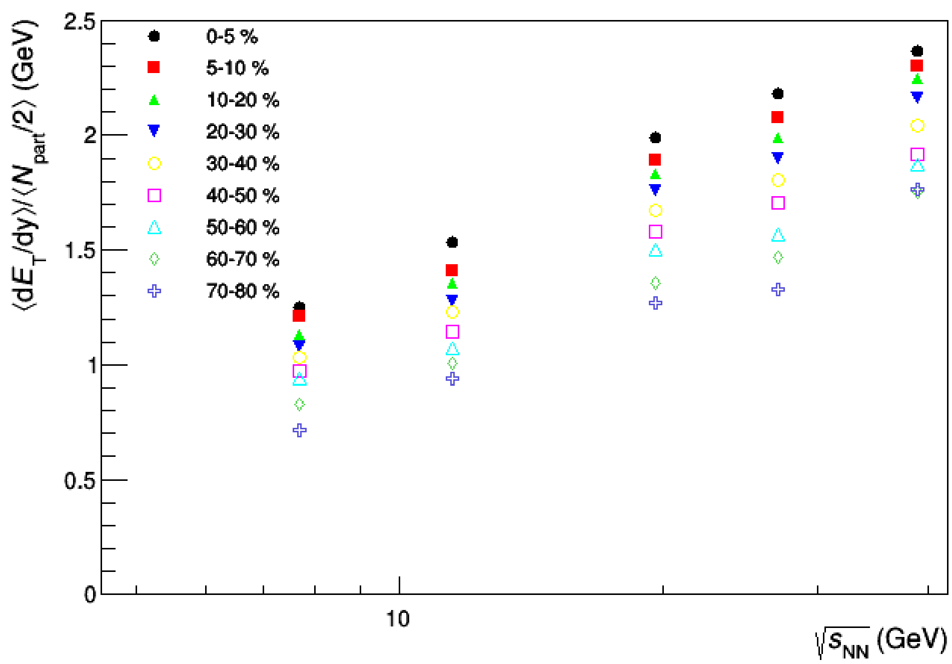

Figure 6.6: $(dE_T/dy)/0.5N_{part}$ at midrapidity as a function of $\sqrt{s_{NN}}$ for different centralities.

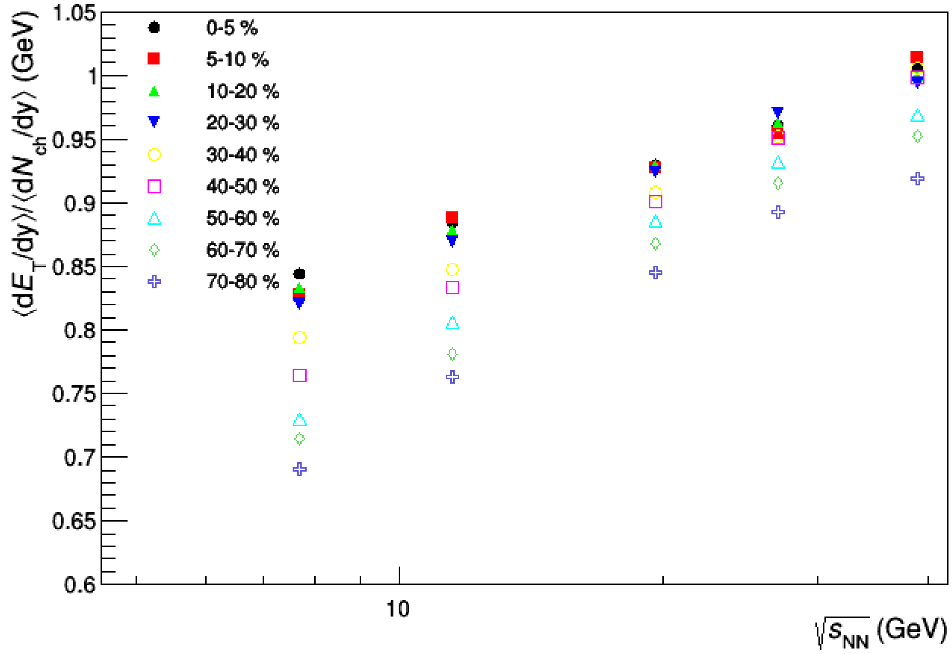

Figure 6.7: $(dE_T/dy)/(dN_{ch}/dy)$ at midrapidity as a function of $\sqrt{s_{NN}}$ for different centralities.

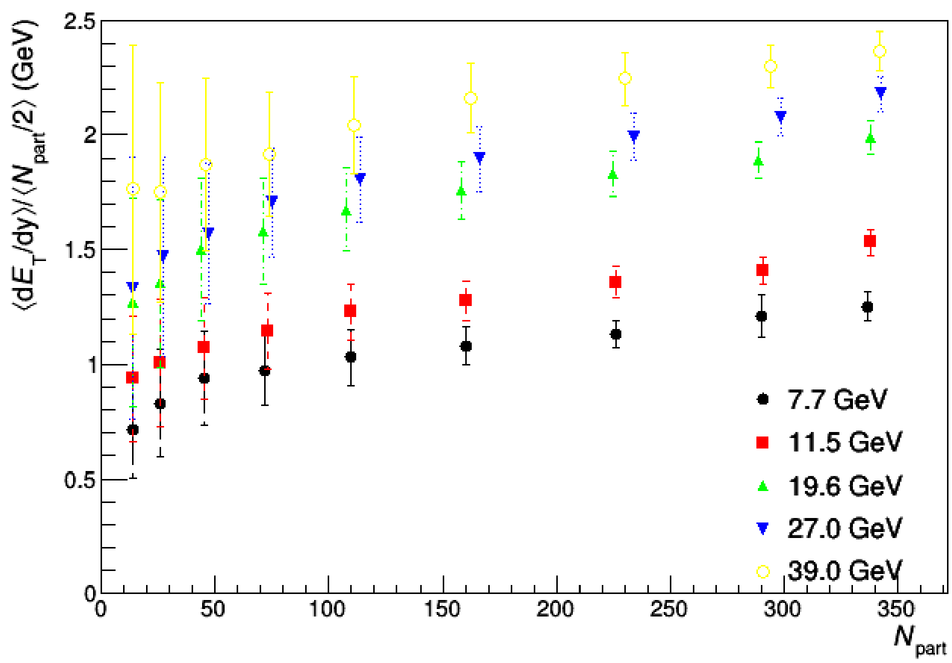

Figure 6.8: $(dE_T/dy)/0.5N_{part}$ at midrapidity as a function of N_{part} for different collision energies.

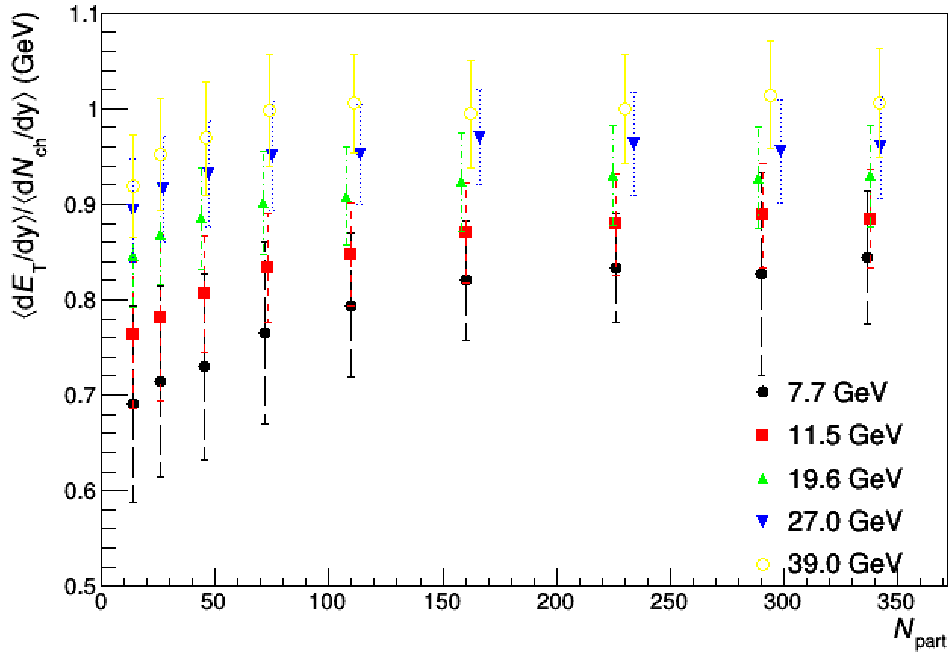

Figure 6.9: $(dE_T/dy)/(dN_{ch}/dy)$ at midrapidity as a function of N_{part} for different collision energies.

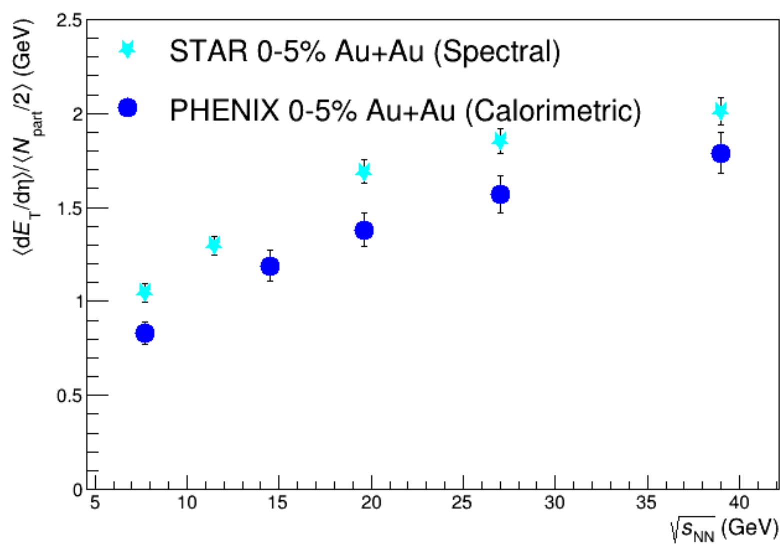

Figure 6.10: $\frac{dE_T}{d\eta}/0.5N_{part}$ for 0-5% central collisions at midrapidity as a function of $\sqrt{s_{NN}}$. The PHENIX data are from [4]. The error bars represent the total statistical and systematic uncertainties.

Chapter 7

Conclusion

Summary and implications

Chapter 8

Future Work

8.1 Goodness of Fit

A maximum likelihood? fit method can be adopted to compare the results with those using the chi-squared fits.

8.2 Bjorken Energy Density Estimate

Apart from the transverse energy, the calculation of the initial energy density, ϵ, as given by the Bjorken formula in eq. 3.2, requires the estimate of other physical quantities. Adare et al.[4] use the Glauber model to determine A_T, the area of the intersection of the two nuclei in the transverse plane. Since the results in this thesis are cross-checked with those in [4], it would be reasonable to use the same model in the future work pertaining to this thesis. τ_0, the proper time at the moment of QGP equilibration, also depends on the model of the collision. However, the product of ϵ and τ_0 is often used instead of just ϵ to study how the energy density scales with the collision energy and the number of participants.

8.3 Asymmetric beams

The codes in the repository can be used to analyze more data. In fact, since there is more data available on collisions of asymmetric systems such as d+Au?, we can expect it to be a test to tell if the assumptions? used in this analysis scale to such domains?

Bibliography

[1] Adam, J., Adamova, D., Aggarwal, M. M., Aglieri Rinella, G., Agnello, M., Agrawal, N., Ahammed, Z., Ahmad, S., Ahn, S. U., Aiola, S., Akindinov, A., Alam, S. N., Silva De Albuquerque, D., Aleksandrov, D., Alessandro, B., Alexandre, D., Alfaro Molina, J. R., Alici, A., Alkin, A., Millan Almaraz, J. R., Alme, J., Alt, T., Altinpinar, S., Altsybeev, I., Alves Garcia Prado, C., Andrei, C., Andronic, A., Anguelov, V., Anticic, T., Antinori, F., Antonioli, P., Aphecetche, L. B., Appelshaeuser, H., Arcelli, S., Arnaldi, R., Arnold, O. W., Arsene, I. C., Arslandok, M., Audurier, B., Augustinus, A., Averbeck, R. P., Azmi, M. D., Badala, A., Baek, Y. W., Bagnasco, S., Bailhache, R. M., Bala, R., Balasubramanian, S., Baldisseri, A., Baral, R. C., Barbano, A. M., Barbera, R., Barile, F., Barnafoldi, G. G., Barnby, L. S., Ramillien Barret, V., Bartalini, P., Barth, K., Bartke, J. G., Bartsch, E., Basile, M., Bastid, N., Basu, S., Bathen, B., Batigne, G., Batista Camejo, A., Batyunya, B., Batzing, P. C., Bearden, I. G., Beck, H., Bedda, C., Behera, N. K., Belikov, I., Bellini, F., Bello Martinez, H., Bellwied, R., Belmont Iii, R. J., Belmont Moreno, E., Belyaev, V., Bencedi, G., Beole, S., Berceanu, I., Bercuci, A., Berdnikov, Y., Berenyi, D., Bertens, R. A., Berzano, D., Betev, L., Bhasin, A., Bhat, I. R., Bhati, A. K., Bhattacharjee, B., Bhom, J., Bianchi, L., Bianchi, N., Bianchin, C., Bielcik, J., Bielcikova, J., Bilandzic, A., Biro, G., Biswas, R., Biswas, S., Bjelogrlic, S., Blair, J. T., Blau, D., Blume, C., Bock, F., Bogdanov, A., Boggild, H., Boldizsar, L., Bombara, M., Book, J. H., Borel, H., Borissov, A., Borri, M., Bossu, F., Botta, E., Bourjau, C., Braun-Munzinger, P., Bregant, M., Breitner, T. G., Broker, T. A., Browning, T. A., Broz, M., Brucken, E. J., Bruna, E., Bruno, G. E., Budnikov, D., Buesching, H., Bufalino, S., Buncic, P., Busch, O., Buthelezi, E. Z., Bashir Butt, J., Buxton, J. T., Cabala, J., Caffarri, D., Cai, X., Caines, H. L., Calero Diaz, L., Caliva, A., Calvo Villar, E., Camerini, P., Carena, F., Carena, W., Carnesecchi, F., Castillo Castellanos, J. E., Castro, A. J., Casula, E. A. R., Ceballos Sanchez, C., Cepila, J., Cerello, P., Cerkala, J., Chang, B., Chapeland, S., Chartier, M., Charvet, J.-L. F., Chattopadhyay, S., Chattopadhyay, S., Chauvin, A., Chelnokov, V., Cherney, M. G., Cheshkov, C. V., Cheynis, B., Chibante Barroso, V. M., Dobrigkeit Chinellato, D., Cho, S., Chochula, P., Choi, K., Chojnacki, M., Choudhury, S., Christakoglou, P., Christensen, C. H., Christiansen, P., Chujo, T., Chung, S.-U., Cicalo, C., Cifarelli, L., Cindolo, F., Cleymans, J. W. A., Colamaria, F. F., Colella, D., Collu, A.,

Colocci, M., Conesa Balbastre, G., Conesa Del Valle, Z., Connors, M. E., Contreras Nuno, J. G., Cormier, T. M., Corrales Morales, Y., Cortes Maldonado, I., Cortese, P., Cosentino, M. R., Costa, F., Crochet, P., Cruz Albino, R., Cuautle Flores, E., Cunqueiro Mendez, L., Dahms, T., Dainese, A., Danisch, M. C., Danu, A., Das, D., Das, I., Das, S., Dash, A. K., Dash, S., De, S., De Caro, A., De Cataldo, G., De Conti, C., De Cuveland, J., De Falco, A., De Gruttola, D., De Marco, N., De Pasquale, S., Deisting, A., Deloff, A., Denes, E. S., Deplano, C., Dhankher, P., Di Bari, D., Di Mauro, A., Di Nezza, P., Diaz Corchero, M. A., Dietel, T., Dillenseger, P., Divia, R., Djuvsland, O., Dobrin, A. F., Domenicis Gimenez, D., Donigus, B., Dordic, O., Drozhzhova, T., Dubey, A. K., Dubla, A., Ducroux, L., Dupieux, P., Ehlers Iii, R. J., Elia, D., Endress, E., Engel, H., Epple, E., Erazmus, B. E., Erdemir, I., Erhardt, F., Espagnon, B., Estienne, M. D., Esumi, S., Eum, J., Evans, D., Evdokimov, S., Eyyubova, G., Fabbietti, L., Fabris, D., Faivre, J., Fantoni, A., Fasel, M., Feldkamp, L., Feliciello, A., Feofilov, G., Ferencei, J., Fernandez Tellez, A., Gonzalez Ferreiro, E., Ferretti, A., Festanti, A., Feuillard, V. J. G., Figiel, J., Araujo Silva Figueredo, M., Filchagin, S., Finogeev, D., Fionda, F., Fiore, E. M., Fleck, M. G., Floris, M., Foertsch, S. V., Foka, P., Fokin, S., Fragiacomo, E., Francescon, A., Frankenfeld, U. M., Fronze, G. G., Fuchs, U., Furget, C., Furs, A., Fusco Girard, M., Gaardhoeje, J. J., Gagliardi, M., Gago Medina, A. M., Gallio, M., Gangadharan, D. R., Ganoti, P., Gao, C., Garabatos Cuadrado, J., Garcia-Solis, E. J., Gargiulo, C., Gasik, P. J., Gauger, E. F., Germain, M., Gheata, M., Ghosh, P., Ghosh, S. K., Gianotti, P., Giubellino, P., Giubilato, P., Gladysz-Dziadus, E., Glassel, P., Gomez Coral, D. M., Gomez Ramirez, A., Sanchez Gonzalez, A., Gonzalez, V., Gonzalez Zamora, P., Gorbunov, S., Gorlich, L. M., Gotovac, S., Grabski, V., Grachov, O. A., Graczykowski, L. K., Graham, K. L., Grelli, A., Grigoras, A. G., Grigoras, C., Grigoryev, V., Grigoryan, A., Grigoryan, S., Grynyov, B., Grion, N., Gronefeld, J. M., Grosse-Oetringhaus, J. F., Grosso, R., Guber, F., Guernane, R., Guerzoni, B., Gulbrandsen, K. H., Gunji, T., Gupta, A., Gupta, R., Haake, R., Haaland, O. S., Hadjidakis, C. M., Haiduc, M., Hamagaki, H., Hamar, G., Hamon, J. C., Harris, J. W., Harton, A. V., Hatzifotiadou, D., Hayashi, S., Heckel, S. T., Hellbar, E., Helstrup, H., Herghelegiu, A. I., Herrera Corral, G. A., Hess, B. A., Hetland, K. F., Hillemanns, H., Hippolyte, B., Horak, D., Hosokawa, R., Hristov, P. Z., Humanic, T., Hussain, N., Hussain, T., Hutter, D., Hwang, D. S., Ilkaev, R., Inaba, M., Incani, E., Ippolitov, M., Irfan, M., Ivanov, M., Ivanov, V., Izucheev, V., Jacazio, N., Jacobs, P. M., Jadhav, M. B., Jadlovska, S., Jadlovsky, J., Jahnke, C., Jakubowska, M. J., Jang, H. J., Janik, M. A., Pahula Hewage, S., Jena, C., Jena, S., Jimenez Bustamante, R. T., Jones, P. G., Jusko, A., Kalinak, P., Kalweit, A. P., Kamin, J. A., Kang, J. H., Kaplin, V., Kar, S., Karasu Uysal, A., Karavichev, O., Karavicheva, T., Karayan, L., Karpechev, E., Kebschull, U. W., Keidel, R., Keijdener, D. L., Keil, M., Khan, M. M., Khan, P., Khan, S. A., Khanzadeev, A., Kharlov, Y., Kileng, B., Kim, D. W., Kim, D. J., Kim, D., Kim, H., Kim, J., Kim, M., Kim, S. Y., Kim, T., Kirsch, S., Kisel, I., Kiselev, S., Kisiel, A. R., Kiss, G., Klay, J. L., Klein, C., Klein, J., Klein-Boesing, C., Klewin, S., Kluge, A., Knichel, M. L., Knospe, A. G., Kobdaj, C., Kofarago, M., Kollegger, T., Kolozhvari, A., Kondratev, V., Kondratyeva, N., Kondratyuk, E., Konevskikh, A., Kopcik, M., Kostarakis, P., Kour, M., Kouzinopoulos, C., Kovalenko, O., Kovalenko, V., Kowalski, M., Koyithatta Meethaleveedu, G., Kralik, I., Kravcakova, A., Krivda, M., Krizek, F., Kryshen, E., Krzewicki, M., Kubera, A. M., Kucera, V., Kuhn, C. C., Kuijer, P. G., Kumar, A., Kumar, J., Kumar, L., Kumar, S., Kurashvili, P., Kurepin, A., Kurepin, A., Kuryakin, A., Kweon, M. J., Kwon, Y., La Pointe, S. L., La Rocca, P., Ladron De Guevara, P., Lagana Fernandes, C., Lakomov, I., Langoy, R., Lapidus, K., Lara Martinez, C. E., Lardeux, A. X., Lattuca, A., Laudi, E., Lea, R., Leardini, L., Lee, G. R., Lee, S., Lehas, F., Lemmon, R. C., Lenti, V., Leogrande, E., Leon Monzon, I., Leon Vargas, H., Leoncino, M., Levai, P., Li, S., Li, X., Lien, J. A., Lietava, R., Lindal, S., Lindenstruth, V., Lippmann, C., Lisa, M. A., Ljunggren, H. M., Lodato, D. F., Lonne, P.-I., Loginov, V., Loizides, C., Lopez, X. B., Lopez Torres, E., Lowe, A. J., Luettig, P. J., Lunardon, M., Luparello, G., Lutz, T. H., Maevskaya, A., Mager, M., Mahajan, S., Mahmood, S. M., Maire, A., Majka, R. D., Malaev, M., Maldonado Cervantes, I. A., Malinina, L., Mal'Kevich, D., Malzacher, P., Mamonov, A., Manko, V., Manso, F., Manzari, V., Marchisone, M., Mares, J., Margagliotti, G. V., Margotti, A., Margutti, J., Marin, A. M., Markert, C., Marquard, M., Martin, N. A., Martin Blanco, J., Martinengo, P., Martinez Hernandez, M. I., Martinez-Garcia, G., Martinez Pedreira, M., Mas, A. J.-M., Masciocchi, S., Masera, M., Masoni, A., Mastroserio, A., Matyja, A. T., Mayer, C., Mazer, J. A., Mazzoni,

A. M., Mcdonald, D., Meddi, F., Melikyan, Y., Menchaca-Rocha, A. A., Meninno, E., Mercado-Perez, J., Meres, M., Miake, Y., Mieskolainen, M. M., Mikhaylov, K., Milano, L., Milosevic, J., Mischke, A., Mishra, A. N., Miskowiec, D. C., Mitra, J., Mitu, C. M., Mohammadi, N., Mohanty, B., Molnar, L., Montano Zetina, L. M., Montes Prado, E., Moreira De Godoy, D. A., Perez Moreno, L. A., Moretto, S., Morreale, A., Morsch, A., Muccifora, V., Mudnic, E., Muhlheim, D. M., Muhuri, S., Mukherjee, M., Mulligan, J. D., Gameiro Munhoz, M., Munzer, R. H., Murakami, H., Murray, S., Musa, L., Musinsky, J., Naik, B., Nair, R., Nandi, B. K., Nania, R., Nappi, E., Naru, M. U., Ferreira Natal Da Luz, P. H., Nattrass, C., Rosado Navarro, S., Nayak, K., Nayak, R., Nayak, T. K., Nazarenko, S., Nedosekin, A., Nellen, L., Ng, F., Nicassio, M., Niculescu, M., Niedziela, J., Nielsen, B. S., Nikolaev, S., Nikulin, S., Nikulin, V., Noferini, F., Nomokonov, P., Nooren, G., Cabanillas Noris, J. C., Norman, J., Nyanin, A., Nystrand, J. I., Oeschler, H. O., Oh, S., Oh, S. K., Ohlson, A. E., Okatan, A., Okubo, T., Olah, L., Oleniacz, J., Oliveira Da Silva, A. C., Oliver, M. H., Onderwaater, J., Oppedisano, C., Orava, R., Oravec, M., Ortiz Velasquez, A., Oskarsson, A. N. E., Otwinowski, J. T., Oyama, K., Ozdemir, M., Pachmayer, Y. C., Pagano, D., Pagano, P., Paic, G., Pal, S. K., Pan, J., Pandey, A. K., Papikyan, V., Pappalardo, G., Pareek, P., Park, W., Parmar, S., Passfeld, A., Paticchio, V., Patra, R. N., Paul, B., Pei, H., Peitzmann, T., Pereira Da Costa, H. D. A., Peresunko, D. Y., Perez Lara, C. E., Perez Lezama, E., Peskov, V., Pestov, Y., Petracek, V., Petrov, V., Petrovici, M., Petta, C., Piano, S., Pikna, M., Pillot, P., Ozelin De Lima Pimentel, L., Pinazza, O., Pinsky, L., Piyarathna, D., Ploskon, M. A., Planinic, M., Pluta, J. M., Pochybova, S., Podesta Lerma, P. L. M., Poghosyan, M., Polishchuk, B., Poljak, N., Poonsawat, W., Pop, A., Porteboeuf, S. J., Porter, R. J., Pospisil, J., Prasad, S. K., Preghenella, R., Prino, F., Pruneau, C. A., Pshenichnov, I., Puccio, M., Puddu, G., Pujahari, P. R., Punin, V., Putschke, J. H., Qvigstad, H., Rachevski, A., Raha, S., Rajput, S., Rak, J., Rakotozafindrabe, A. M., Ramello, L., Rami, F., Raniwala, R., Raniwala, S., Rasanen, S. S., Rascanu, B. T., Rathee, D., Read, K. F., Redlich, K., Reed, R. J., Rehman, A. U., Reichelt, P. S., Reidt, F., Ren, X., Renfordt, R. A. E., Reolon, A. R., Reshetin, A., Reygers, K. J., Riabov, V., Ricci, R. A., Richert, T. O. H., Richter, M. R., Riedler, P., Riegler, W., Riggi, F., Ristea, C.-L., Rocco, E., Rodriguez Cahuantzi, M., Rodriguez Manso, A., Roeed, K., Rogochaya, E., Rohr, D. M., Roehrich, D., Ronchetti, F., Ronflette, L., Rosnet, P., Rossi, A., Roukoutakis, F., Roy, A., Roy, C. S., Roy, P. K., Rubio Montero, A. J., Rui, R., Russo, R., Di Ruzza, B., Ryabinkin, E., Ryabov, Y., Rybicki, A., Saarinen, S., Sadhu, S., Sadovskiy, S., Safarik, K., Sahlmuller, B., Sahoo, P., Sahoo, R., Sahoo, S., Sahu, P. K., Saini, J., Sakai, S., Saleh, M. A., Salzwedel, J. S. N., Sambyal, S. S., Samsonov, V., Sandor, L., Sandoval, A., Sano, M., Sarkar, D., Sarkar, N., Sarma, P., Scapparone, E., Scarlassara, F., Schiaua, C. C., Schicker, R. M., Schmidt, C. J., Schmidt, H. R., Schuchmann, S., Schukraft, J., Schulc, M., Schutz, Y. R., Schwarz, K. E., Schweda, K. O., Scioli, G., Scomparin, E., Scott, R. M., Sefcik, M., Seger, J. E., Sekiguchi, Y., Sekihata, D., Selyuzhenkov, I., Senosi, K., Senyukov, S., Serradilla Rodriguez, E., Sevcenco, A., Shabanov, A., Shabetai, A., Shadura, O., Shahoyan, R., Shahzad, M. I., Shangaraev, A., Sharma, A., Sharma, M., Sharma, M., Sharma, N., Sheikh, A. I., Shigaki, K., Shou, Q., Shtejer Diaz, K., Sibiryak, Y., Siddhanta, S., Sielewicz, K. M., Siemiarczuk, T., Silvermyr, D. O. R., Silvestre, C. M., Simatovic, G., Simonetti, G., Singaraju, R. N., Singh, R., Singha, S., Singhal, V., Sinha, B., Sarkar Sinha, T., Sitar, B., Sitta, M., Skaali, B., Slupecki, M., Smirnov, N., Snellings, R., Snellman, T. W., Song, J., Song, M., Song, Z., Soramel, F., Sorensen, S. P., Derradi De Souza, R., Sozzi, F., Spacek, M., Spiriti, E., Sputowska, I. A., Spyropoulou-Stassinaki, M., Stachel, J., Stan, I., Stankus, P., Stenlund, E. A., Steyn, G. F., Stiller, J. H., Stocco, D., Strmen, P., Alarcon Do Passo Suaide, A., Sugitate, T., Suire, C. P., Suleymanov, M. K. O., Suljic, M., Sultanov, R., Sumbera, M., Sumowidagdo, S., Szabo, A., Szanto De Toledo, A., Szarka, I., Szczepankiewicz, A., Szymanski, M. P., Tabassam, U., Takahashi, J., Tambave, G. J., Tanaka, N., Tarhini, M., Tariq, M., Tarzila, M.-G., Tauro, A., Tejeda Munoz, G., Telesca, A., Terasaki, K., Terrevoli, C., Teyssier, B., Thaeder, J. M., Thakur, D., Thomas, D., Tieulent, R. N., Tikhonov, A., Timmins, A. R., Toia, A., Trogolo, S., Trombetta, G., Trubnikov, V., Trzaska, W. H., Tsuji, T., Tumkin, A., Turrisi, R., Tveter, T. S., Ullaland, K., Uras, A., Usai, G., Utrobicic, A., Vala, M., Valencia Palomo, L., Vallero, S., Van Der Maarel, J., Van Hoorne, J. W., Van Leeuwen, M., Vanat, T., Vande Vyvre, P., Varga, D., Diozcora Vargas Trevino, A., Vargyas, M., Varma, R., Vasileiou, M., Vasiliev, A., Vauthier, A., Vazquez Doce, O., Vechernin, V., Veen, A. M., Veldhoen, M., Velure, A., Vercellin, E., Vergara Limon, S., Vernet, R., Verweij, M., Vickovic, L., Viinikainen, J. S., Vilakazi, Z., Villalobos Baillie, O., Villatoro Tello, A., Vinogradov, A., Vinogradov, L., Vinogradov, Y., Virgili, T., Vislavicius, V., Viyogi, Y., Vodopyanov, A., Volkl, M. A., Voloshin, K., Voloshin, S., Volpe, G., Von Haller, B., Vorobyev, I., Vranic, D., Vrlakova, J., Vulpescu, B., Wagner, B., Wagner, J., Wang, H., Wang, M., Watanabe, D., Watanabe, Y., Weber, M., Weber, S. G., Weiser, D. F., Wessels, J. P., Westerhoff, U., Whitehead, A. M., Wiechula, J., Wikne, J., Wilk, G. A., Wilkinson, J. J., Williams, C., Windelband, B. S., Winn, M. A., Yang, P., Yano, S., Yasin, Z., Yin, Z., Yokoyama, H., Yoo, I.-K., Yoon, J. H., Yurchenko, V., Yushmanov, I., Zaborowska, A., Zaccolo, V., Zaman, A., Zampolli, C., Correia Zanoli, H. J., Zaporozhets, S., Zardoshti, N., Zarochentsev, A., Zavada, P., Zavyalov, N., Zbroszczyk, H. P., Zgura, S. I., Zhalov, M., Zhang, H., Zhang, X., Zhang, Y., Chunhui, Z., Zhang, Z., Zhao, C., Zhigareva, N., Zhou, D., Zhou, Y., Zhou, Z., Zhu, H., Zhu, J., Zichichi, A., Zimmermann, A., Zimmermann, M. B., Zinovjev, G., and Zyzak, M. (2016). Measurement of transverse energy at midrapidity in Pb-Pb collisions at $\sqrt{s_{\mathrm{NN}}} = 2.76$ TeV. *Phys. Rev. C*, 94(CERN-EP-2016-071. CERN-EP-2016-071):034903. 30 p. 30 pages, 14 captioned figures, 2 tables, authors from page 25, published version, figures at http://aliceinfo.cern.ch/ArtSubmission/node/2400. 6, 14

[2] Adamczyk, L., Adkins, J. K., Agakishiev, G., Aggarwal, M. M., Ahammed, Z., Ajitanand, N. N., Alekseev, I., Anderson, D. M., Aoyama, R., Aparin, A., Arkhipkin, D., Aschenauer, E. C., Ashraf, M. U., Attri, A., Averichev, G. S., Bai, X., Bairathi, V., Behera, A., Bellwied, R., Bhasin, A., Bhati, A. K., Bhattarai, P., Bielcik, J., Bielcikova, J., Bland, L. C., Bordyuzhin, I. G., Bouchet, J., Brandenburg, J. D., Brandin, A. V., Brown, D., Bunzarov, I., Butterworth, J., Caines, H., Calderón de la Barca Sánchez, M., Campbell, J. M., Cebra, D., Chakaberia, I., Chaloupka, P., Chang, Z., Chankova-Bunzarova, N., Chatterjee, A., Chattopadhyay, S., Chen, X., Chen, J. H., Chen, X., Cheng, J., Cherney, M., Christie, W., Contin, G., Crawford, H. J., Das, S., De Silva, L. C., Debbe, R. R., Dedovich, T. G., Deng, J., Derevschikov, A. A., Didenko, L., Dilks, C., Dong, X., Drachenberg, J. L., Draper, J. E., Dunkelberger, L. E., Dunlop, J. C., Efimov, L. G., Elsey, N., Engelage, J., Eppley, G., Esha, R., Esumi, S., Evdokimov, O., Ewigleben,

J., Eyser, O., Fatemi, R., Fazio, S., Federic, P., Federicova, P., Fedorisin, J., Feng, Z., Filip, P., Finch, E., Fisyak, Y., Flores, C. E., Fulek, L., Gagliardi, C. A., Garand, D., Geurts, F., Gibson, A., Girard, M., Grosnick, D., Gunarathne, D. S., Guo, Y., Gupta, A., Gupta, S., Guryn, W., Hamad, A. I., Hamed, A., Harlenderova, A., Harris, J. W., He, L., Heppelmann, S., Heppelmann, S., Hirsch, A., Hoffmann, G. W., Horvat, S., Huang, T., Huang, B., Huang, X., Huang, H. Z., Humanic, T. J., Huo, P., Igo, G., Jacobs, W. W., Jentsch, A., Jia, J., Jiang, K., Jowzaee, S., Judd, E. G., Kabana, S., Kalinkin, D., Kang, K., Kauder, K., Ke, H. W., Keane, D., Kechechyan, A., Khan, Z., Kikoła, D. P., Kisel, I., Kisiel, A., Kochenda, L., Kocmanek, M., Kollegger, T., Kosarzewski, L. K., Kraishan, A. F., Kravtsov, P., Krueger, K., Kulathunga, N., Kumar, L., Kvapil, J., Kwasizur, J. H., Lacey, R., Landgraf, J. M., Landry, K. D., Lauret, J., Lebedev, A., Lednicky, R., Lee, J. H., Li, X., Li, C., Li, W., Li, Y., Lidrych, J., Lin, T., Lisa, M. A., Liu, H., Liu, P., Liu, Y., Liu, F., Ljubicic, T., Llope, W. J., Lomnitz, M., Longacre, R. S., Luo, S., Luo, X., Ma, G. L., Ma, L., Ma, Y. G., Ma, R., Magdy, N., Majka, R., Mallick, D., Margetis, S., Markert, C., Matis, H. S., Meehan, K., Mei, J. C., Miller, Z. W., Minaev, N. G., Mioduszewski, S., Mishra, D., Mizuno, S., Mohanty, B., Mondal, M. M., Morozov, D. A., Mustafa, M. K., Nasim, M., Nayak, T. K., Nelson, J. M., Nie, M., Nigmatkulov, G., Niida, T., Nogach, L. V., Nonaka, T., Nurushev, S. B., Odyniec, G., Ogawa, A., Oh, K., Okorokov, V. A., Olvitt, D., Page, B. S., Pak, R., Pandit, Y., Panebratsev, Y., Pawlik, B., Pei, H., Perkins, C., Pile, P., Pluta, J., Poniatowska, K., Porter, J., Posik, M., Poskanzer, A. M., Pruthi, N. K., Przybycien, M., Putschke, J., Qiu, H., Quintero, A., Ramachandran, S., Ray, R. L., Reed, R., Rehbein, M. J., Ritter, H. G., Roberts, J. B., Rogachevskiy, O. V., Romero, J. L., Roth, J. D., Ruan, L., Rusnak, J., Rusnakova, O., Sahoo, N. R., Sahu, P. K., Salur, S., Sandweiss, J., Saur, M., Schambach, J., Schmah, A. M., Schmidke, W. B., Schmitz, N., Schweid, B. R., Seger, J., Sergeeva, M., Seyboth, P., Shah, N., Shahaliev, E., Shanmuganathan, P. V., Shao, M., Sharma, A., Sharma, M. K., Shen, W. Q., Shi, Z., Shi, S. S., Shou, Q. Y., Sichtermann, E. P., Sikora, R., Simko, M., Singha, S., Skoby, M. J., Smirnov, N., Smirnov, D., Solyst, W., Song, L., Sorensen, P., Spinka, H. M., Srivastava, B., Stanislaus, T. D. S., Strikhanov, M., Stringfellow, B., Sugiura, T., Sumbera, M., Summa, B., Sun, Y., Sun, X. M., Sun, X., Surrow, B., Svirida,

D. N., Tang, A. H., Tang, Z., Taranenko, A., Tarnowsky, T., Tawfik, A., Thäder, J., Thomas, J. H., Timmins, A. R., Tlusty, D., Todoroki, T., Tokarev, M., Trentalange, S., Tribble, R. E., Tribedy, P., Tripathy, S. K., Trzeciak, B. A., Tsai, O. D., Ullrich, T., Underwood, D. G., Upsal, I., Van Buren, G., van Nieuwenhuizen, G., Vasiliev, A. N., Videbæk, F., Vokal, S., Voloshin, S. A., Vossen, A., Wang, G., Wang, Y., Wang, F., Wang, Y., Webb, J. C., Webb, G., Wen, L., Westfall, G. D., Wieman, H., Wissink, S. W., Witt, R., Wu, Y., Xiao, Z. G., Xie, W., Xie, G., Xu, J., Xu, N., Xu, Q. H., Xu, Y. F., Xu, Z., Yang, Y., Yang, Q., Yang, C., Yang, S., Ye, Z., Ye, Z., Yi, L., Yip, K., Yoo, I.-K., Yu, N., Zbroszczyk, H., Zha, W., Zhang, Z., Zhang, X. P., Zhang, J. B., Zhang, S., Zhang, J., Zhang, Y., Zhang, J., Zhang, S., Zhao, J., Zhong, C., Zhou, L., Zhou, C., Zhu, X., Zhu, Z., and Zyzak, M. (2017). Bulk properties of the medium produced in relativistic heavy-ion collisions from the beam energy scan program. *Phys. Rev. C*, 96:044904. vii, 23, 27, 28, 29

[3] Adams, J., Aggarwal, M., Ahammed, Z., Amonett, J., Anderson, B., Arkhipkin, D., Averichev, G., Badyal, S., Bai, Y., Balewski, J., Barannikova, O., Barnby, L., Baudot, J., Bekele, S., Belaga, V., Bellingeri-Laurikainen, A., Bellwied, R., Berger, J., Bezverkhny, B., Bharadwaj, S., Bhasin, A., Bhati, A., Bhatia, V., Bichsel, H., Bielcik, J., Bielcikova, J., Billmeier, A., Bland, L., Blyth, C., Bonner, B., Botje, M., Boucham, A., Bouchet, J., Brandin, A., Bravar, A., Bystersky, M., Cadman, R., Cai, X., Caines, H., de la Barca Snchez, M. C., Castillo, J., Catu, O., Cebra, D., Chajecki, Z., Chaloupka, P., Chattopadhyay, S., Chen, H., Chen, Y., Cheng, J., Cherney, M., Chikanian, A., Christie, W., Coffin, J., Cormier, T., Cramer, J., Crawford, H., Das, D., Das, S., de Moura, M., Dedovich, T., Derevschikov, A., Didenko, L., Dietel, T., Dogra, S., Dong, W., Dong, X., Draper, J., Du, F., Dubey, A., Dunin, V., Dunlop, J., Mazumdar, M. D., Eckardt, V., Edwards, W., Efimov, L., Emelianov, V., Engelage, J., Eppley, G., Erazmus, B., Estienne, M., Fachini, P., Faivre, J., Fatemi, R., Fedorisin, J., Filimonov, K., Filip, P., Finch, E., Fine, V., Fisyak, Y., Fu, J., Gagliardi, C., Gaillard, L., Gans, J., Ganti, M., Geurts, F., Ghazikhanian, V., Ghosh, P., Gonzalez, J., Gos, H., Grachov, O., Grebenyuk, O., Grosnick, D., Guertin, S., Guo, Y., Gupta, A., Gutierrez, T., Hallman, T., Hamed, A.,

Hardtke, D., Harris, J., Heinz, M., Henry, T., Hepplemann, S., Hippolyte, B., Hirsch, A., Hjort, E., Hoffmann, G., Huang, H., Huang, S., Hughes, E., Humanic, T., Igo, G., Ishihara, A., Jacobs, P., Jacobs, W., Jedynak, M., Jiang, H., Jones, P., Judd, E., Kabana, S., Kang, K., Kaplan, M., Keane, D., Kechechyan, A., Khodyrev, V., Kiryluk, J., Kisiel, A., Kislov, E., Klay, J., Klein, S., Koetke, D., Kollegger, T., Kopytine, M., Kotchenda, L., Kramer, M., Kravtsov, P., Kravtsov, V., Krueger, K., Kuhn, C., Kulikov, A., Kumar, A., Kutuev, R., Kuznetsov, A., Lamont, M., Landgraf, J., Lange, S., Laue, F., Lauret, J., Lebedev, A., Lednicky, R., Lehocka, S., LeVine, M., Li, C., Li, Q., Li, Y., Lin, G., Lindenbaum, S., Lisa, M., Liu, F., Liu, H., Liu, L., Liu, Q., Liu, Z., Ljubicic, T., Llope, W., Long, H., Longacre, R., Lopez-Noriega, M., Love, W., Lu, Y., Ludlam, T., Lynn, D., Ma, G., Ma, J., Ma, Y., Magestro, D., Mahajan, S., Mahapatra, D., Majka, R., Mangotra, L., Manweiler, R., Margetis, S., Markert, C., Martin, L., Marx, J., Matis, H., Matulenko, Y., McClain, C., McShane, T., Meissner, F., Melnick, Y., Meschanin, A., Miller, M., Minaev, N., Mironov, C., Mischke, A., Mishra, D., Mitchell, J., Mohanty, B., Molnar, L., Moore, C., Morozov, D., Munhoz, M., Nandi, B., Nayak, S., Nayak, T., Nelson, J., Netrakanti, P., Nikitin, V., Nogach, L., Nurushev, S., Odyniec, G., Ogawa, A., Okorokov, V., Oldenburg, M., Olson, D., Pal, S., Panebratsev, Y., Panitkin, S., Pavlinov, A., Pawlak, T., Peitzmann, T., Perevoztchikov, V., Perkins, C., Peryt, W., Petrov, V., Phatak, S., Picha, R., Planinic, M., Pluta, J., Porile, N., Porter, J., Poskanzer, A., Potekhin, M., Potrebenikova, E., Potukuchi, B., Prindle, D., Pruneau, C., Putschke, J., Rakness, G., Raniwala, R., Raniwala, S., Ravel, O., Ray, R., Razin, S., Reichhold, D., Reid, J., Reinnarth, J., Renault, G., Retiere, F., Ridiger, A., Ritter, H., Roberts, J., Rogachevskiy, O., Romero, J., Rose, A., Roy, C., Ruan, L., Russcher, M., Sahoo, R., Sakrejda, I., Salur, S., Sandweiss, J., Sarsour, M., Savin, I., Sazhin, P., Schambach, J., Scharenberg, R., Schmitz, N., Seger, J., Seyboth, P., Shahaliev, E., Shao, M., Shao, W., Sharma, M., Shen, W., Shestermanov, K., Shimanskiy, S., Sichtermann, E., Simon, F., Singaraju, R., Smirnov, N., Snellings, R., Sood, G., Sorensen, P., Sowinski, J., Speltz, J., Spinka, H., Srivastava, B., Stadnik, A., Stanislaus, T., Stock, R., Stolpovsky, A., Strikhanov, M., Stringfellow, B., Suaide, A., Sugarbaker, E., Suire, C., Sumbera, M., Surrow, B., Swanger, M., Symons, T., de Toledo, A. S., Tai, A., Takahashi, J., Tang, A., Tarnowsky, T., Thein, D., Thomas, J., Timoshenko, S., Tokarev, M., Trentalange, S., Tribble, R., Tsai, O., Ulery, J., Ullrich, T., Underwood, D., Buren, G. V., van Leeuwen, M., Molen, A. V., Varma, R., Vasilevski, I., Vasiliev, A., Vernet, R., Vigdor, S., Viyogi, Y., Vokal, S., Voloshin, S., Waggoner, W., Wang, F., Wang, G., Wang, G., Wang, X., Wang, Y., Wang, Y., Wang, Z., Ward, H., Watson, J., Webb, J., Westfall, G., Wetzler, A., Whitten, C., Wieman, H., Wissink, S., Witt, R., Wood, J., Wu, J., Xu, N., Xu, Z., Xu, Z., Yamamoto, E., Yepes, P., Yurevich, V., Zborovsky, I., Zhang, H., Zhang, W., Zhang, Y., Zhang, Z., Zoulkarneev, R., Zoulkarneeva, Y., and Zubarev, A. (2005). Experimental and theoretical challenges in the search for the quarkgluon plasma: The star collaboration's critical assessment of the evidence from rhic collisions. *Nuclear Physics A*, 757(1):102 – 183. First Three Years of Operation of RHIC. 1

[4] Adare, A., Afanasiev, S., Aidala, C., Ajitanand, N. N., Akiba, Y., Akimoto, R., Al-Bataineh, H., Alexander, J., Alfred, M., Al-Jamel, A., Al-Ta'ani, H., Angerami, A., Aoki, K., Apadula, N., Aphecetche, L., Aramaki, Y., Armendariz, R., Aronson, S. H., Asai, J., Asano, H., Aschenauer, E. C., Atomssa, E. T., Averbeck, R., Awes, T. C., Azmoun, B., Babintsev, V., Bai, M., Bai, X., Baksay, G., Baksay, L., Baldisseri, A., Bandara, N. S., Bannier, B., Barish, K. N., Barnes, P. D., Bassalleck, B., Basye, A. T., Bathe, S., Batsouli, S., Baublis, V., Bauer, F., Baumann, C., Baumgart, S., Bazilevsky, A., Beaumier, M., Beckman, S., Belikov, S., Belmont, R., Bennett, R., Berdnikov, A., Berdnikov, Y., Bhom, J. H., Bickley, A. A., Bjorndal, M. T., Black, D., Blau, D. S., Boissevain, J. G., Bok, J. S., Borel, H., Boyle, K., Brooks, M. L., Brown, D. S., Bryslawskyj, J., Bucher, D., Buesching, H., Bumazhnov, V., Bunce, G., Burward-Hoy, J. M., Butsyk, S., Campbell, S., Caringi, A., Castera, P., Chai, J.-S., Chang, B. S., Charvet, J.-L., Chen, C.-H., Chernichenko, S., Chi, C. Y., Chiba, J., Chiu, M., Choi, I. J., Choi, J. B., Choi, S., Choudhury, R. K., Christiansen, P., Chujo, T., Chung, P., Churyn, A., Chvala, O., Cianciolo, V., Citron, Z., Cleven, C. R., Cobigo, Y., Cole, B. A., Comets, M. P., Conesa del Valle, Z., Connors, M., Constantin, P., Cronin, N., Crossette, N., Csanád, M., Csörgő, T., Dahms, T., Dairaku, S., Danchev, I., Danley, T. W., Das, K., Datta, A., Daugherity, M. S., David, G., Dayananda, M. K., Deaton, M. B., DeBlasio, K., Dehmelt, K., Delagrange,

H., Denisov, A., d'Enterria, D., Deshpande, A., Desmond, E. J., Dharmawardane, K. V., Dietzsch, O., Ding, L., Dion, A., Diss, P. B., Do, J. H., Donadelli, M., D'Orazio, L., Drachenberg, J. L., Drapier, O., Drees, A., Drees, K. A., Dubey, A. K., Durham, J. M., Durum, A., Dutta, D., Dzhordzhadze, V., Edwards, S., Efremenko, Y. V., Egdemir, J., Ellinghaus, F., Emam, W. S., Engelmore, T., Enokizono, A., En'yo, H., Espagnon, B., Esumi, S., Eyser, K. O., Fadem, B., Feege, N., Fields, D. E., Finger, M., Finger, M., Fleuret, F., Fokin, S. L., Forestier, B., Fraenkel, Z., Frantz, J. E., Franz, A., Frawley, A. D., Fujiwara, K., Fukao, Y., Fung, S.-Y., Fusayasu, T., Gadrat, S., Gainey, K., Gal, C., Gallus, P., Garg, P., Garishvili, A., Garishvili, I., Gastineau, F., Ge, H., Germain, M., Giordano, F., Glenn, A., Gong, H., Gong, X., Gonin, M., Gosset, J., Goto, Y., Granier de Cassagnac, R., Grau, N., Greene, S. V., Grim, G., Grosse Perdekamp, M., Gu, Y., Gunji, T., Guo, L., Guragain, H., Gustafsson, H.-A., Hachiya, T., Hadj Henni, A., Haegemann, C., Haggerty, J. S., Hagiwara, M. N., Hahn, K. I., Hamagaki, H., Hamblen, J., Hamilton, H. F., Han, R., Han, S. Y., Hanks, J., Harada, H., Hartouni, E. P., Haruna, K., Harvey, M., Hasegawa, S., Haseler, T. O. S., Hashimoto, K., Haslum, E., Hasuko, K., Hayano, R., Hayashi, S., He, X., Heffner, M., Hemmick, T. K., Hester, T., Heuser, J. M., Hiejima, H., Hill, J. C., Hobbs, R., Hohlmann, M., Hollis, R. S., Holmes, M., Holzmann, W., Homma, K., Hong, B., Horaguchi, T., Hori, Y., Hornback, D., Hoshino, T., Hotvedt, N., Huang, J., Huang, S., Hur, M. G., Ichihara, T., Ichimiya, R., Iinuma, H., Ikeda, Y., Imai, K., Imazu, Y., Imrek, J., Inaba, M., Inoue, Y., Iordanova, A., Isenhower, D., Isenhower, L., Ishihara, M., Isinhue, A., Isobe, T., Issah, M., Isupov, A., Ivanishchev, D., Iwanaga, Y., Jacak, B. V., Javani, M., Jeon, S. J., Jezghani, M., Jia, J., Jiang, X., Jin, J., Jinnouchi, O., Johnson, B. M., Jones, T., Joo, K. S., Jouan, D., Jumper, D. S., Kajihara, F., Kametani, S., Kamihara, N., Kamin, J., Kanda, S., Kaneta, M., Kaneti, S., Kang, B. H., Kang, J. H., Kang, J. S., Kanou, H., Kapustinsky, J., Karatsu, K., Kasai, M., Kawagishi, T., Kawall, D., Kawashima, M., Kazantsev, A. V., Kelly, S., Kempel, T., Key, J. A., Khachatryan, V., Khandai, P. K., Khanzadeev, A., Kijima, K. M., Kikuchi, J., Kim, A., Kim, B. I., Kim, C., Kim, D. H., Kim, D. J., Kim, E., Kim, E.-J., Kim, G. W., Kim, H. J., Kim, K.-B., Kim, M., Kim, Y.-J., Kim, Y. K., Kim, Y.-S., Kimelman, B., Kinney, E., Kiss, A., Kistenev, E., Kitamura, R., Kiyomichi, A., Klatsky, J., Klay, J., Klein-Boesing, C., Kleinjan, D., Kline, P., Koblesky, T., Kochenda, L., Kochetkov, V., Kofarago, M., Komatsu, Y., Komkov, B., Konno, M., Koster, J., Kotchetkov, D., Kotov, D., Kozlov, A., Král, A., Kravitz, A., Krizek, F., Kroon, P. J., Kubart, J., Kunde, G. J., Kurihara, N., Kurita, K., Kurosawa, M., Kweon, M. J., Kwon, Y., Kyle, G. S., Lacey, R., Lai, Y. S., Lajoie, J. G., Lebedev, A., Le Bornec, Y., Leckey, S., Lee, B., Lee, D. M., Lee, G. H., Lee, J., Lee, K. B., Lee, K. S., Lee, M. K., Lee, S., Lee, S. H., Lee, S. R., Lee, T., Leitch, M. J., Leite, M. A. L., Leitgab, M., Lenzi, B., Lewis, B., Li, X., Li, X. H., Lichtenwalner, P., Liebing, P., Lim, H., Lim, S. H., Linden Levy, L. A., Liška, T., Litvinenko, A., Liu, H., Liu, M. X., Love, B., Lynch, D., Maguire, C. F., Makdisi, Y. I., Makek, M., Malakhov, A., Malik, M. D., Manion, A., Manko, V. I., Mannel, E., Mao, Y., Maruyama, T., Mašek, L., Masui, H., Masumoto, S., Matathias, F., McCain, M. C., McCumber, M., McGaughey, P. L., McGlinchey, D., McKinney, C., Means, N., Meles, A., Mendoza, M., Meredith, B., Miake, Y., Mibe, T., Midori, J., Mignerey, A. C., Mikeš, P., Miki, K., Miller, T. E., Milov, A., Mioduszewski, S., Mishra, D. K., Mishra, G. C., Mishra, M., Mitchell, J. T., Mitrovski, M., Miyachi, Y., Miyasaka, S., Mizuno, S., Mohanty, A. K., Mohapatra, S., Montuenga, P., Moon, H. J., Moon, T., Morino, Y., Morreale, A., Morrison, D. P., Moskowitz, M., Moss, J. M., Motschwiller, S., Moukhanova, T. V., Mukhopadhyay, D., Murakami, T., Murata, J., Mwai, A., Nagae, T., Nagamiya, S., Nagashima, K., Nagata, Y., Nagle, J. L., Naglis, M., Nagy, M. I., Nakagawa, I., Nakagomi, H., Nakamiya, Y., Nakamura, K. R., Nakamura, T., Nakano, K., Nam, S., Nattrass, C., Nederlof, A., Netrakanti, P. K., Newby, J., Nguyen, M., Nihashi, M., Niida, T., Nishimura, S., Norman, B. E., Nouicer, R., Novák, T., Novitzky, N., Nukariya, A., Nyanin, A. S., Nystrand, J., Oakley, C., Obayashi, H., O'Brien, E., Oda, S. X., Ogilvie, C. A., Ohnishi, H., Oide, H., Ojha, I. D., Oka, M., Okada, K., Omiwade, O. O., Onuki, Y., Orjuela Koop, J. D., Osborn, J. D., Oskarsson, A., Otterlund, I., Ouchida, M., Ozawa, K., Pak, R., Pal, D., Palounek, A. P. T., Pantuev, V., Papavassiliou, V., Park, B. H., Park, I. H., Park, J., Park, J. S., Park, S., Park, S. K., Park, W. J., Pate, S. F., Patel, L., Patel, M., Pei, H., Peng, J.-C., Pereira, H., Perepelitsa, D. V., Perera, G. D. N., Peresedov, V., Peressounko, D., Perry, J., Petti, R., Pinkenburg, C., Pinson, R., Pisani, R. P., Proissl, M., Purschke, M. L., Purwar, A. K., Qu, H., Rak, J., Rakotozafindrabe, A., Ramson, B. J., Ravinovich, I., Read, K. F., Rembeczki, S., Reuter, M., Reygers, K., Reynolds, D., Riabov, V., Riabov, Y., Richardson, E., Rinn, T., Riveli, N., Roach, D., Roche, G., Rolnick, S. D., Romana, A., Rosati, M., Rosen, C. A., Rosendahl, S. S. E., Rosnet, P., Rowan, Z., Rubin, J. G., Rukoyatkin, P., Ružička, P., Rykov, V. L., Ryu, M. S., Ryu, S. S., Sahlmueller, B., Saito, N., Sakaguchi, T., Sakai, S., Sakashita, K., Sakata, H., Sako, H., Samsonov, V., Sano, M., Sano, S., Sarsour, M., Sato, H. D., Sato, S., Sato, T., Sawada, S., Schaefer, B., Schmoll, B. K., Sedgwick, K., Seele, J., Seidl, R., Sekiguchi, Y., Semenov, V., Sen, A., Seto, R., Sett, P., Sexton, A., Sharma, D., Shaver, A., Shea, T. K., Shein, I., Shevel, A., Shibata, T.-A., Shigaki, K., Shimomura, M., Shohjoh, T., Shoji, K., Shukla, P., Sickles, A., Silva, C. L., Silvermyr, D., Silvestre, C., Sim, K. S., Singh, B. K., Singh, C. P., Singh, V., Skolnik, M., Skutnik, S., Slunečka, M., Smith, W. C., Snowball, M., Solano, S., Soldatov, A., Soltz, R. A., Sondheim, W. E., Sorensen, S. P., Sourikova, I. V., Staley, F., Stankus, P. W., Steinberg, P., Stenlund, E., Stepanov, M., Ster, A., Stoll, S. P., Stone, M. R., Sugitate, T., Suire, C., Sukhanov, A., Sullivan, J. P., Sumita, T., Sun, J., Sziklai, J., Tabaru, T., Takagi, S., Takagui, E. M., Takahara, A., Taketani, A., Tanabe, R., Tanaka, K. H., Tanaka, Y., Taneja, S., Tanida, K., Tannenbaum, M. J., Tarafdar, S., Taranenko, A., Tarján, P., Tennant, E., Themann, H., Thomas, D., Thomas, T. L., Tieulent, R., Timilsina, A., Todoroki, T., Togawa, M., Toia, A., Tojo, J., Tomášek, L., Tomášek, M., Torii, H., Towell, C. L., Towell, R., Towell, R. S., Tram, V.-N., Tserruya, I., Tsuchimoto, Y., Tsuji, T., Tuli, S. K., Tydesjö, H., Tyurin, N., Vale, C., Valle, H., van Hecke, H. W., Vargyas, M., Vazquez-Zambrano, E., Veicht, A., Velkovska, J., Vértesi, R., Vinogradov, A. A., Virius, M., Voas, B., Vossen, A., Vrba, V., Vznuzdaev, E., Wagner, M., Walker, D., Wang, X. R., Watanabe, D., Watanabe, K., Watanabe, Y., Watanabe, Y. S., Wei, F., Wei, R., Wessels, J., Whitaker, S., White, A. S., White, S. N., Willis, N., Winter, D., Wolin, S., Woody, C. L., Wright, R. M., Wysocki, M., Xia, B., Xie, W., Xue, L., Yalcin, S., Yamaguchi, Y. L., Yamaura, K., Yang, R., Yanovich, A., Yasin, Z., Ying, J., Yokkaichi, S., Yoo, J. H., Yoon, I., You, Z., Young, G. R., Younus, I., Yu, H., Yushmanov, I. E., Zajc, W. A., Zaudtke, O., Zelenski, A., Zhang, C., Zhou, S., Zimamyi, J., Zolin, L., and Zou, L. (2016). Transverse energy production and charged-particle multiplicity at midrapidity in various systems from $\sqrt{s_{NN}} = 7.7$ to 200 gev. *Phys. Rev. C*, 93:024901. vii, viii, 5, 22, 23, 33, 37, 39

[5] Adare, A., Afanasiev, S., Aidala, C., Ajitanand, N. N., Akiba, Y., Al-Bataineh, H., Alexander, J., Al-Jamel, A., Aoki, K., Aphecetche, L., and et al. (2007). Scaling Properties of Azimuthal Anisotropy in Au+Au and Cu+Cu Collisions at s_{NN}=200GeV. *Physical Review Letters*, 98(16):162301. vi, 15, 16

[6] Adler, S. S., Afanasiev, S., Aidala, C., Ajitanand, N. N., Akiba, Y., Al-Jamel, A., Alexander, J., Aoki, K., Aphecetche, L., Armendariz, R., Aronson, S. H., Averbeck, R., Awes, T. C., Azmoun, B., Babintsev, V., Baldisseri, A., Barish, K. N., Barnes, P. D., Bassalleck, B., Bathe, S., Batsouli, S., Baublis, V., Bauer, F., Bazilevsky, A., Belikov, S., Bennett, R., Berdnikov, Y., Bjorndal, M. T., Boissevain, J. G., Borel, H., Boyle, K., Brooks, M. L., Brown, D. S., Bruner, N., Bucher, D., Buesching, H., Bumazhnov, V., Bunce, G., Burward-Hoy, J. M., Butsyk, S., Camard, X., Campbell, S., Chai, J.-S., Chand, P., Chang, W. C., Chernichenko, S., Chi, C. Y., Chiba, J., Chiu, M., Choi, I. J., Choudhury, R. K., Chujo, T., Cianciolo, V., Cleven, C. R., Cobigo, Y., Cole, B. A., Comets, M. P., Constantin, P., Csanád, M., Csörgő, T., Cussonneau, J. P., Dahms, T., Das, K., David, G., Deák, F., Delagrange, H., Denisov, A., d'Enterria, D., Deshpande, A., Desmond, E. J., Devismes, A., Dietzsch, O., Dion, A., Drachenberg, J. L., Drapier, O., Drees, A., Dubey, A. K., Durum, A., Dutta, D., Dzhordzhadze, V., Efremenko, Y. V., Egdemir, J., Enokizono, A., En'yo, H., Espagnon, B., Esumi, S., Fields, D. E., Finck, C., Fleuret, F., Fokin, S. L., Forestier, B., Fox, B. D., Fraenkel, Z., Frantz, J. E., Franz, A., Frawley, A. D., Fukao, Y., Fung, S.-Y., Gadrat, S., Gastineau, F., Germain, M., Glenn, A., Gonin, M., Gosset, J., Goto, Y., Granier de Cassagnac, R., Grau, N., Greene, S. V., Grosse Perdekamp, M., Gunji, T., Gustafsson, H.-A., Hachiya, T., Hadj Henni, A., Haggerty, J. S., Hagiwara, M. N., Hamagaki, H., Hansen, A. G., Harada, H., Hartouni, E. P., Haruna, K., Harvey, M., Haslum, E., Hasuko, K., Hayano, R., He, X., Heffner, M., Hemmick, T. K., Heuser, J. M., Hidas, P., Hiejima, H., Hill, J. C., Hobbs, R., Holmes, M., Holzmann, W., Homma, K., Hong, B., Hoover, A., Horaguchi, T., Hur, M. G., Ichihara, T., Iinuma, H., Ikonnikov, V. V., Imai, K., Inaba, M., Inuzuka, M., Isenhower, D., Isenhower, L., Ishihara, M., Isobe, T., Issah, M., Isupov, A., Jacak, B. V., Jia, J., Jin, J., Jinnouchi, O., Johnson, B. M., Johnson, S. C., Joo, K. S., Jouan, D., Kajihara, F., Kametani,

S., Kamihara, N., Kaneta, M., Kang, J. H., Katou, K., Kawabata, T., Kawagishi, T., Kazantsev, A. V., Kelly, S., Khachaturov, B., Khanzadeev, A., Kikuchi, J., Kim, D. J., Kim, E., Kim, E. J., Kim, G.-B., Kim, H. J., Kim, Y.-S., Kinney, E., Kiss, A., Kistenev, E., Kiyomichi, A., Klein-Boesing, C., Kobayashi, H., Kochenda, L., Kochetkov, V., Kohara, R., Komkov, B., Konno, M., Kotchetkov, D., Kozlov, A., Kroon, P. J., Kuberg, C. H., Kunde, G. J., Kurihara, N., Kurita, K., Kweon, M. J., Kwon, Y., Kyle, G. S., Lacey, R., Lajoie, J. G., Lebedev, A., Le Bornec, Y., Leckey, S., Lee, D. M., Lee, M. K., Leitch, M. J., Leite, M. A. L., Li, X. H., Lim, H., Litvinenko, A., Liu, M. X., Maguire, C. F., Makdisi, Y. I., Malakhov, A., Malik, M. D., Manko, V. I., Mao, Y., Martinez, G., Masui, H., Matathias, F., Matsumoto, T., McCain, M. C., McGaughey, P. L., Miake, Y., Miller, T. E., Milov, A., Mioduszewski, S., Mishra, G. C., Mitchell, J. T., Mohanty, A. K., Morrison, D. P., Moss, J. M., Moukhanova, T. V., Mukhopadhyay, D., Muniruzzaman, M., Murata, J., Nagamiya, S., Nagata, Y., Nagle, J. L., Naglis, M., Nakamura, T., Newby, J., Nguyen, M., Norman, B. E., Nyanin, A. S., Nystrand, J., O'Brien, E., Ogilvie, C. A., Ohnishi, H., Ojha, I. D., Okada, K., Omiwade, O. O., Oskarsson, A., Otterlund, I., Oyama, K., Ozawa, K., Pal, D., Palounek, A. P. T., Pantuev, V., Papavassiliou, V., Park, J., Park, W. J., Pate, S. F., Pei, H., Penev, V., Peng, J.-C., Pereira, H., Peresedov, V., Peressounko, D., Pierson, A., Pinkenburg, C., Pisani, R. P., Purschke, M. L., Purwar, A. K., Qu, H., Qualls, J. M., Rak, J., Ravinovich, I., Read, K. F., Reuter, M., Reygers, K., Riabov, V., Riabov, Y., Roche, G., Romana, A., Rosati, M., Rosendahl, S. S. E., Rosnet, P., Rukoyatkin, P., Rykov, V. L., Ryu, S. S., Sahlmueller, B., Saito, N., Sakaguchi, T., Sakai, S., Samsonov, V., Sanfratello, L., Santo, R., Sarsour, M., Sato, H. D., Sato, S., Sawada, S., Schutz, Y., Semenov, V., Seto, R., Sharma, D., Shea, T. K., Shein, I., Shibata, T.-A., Shigaki, K., Shimomura, M., Shohjoh, T., Shoji, K., Sickles, A., Silva, C. L., Silvermyr, D., Sim, K. S., Singh, C. P., Singh, V., Skutnik, S., Smith, W. C., Soldatov, A., Soltz, R. A., Sondheim, W. E., Sorensen, S. P., Sourikova, I. V., Staley, F., Stankus, P. W., Stenlund, E., Stepanov, M., Ster, A., Stoll, S. P., Sugitate, T., Suire, C., Sullivan, J. P., Sziklai, J., Tabaru, T., Takagi, S., Takagui, E. M., Taketani, A., Tanaka, K. H., Tanaka, Y., Tanida, K., Tannenbaum, M. J., Taranenko, A., Tarján, P., Thomas, T. L., Togawa, M., Tojo, J., Torii, H., Towell, R. S., Tram, V.-N., Tserruya, I., Tsuchimoto, Y., Tuli, S. K., Tydesjö, H., Tyurin, N., Uam, T. J., Vale, C., Valle, H., van Hecke, H. W., Velkovska, J., Velkovsky, M., Vértesi, R., Veszprémi, V., Vinogradov, A. A., Volkov, M. A., Vznuzdaev, E., Wagner, M., Wang, X. R., Watanabe, Y., Wessels, J., White, S. N., Willis, N., Winter, D., Wohn, F. K., Woody, C. L., Wysocki, M., Xie, W., Yanovich, A., Yokkaichi, S., Young, G. R., Younus, I., Yushmanov, I. E., Zajc, W. A., Zaudtke, O., Zhang, C., Zhou, S., Zimányi, J., Zolin, L., and Zong, X. (2014). Transverse-energy distributions at midrapidity in $p+p$, $d+$Au, and Au $+$ Au collisions at $\sqrt{s_{\mathrm{NN}}} = 62.4$˘200 gev and implications for particle-production models. *Phys. Rev. C*, 89:044905. 20

[7] Adler, S. S., Afanasiev, S., Aidala, C., Ajitanand, N. N., Akiba, Y., Alexander, J., Amirikas, R., Aphecetche, L., Aronson, S. H., Averbeck, R., Awes, T. C., Azmoun, R., Babintsev, V., Baldisseri, A., Barish, K. N., Barnes, P. D., Bassalleck, B., Bathe, S., Batsouli, S., Baublis, V., Bazilevsky, A., Belikov, S., Berdnikov, Y., Bhagavatula, S., Boissevain, J. G., Borel, H., Borenstein, S., Brooks, M. L., Brown, D. S., Bruner, N., Bucher, D., Buesching, H., Bumazhnov, V., Bunce, G., Burward-Hoy, J. M., Butsyk, S., Camard, X., Chai, J.-S., Chand, P., Chang, W. C., Chernichenko, S., Chi, C. Y., Chiba, J., Chiu, M., Choi, I. J., Choi, J., Choudhury, R. K., Chujo, T., Cianciolo, V., Cobigo, Y., Cole, B. A., Constantin, P., d'Enterria, D. G., David, G., Delagrange, H., Denisov, A., Deshpande, A., Desmond, E. J., Dietzsch, O., Drapier, O., Drees, A., Rietz, R. d., Durum, A., Dutta, D., Efremenko, Y. V., Chenawi, K. E., Enokizono, A., En'yo, H., Esumi, S., Ewell, L., Fields, D. E., Fleuret, F., Fokin, S. L., Fox, B. D., Fraenkel, Z., Frantz, J. E., Franz, A., Frawley, A. D., Fung, S.-Y., Garpman, S., Ghosh, T. K., Glenn, A., Gogiberidze, G., Gonin, M., Gosset, J., Goto, Y., Cassagnac, R. G. d., Grau, N., Greene, S. V., Perdekamp, M. G., Guryn, W., Gustafsson, H.-A., Hachiya, T., Haggerty, J. S., Hamagaki, H., Hansen, A. G., Hartouni, E. P., Harvey, M., Hayano, R., He, X., Heffner, M., Hemmick, T. K., Heuser, J. M., Hibino, M., Hill, J. C., Holzmann, W., Homma, K., Hong, B., Hoover, A., Ichihara, T., Ikonnikov, V. V., Imai, K., Isenhower, D., Ishihara, M., Issah, M., Isupov, A., Jacak, B. V., Jang, W. Y., Jeong, Y., Jia, J., Jinnouchi, O., Johnson, B. M., Johnson, S. C., Joo, K. S., Jouan, D., Kametani, S., Kamihara, N., Kang, J. H., Kapoor, S. S., Katou, K., Kelly, S., Khachaturov, B., Khanzadeev, A.,

Kikuchi, J., Kim, D. H., Kim, D. J., Kim, D. W., Kim, E., Kim, G.-B., Kim, H. J., Kistenev, E., Kiyomichi, A., Kiyoyama, K., Klein-Boesing, C., Kobayashi, H., Kochenda, L., Kochetkov, V., Koehler, D., Kohama, T., Kopytine, M., Kotchetkov, D., Kozlov, A., Kroon, P. J., Kuberg, C. H., Kurita, K., Kuroki, Y., Kweon, M. J., Kwon, Y., Kyle, G. S., Lacey, R., Ladygin, V., Lajoie, J. G., Lebedev, A., Leckey, S., Lee, D. M., Lee, S., Leitch, M. J., Li, X. H., Lim, H., Litvinenko, A., Liu, M. X., Liu, Y., Maguire, C. F., Makdisi, Y. I., Malakhov, A., Manko, V. I., Mao, Y., Martinez, G., Marx, M. D., Masui, H., Matathias, F., Matsumoto, T., McGaughey, P. L., Melnikov, E., Mendenhall, M., Messer, F., Miake, Y., Milan, J., Miller, T. E., Milov, A., Mioduszewski, S., Mischke, R. E., Mishra, G. C., Mitchell, J. T., Mohanty, A. K., Morrison, D. P., Moss, J. M., Mühlbacher, F., Mukhopadhyay, D., Muniruzzaman, M., Murata, J., Nagamiya, S., Nagle, J. L., Nakamura, T., Nandi, B. K., Nara, M., Newby, J., Nilsson, P., Nyanin, A. S., Nystrand, J., O'Brien, E., Ogilvie, C. A., Ohnishi, H., Ojha, I. D., Okada, K., Ono, M., Onuchin, V., Oskarsson, A., Otterlund, I., Oyama, K., Ozawa, K., Pal, D., Palounek, A. P. T., Pantuev, V. S., Papavassiliou, V., Park, J., Parmar, A., Pate, S. F., Peitzmann, T., Peng, J.-C., Peresedov, V., Pinkenburg, C., Pisani, R. P., Plasil, F., Purschke, M. L., Purwar, A. K., Rak, J., Ravinovich, I., Read, K. F., Reuter, M., Reygers, K., Riabov, V., Riabov, Y., Roche, G., Romana, A., Rosati, M., Rosnet, P., Ryu, S. S., Sadler, M. E., Saito, N., Sakaguchi, T., Sakai, M., Sakai, S., Samsonov, V., Sanfratello, L., Santo, R., Sato, H. D., Sato, S., Sawada, S., Schutz, Y., Semenov, V., Seto, R., Shaw, M. R., Shea, T. K., Shibata, T.-A., Shigaki, K., Shiina, T., Silva, C. L., Silvermyr, D., Sim, K. S., Singh, C. P., Singh, V., Sivertz, M., Soldatov, A., Soltz, R. A., Sondheim, W. E., Sorensen, S. P., Sourikova, I. V., Staley, F., Stankus, P. W., Stenlund, E., Stepanov, M., Ster, A., Stoll, S. P., Sugitate, T., Sullivan, J. P., Takagui, E. M., Taketani, A., Tamai, M., Tanaka, K. H., Tanaka, Y., Tanida, K., Tannenbaum, M. J., Tarján, P., Tepe, J. D., Thomas, T. L., Tojo, J., Torii, H., Towell, R. S., Tserruya, I., Tsuruoka, H., Tuli, S. K., Tydesjö, H., Tyurin, N., Hecke, H. W. v., Velkovska, J., Velkovsky, M., Villatte, L., Vinogradov, A. A., Volkov, M. A., Vznuzdaev, E., Wang, X. R., Watanabe, Y., White, S. N., Wohn, F. K., Woody, C. L., Xie, W., Yang, Y., Yanovich, A., Yokkaichi, S., Young, G. R., Yushmanov, I. E., Zajc, W. A., Zhang, C., Zhou, S., Zhou, S. J., and Zolin, L. (2005). Systematic studies of the centrality and $\sqrt{s_{NN}}$ dependence of the $de_T/d\eta$ and $dn_{\mathrm{ch}}/d\eta$ in heavy ion collisions at midrapidity. *Phys. Rev. C*, 71:034908. 21

[8] Aitchison, I. and Hey, A. (2003). *Gauge Theories in Particle Physics, Volume II: QCD and the Electroweak Theory, Third Edition.* Graduate Student Series in Physics. CRC Press. 3

[9] Anderson, M. et al. (2003). The Star time projection chamber: A Unique tool for studying high multiplicity events at RHIC. *Nucl. Instrum. Meth.*, A499:659–678. vii, 25, 26

[10] Ayala, A. (2016). Hadronic matter at the edge: A survey of some theoretical approaches to the physics of the qcd phase diagram. *Journal of Physics: Conference Series*, 761(1):012066. vi, 5, 6

[11] Bali, G. S. (2001). QCD forces and heavy quark bound states. *Phys. Rept.*, 343:1–136. 4

[12] Behera, N. K., Sahoo, R., and Nandi, B. K. (2013). Constituent Quark Scaling of Strangeness Enhancement in Heavy-Ion Collisions. *Adv. High Energy Phys.*, 2013:273248. 16

[13] Bethe, H. A. and Ashkin, J. (1953). Passage of radiations through matter experimental nuclear physics vol 1 ed e segre. 24

[14] Bjorken, J. D. (1983). Highly relativistic nucleus-nucleus collisions: The central rapidity region. *Phys. Rev. D*, 27:140–151. 13

[15] Bratkovskaya, E.L., Moreau, P., Palmese, A., Cassing, W., Seifert, E., and Steinert, T. (2018). Signatures of chiral symmetry restoration and its survival throughout the hadronic phase interactions. *EPJ Web Conf.*, 171:02004. 16

[16] Chatrchyan, S., Khachatryan, V., Sirunyan, A. M., Tumasyan, A., Adam, W., Bergauer, T., Dragicevic, M., Erö, J., Fabjan, C., Friedl, M., Frühwirth, R., Ghete, V. M., Hammer, J., Hörmann, N., Hrubec, J., Jeitler, M., Kiesenhofer, W., Knünz, V., Krammer, M., Liko, D., Mikulec, I., Pernicka, M., Rahbaran, B., Rohringer, C., Rohringer, H., Schöfbeck, R.,

Strauss, J., Taurok, A., Wagner, P., Waltenberger, W., Walzel, G., Widl, E., Wulz, C.-E., Mossolov, V., Shumeiko, N., Suarez Gonzalez, J., Bansal, S., Cornelis, T., De Wolf, E. A., Janssen, X., Luyckx, S., Maes, T., Mucibello, L., Ochesanu, S., Roland, B., Rougny, R., Selvaggi, M., Staykova, Z., Van Haevermaet, H., Van Mechelen, P., Van Remortel, N., Van Spilbeeck, A., Blekman, F., Blyweert, S., D'Hondt, J., Gonzalez Suarez, R., Kalogeropoulos, A., Maes, M., Olbrechts, A., Van Doninck, W., Van Mulders, P., Van Onsem, G. P., Villella, I., Clerbaux, B., De Lentdecker, G., Dero, V., Gay, A. P. R., Hreus, T., Léonard, A., Marage, P. E., Reis, T., Thomas, L., Vander Velde, C., Vanlaer, P., Wang, J., Adler, V., Beernaert, K., Cimmino, A., Costantini, S., Garcia, G., Grunewald, M., Klein, B., Lellouch, J., Marinov, A., Mccartin, J., Ocampo Rios, A. A., Ryckbosch, D., Strobbe, N., Thyssen, F., Tytgat, M., Verwilligen, P., Walsh, S., Yazgan, E., Zaganidis, N., Basegmez, S., Bruno, G., Castello, R., Ceard, L., Delaere, C., du Pree, T., Favart, D., Forthomme, L., Giammanco, A., Hollar, J., Lemaitre, V., Liao, J., Militaru, O., Nuttens, C., Pagano, D., Pin, A., Piotrzkowski, K., Schul, N., Vizan Garcia, J. M., Beliy, N., Caebergs, T., Daubie, E., Hammad, G. H., Alves, G. A., Correa Martins Junior, M., De Jesus Damiao, D., Martins, T., Pol, M. E., Souza, M. H. G., Aldá Júnior, W. L., Carvalho, W., Custódio, A., Da Costa, E. M., De Oliveira Martins, C., Fonseca De Souza, S., Matos Figueiredo, D., Mundim, L., Nogima, H., Oguri, V., Prado Da Silva, W. L., Santoro, A., Soares Jorge, L., Sznajder, A., Bernardes, C. A., Dias, F. A., Fernandez Perez Tomei, T. R., Gregores, E. M., Lagana, C., Marinho, F., Mercadante, P. G., Novaes, S. F., Padula, S. S., Genchev, V., Iaydjiev, P., Piperov, S., Rodozov, M., Stoykova, S., Sultanov, G., Tcholakov, V., Trayanov, R., Vutova, M., Dimitrov, A., Hadjiiska, R., Kozhuharov, V., Litov, L., Pavlov, B., Petkov, P., Bian, J. G., Chen, G. M., Chen, H. S., Jiang, C. H., Liang, D., Liang, S., Meng, X., Tao, J., Wang, J., Wang, X., Wang, Z., Xiao, H., Xu, M., Zang, J., Zhang, Z., Asawatangtrakuldee, C., Ban, Y., Guo, S., Guo, Y., Li, W., Liu, S., Mao, Y., Qian, S. J., Teng, H., Wang, S., Zhu, B., Zou, W., Avila, C., Gomez, J. P., Gomez Moreno, B., Osorio Oliveros, A. F., Sanabria, J. C., Godinovic, N., Lelas, D., Plestina, R., Polic, D., Puljak, I., Antunovic, Z., Kovac, M., Brigljevic, V., Duric, S., Kadija, K., Luetic, J., Morovic, S., Attikis, A., Galanti, M., Mavromanolakis, G., Mousa, J., Nicolaou, C., Ptochos, F., Razis, P. A., Finger, M., Finger, M., Assran,

Y., Elgammal, S., Ellithi Kamel, A., Khalil, S., Mahmoud, M. A., Radi, A., Kadastik, M., Müntel, M., Raidal, M., Rebane, L., Tiko, A., Azzolini, V., Eerola, P., Fedi, G., Voutilainen, M., Härkönen, J., Heikkinen, A., Karimäki, V., Kinnunen, R., Kortelainen, M. J., Lampén, T., Lassila-Perini, K., Lehti, S., Lindén, T., Luukka, P., Mäenpää, T., Peltola, T., Tuominen, E., Tuominiemi, J., Tuovinen, E., Ungaro, D., Wendland, L., Banzuzi, K., Karjalainen, A., Korpela, A., Tuuva, T., Besancon, M., Choudhury, S., Dejardin, M., Denegri, D., Fabbro, B., Faure, J. L., Ferri, F., Ganjour, S., Givernaud, A., Gras, P., Hamel de Monchenault, G., Jarry, P., Locci, E., Malcles, J., Millischer, L., Nayak, A., Rander, J., Rosowsky, A., Shreyber, I., Titov, M., Baffioni, S., Beaudette, F., Benhabib, L., Bianchini, L., Bluj, M., Broutin, C., Busson, P., Charlot, C., Daci, N., Dahms, T., Dobrzynski, L., Granier de Cassagnac, R., Haguenauer, M., Miné, P., Mironov, C., Nguyen, M., Ochando, C., Paganini, P., Sabes, D., Salerno, R., Sirois, Y., Veelken, C., Zabi, A., Agram, J.-L., Andrea, J., Bloch, D., Bodin, D., Brom, J.-M., Cardaci, M., Chabert, E. C., Collard, C., Conte, E., Drouhin, F., Ferro, C., Fontaine, J.-C., Gelé, D., Goerlach, U., Juillot, P., Le Bihan, A.-C., Van Hove, P., Fassi, F., Mercier, D., Beauceron, S., Beaupere, N., Bondu, O., Boudoul, G., Chasserat, J., Chierici, R., Contardo, D., Depasse, P., El Mamouni, H., Fay, J., Gascon, S., Gouzevitch, M., Ille, B., Kurca, T., Lethuillier, M., Mirabito, L., Perries, S., Sordini, V., Tosi, S., Tschudi, Y., Verdier, P., Viret, S., Tsamalaidze, Z., Anagnostou, G., Beranek, S., Edelhoff, M., Feld, L., Heracleous, N., Hindrichs, O., Jussen, R., Klein, K., Merz, J., Ostapchuk, A., Perieanu, A., Raupach, F., Sammet, J., Schael, S., Sprenger, D., Weber, H., Wittmer, B., Zhukov, V., Ata, M., Caudron, J., Dietz-Laursonn, E., Erdmann, M., Güth, A., Hebbeker, T., Heidemann, C., Hoepfner, K., Klingebiel, D., Kreuzer, P., Lingemann, J., Magass, C., Merschmeyer, M., Meyer, A., Olschewski, M., Papacz, P., Pieta, H., Reithler, H., Schmitz, S. A., Sonnenschein, L., Steggemann, J., Teyssier, D., Weber, M., Bontenackels, M., Cherepanov, V., Flügge, G., Geenen, H., Geisler, M., Haj Ahmad, W., Hoehle, F., Kargoll, B., Kress, T., Kuessel, Y., Nowack, A., Perchalla, L., Pooth, O., Rennefeld, J., Sauerland, P., Stahl, A., Aldaya Martin, M., Behr, J., Behrenhoff, W., Behrens, U., Bergholz, M., Bethani, A., Borras, K., Burgmeier, A., Cakir, A., Calligaris, L., Campbell, A., Castro, E., Costanza, F., Dammann, D., Diez Pardos, C., Eckerlin, G., Eckstein, D., Flucke, G., Geiser, A., Glushkov, I., Gunnellini, P., Habib, S., Hauk, J., Jung, H., Kasemann, M., Katsas, P., Kleinwort, C., Kluge, H., Knutsson, A., Krämer, M., Krücker, D., Kuznetsova, E., Lange, W., Lohmann, W., Lutz, B., Mankel, R., Marfin, I., Marienfeld, M., Melzer-Pellmann, I.-A., Meyer, A. B., Mnich, J., Mussgiller, A., Naumann-Emme, S., Olzem, J., Perrey, H., Petrukhin, A., Pitzl, D., Raspereza, A., Ribeiro Cipriano, P. M., Riedl, C., Ron, E., Rosin, M., Salfeld-Nebgen, J., Schmidt, R., Schoerner-Sadenius, T., Sen, N., Spiridonov, A., Stein, M., Walsh, R., Wissing, C., Autermann, C., Blobel, V., Draeger, J., Enderle, H., Erfle, J., Gebbert, U., Görner, M., Hermanns, T., Höing, R. S., Kaschube, K., Kaussen, G., Kirschenmann, H., Klanner, R., Lange, J., Mura, B., Nowak, F., Peiffer, T., Pietsch, N., Sander, C., Schettler, H., Schleper, P., Schlieckau, E., Schmidt, A., Schröder, M., Schum, T., Sola, V., Stadie, H., Steinbrück, G., Thomsen, J., Vanelderen, L., Barth, C., Berger, J., Chwalek, T., De Boer, W., Dierlamm, A., Feindt, M., Guthoff, M., Hackstein, C., Hartmann, F., Heinrich, M., Held, H., Hoffmann, K. H., Honc, S., Katkov, I., Komaragiri, J. R., Lobelle Pardo, P., Martschei, D., Mueller, S., Müller, T., Niegel, M., Nürnberg, A., Oberst, O., Oehler, A., Ott, J., Quast, G., Rabbertz, K., Ratnikov, F., Ratnikova, N., Röcker, S., Scheurer, A., Schilling, F.-P., Schott, G., Simonis, H. J., Stober, F. M., Troendle, D., Ulrich, R., Wagner-Kuhr, J., Weiler, T., Zeise, M., Daskalakis, G., Geralis, T., Kesisoglou, S., Kyriakis, A., Loukas, D., Manolakos, I., Markou, A., Markou, C., Mavrommatis, C., Ntomari, E., Gouskos, L., Mertzimekis, T. J., Panagiotou, A., Saoulidou, N., Evangelou, I., Foudas, C., Kokkas, P., Manthos, N., Papadopoulos, I., Patras, V., Bencze, G., Hajdu, C., Hidas, P., Horvath, D., Sikler, F., Veszpremi, V., Vesztergombi, G., Beni, N., Czellar, S., Molnar, J., Palinkas, J., Szillasi, Z., Karancsi, J., Raics, P., Trocsanyi, Z. L., Ujvari, B., Beri, S. B., Bhatnagar, V., Dhingra, N., Gupta, R., Jindal, M., Kaur, M., Mehta, M. Z., Nishu, N., Saini, L. K., Sharma, A., Singh, J., Ahuja, S., Bhardwaj, A., Choudhary, B. C., Kumar, A., Kumar, A., Malhotra, S., Naimuddin, M., Ranjan, K., Sharma, V., Shivpuri, R. K., Banerjee, S., Bhattacharya, S., Dutta, S., Gomber, B., Jain, S., Jain, S., Khurana, R., Sarkar, S., Sharan, M., Abdulsalam, A., Choudhury, R. K., Dutta, D., Kailas, S., Kumar, V., Mehta, P., Mohanty, A. K., Pant, L. M., Shukla, P., Aziz, T., Ganguly, S., Guchait, M., Maity, M., Majumder, G., Mazumdar, K., Mohanty, G. B., Parida, B., Sudhakar, K., Wickramage, N., Banerjee, S., Dugad, S., Arfaei, H., Bakhshiansohi, H., Etesami, S. M., Fahim, A., Hashemi, M., Hesari, H., Jafari, A., Khakzad, M., Mohammadi Najafabadi, M., Paktinat Mehdiabadi, S., Safarzadeh, B., Zeinali, M., Abbrescia, M., Barbone, L., Calabria, C., Chhibra, S. S., Colaleo, A., Creanza, D., De Filippis, N., De Palma, M., Fiore, L., Iaselli, G., Lusito, L., Maggi, G., Maggi, M., Marangelli, B., My, S., Nuzzo, S., Pacifico, N., Pompili, A., Pugliese, G., Selvaggi, G., Silvestris, L., Singh, G., Zito, G., Abbiendi, G., Benvenuti, A. C., Bonacorsi, D., Braibant-Giacomelli, S., Brigliadori, L., Capiluppi, P., Castro, A., Cavallo, F. R., Cuffiani, M., Dallavalle, G. M., Fabbri, F., Fanfani, A., Fasanella, D., Giacomelli, P., Grandi, C., Guiducci, L., Marcellini, S., Masetti, G., Meneghelli, M., Montanari, A., Navarria, F. L., Odorici, F., Perrotta, A., Primavera, F., Rossi, A. M., Rovelli, T., Siroli, G., Travaglini, R., Albergo, S., Cappello, G., Chiorboli, M., Costa, S., Potenza, R., Tricomi, A., Tuve, C., Barbagli, G., Ciulli, V., Civinini, C., D'Alessandro, R., Focardi, E., Frosali, S., Gallo, E., Gonzi, S., Meschini, M., Paoletti, S., Sguazzoni, G., Tropiano, A., Benussi, L., Bianco, S., Colafranceschi, S., Fabbri, F., Piccolo, D., Fabbricatore, P., Musenich, R., Benaglia, A., De Guio, F., Di Matteo, L., Fiorendi, S., Gennai, S., Ghezzi, A., Malvezzi, S., Manzoni, R. A., Martelli, A., Massironi, A., Menasce, D., Moroni, L., Paganoni, M., Pedrini, D., Ragazzi, S., Redaelli, N., Sala, S., Tabarelli de Fatis, T., Buontempo, S., Carrillo Montoya, C. A., Cavallo, N., De Cosa, A., Dogangun, O., Fabozzi, F., Iorio, A. O. M., Lista, L., Meola, S., Merola, M., Paolucci, P., Azzi, P., Bacchetta, N., Bellan, P., Bisello, D., Branca, A., Carlin, R., Checchia, P., Dorigo, T., Dosselli, U., Gasparini, F., Gasparini, U., Gozzelino, A., Kanishchev, K., Lacaprara, S., Lazzizzera, I., Margoni, M., Meneguzzo, A. T., Nespolo, M., Ronchese, P., Simonetto, F., Torassa, E., Vanini, S., Zotto, P., Zumerle, G., Gabusi, M., Ratti, S. P., Riccardi, C., Torre, P., Vitulo, P., Biasini, M., Bilei, G. M., Fanò, L., Lariccia, P., Lucaroni, A., Mantovani, G., Menichelli, M., Nappi, A., Romeo, F., Saha, A., Santocchia, A., Taroni, S., Azzurri, P., Bagliesi, G., Boccali, T., Broccolo, G., Castaldi, R., D'Agnolo, R. T., Dell'Orso, R., Fiori, F., Foà, L., Giassi, A., Kraan, A., Ligabue, F., Lomtadze, T., Martini, L., Messineo, A., Palla, F., Rizzi, A., Serban, A. T., Spagnolo, P., Squillacioti, P., Tenchini, R., Tonelli, G., Venturi, A., Verdini, P. G., Barone, L., Cavallari, F., Del Re, D., Diemoz, M., Grassi, M., Longo, E., Meridiani, P., Micheli, F., Nourbakhsh, S., Organtini, G., Paramatti, R., Rahatlou, S., Sigamani, M., Soffi, L., Amapane, N., Arcidiacono, R., Argiro, S., Arneodo, M., Biino, C., Cartiglia, N., Costa, M., Demaria, N., Graziano, A., Mariotti, C., Maselli, S., Migliore, E., Monaco, V., Musich, M., Obertino, M. M., Pastrone, N., Pelliccioni, M., Potenza, A., Romero, A., Ruspa, M., Sacchi, R., Solano, A., Staiano, A., Vilela Pereira, A., Belforte, S., Candelise, V., Cossutti, F., Della Ricca, G., Gobbo, B., Marone, M., Montanino, D., Penzo, A., Schizzi, A., Heo, S. G., Kim, T. Y., Nam, S. K., Chang, S., Kim, D. H., Kim, G. N., Kong, D. J., Park, H., Ro, S. R., Son, D. C., Son, T., Kim, J. Y., Kim, Z. J., Song, S., Choi, S., Gyun, D., Hong, B., Jo, M., Kim, H., Kim, T. J., Lee, K. S., Moon, D. H., Park, S. K., Choi, M., Kim, J. H., Park, C., Park, I. C., Park, S., Ryu, G., Cho, Y., Choi, Y., Choi, Y. K., Goh, J., Kim, M. S., Kwon, E., Lee, B., Lee, J., Lee, S., Seo, H., Yu, I., Bilinskas, M. J., Grigelionis, I., Janulis, M., Juodagalvis, A., Castilla-Valdez, H., De La Cruz-Burelo, E., Heredia-de La Cruz, I., Lopez-Fernandez, R., Magaña Villalba, R., Martínez-Ortega, J., Sánchez-Hernández, A., Villasenor-Cendejas, L. M., Carrillo Moreno, S., Vazquez Valencia, F., Salazar Ibarguen, H. A., Casimiro Linares, E., Morelos Pineda, A., Reyes-Santos, M. A., Krofcheck, D., Bell, A. J., Butler, P. H., Doesburg, R., Reucroft, S., Silverwood, H., Ahmad, M., Asghar, M. I., Hoorani, H. R., Khalid, S., Khan, W. A., Khurshid, T., Qazi, S., Shah, M. A., Shoaib, M., Bialkowska, H., Boimska, B., Frueboes, T., Gokieli, R., Górski, M., Kazana, M., Nawrocki, K., Romanowska-Rybinska, K., Szleper, M., Wrochna, G., Zalewski, P., Brona, G., Bunkowski, K., Cwiok, M., Dominik, W., Doroba, K., Kalinowski, A., Konecki, M., Krolikowski, J., Almeida, N., Bargassa, P., David, A., Faccioli, P., Ferreira Parracho, P. G., Gallinaro, M., Seixas, J., Varela, J., Vischia, P., Belotelov, I., Bunin, P., Gavrilenko, M., Golutvin, I., Gorbunov, I., Kamenev, A., Karjavin, V., Kozlov, G., Lanev, A., Malakhov, A., Moisenz, P., Palichik, V., Perelygin, V., Shmatov, S., Smirnov, V., Volodko, A., Zarubin, A., Evstyukhin, S., Golovtsov, V., Ivanov, Y., Kim, V., Levchenko, P., Murzin, V., Oreshkin, V., Smirnov, I., Sulimov, V., Uvarov, L., Vavilov, S., Vorobyev, A., Vorobyev, A., Andreev, Y., Dermenev, A., Gninenko, S., Golubev, N., Kirsanov, M., Krasnikov, N., Matveev, V., Pashenkov, A., Tlisov, D., Toropin, A., Epshteyn, V., Erofeeva, M., Gavrilov, V., Kossov, M., Lychkovskaya, N., Popov, V., Safronov, G., Semenov, S., Stolin, V., Vlasov, E., Zhokin, A., Belyaev, A., Boos, E., Ershov, A., Gribushin, A., Klyukhin, V., Kodolova, O., Korotkikh, V., Lokhtin, I., Markina, A., Obraztsov, S., Perfilov, M., Petrushanko, S., Popov, A., Sarycheva, L., Savrin, V., Snigirev, A., Vardanyan, I., Andreev, V., Azarkin, M., Dremin, I., Kirakosyan, M., Leonidov, A., Mesyats, G., Rusakov, S. V., Vinogradov, A., Azhgirey, I., Bayshev, I., Bitioukov, S., Grishin, V., Kachanov, V., Konstantinov, D., Korablev, A., Krychkine, V., Petrov, V., Ryutin, R., Sobol, A., Tourtchanovitch, L., Troshin, S., Tyurin, N., Uzunian, A., Volkov, A., Adzic, P., Djordjevic, M., Ekmedzic, M., Krpic, D., Milosevic, J., Aguilar-Benitez, M., Alcaraz Maestre, J., Arce, P., Battilana, C., Calvo, E., Cerrada, M., Chamizo Llatas, M., Colino, N., De La Cruz, B., Delgado Peris, A., Domínguez Vázquez, D., Fernandez Bedoya, C., Fernández Ramos, J. P., Ferrando, A., Flix, J., Fouz, M. C., Garcia-Abia, P., Gonzalez Lopez, O., Goy Lopez, S., Hernandez, J. M., Josa, M. I., Merino, G., Puerta Pelayo, J., Quintario Olmeda, A., Redondo, I., Romero, L., Santaolalla, J., Soares, M. S., Willmott, C., Albajar, C., Codispoti, G., de Trocóniz, J. F., Brun, H., Cuevas, J., Fernandez Menendez, J., Folgueras, S., Gonzalez Caballero, I., Lloret Iglesias, L., Piedra Gomez, J., Brochero Cifuentes, J. A., Cabrillo, I. J., Calderon, A., Chuang, S. H., Duarte Campderros, J., Felcini, M., Fernandez, M., Gomez, G., Gonzalez Sanchez, J., Jorda, C., Lopez Virto, A., Marco, J., Marco, R., Martinez Rivero, C., Matorras, F., Munoz Sanchez, F. J., Rodrigo, T., Rodríguez-Marrero, A. Y., Ruiz-Jimeno, A., Scodellaro, L., Sobron Sanudo, M., Vila, I., Vilar Cortabitarte, R., Abbaneo, D., Auffray, E., Auzinger, G., Baillon, P., Ball, A. H., Barney, D., Benitez, J. F., Bernet, C., Bianchi, G., Bloch, P., Bocci, A., Bonato, A., Botta, C., Breuker, H., Camporesi, T., Cerminara, G., Christiansen, T., Coarasa Perez, J. A., D'Enterria, D., Dabrowski, A., De Roeck, A., Di Guida, S., Dobson, M., Dupont-Sagorin, N., Elliott-Peisert, A., Frisch, B., Funk, W., Georgiou, G., Giffels, M., Gigi, D., Gill, K., Giordano, D., Giunta, M., Glege, F., Gomez-Reino Garrido, R., Govoni, P., Gowdy, S., Guida, R., Hansen, M., Harris, P., Hartl, C., Harvey, J., Hegner, B., Hinzmann, A., Innocente, V., Janot, P., Kaadze, K., Karavakis, E., Kousouris, K., Lecoq, P., Lee, Y.-J., Lenzi, P., Lourenço, C., Mäki, T., Malberti, M., Malgeri, L., Mannelli, M., Masetti, L., Meijers, F., Mersi, S., Meschi, E., Moser, R., Mozer, M. U., Mulders, M., Musella, P., Nesvold, E., Orimoto, T., Orsini, L., Palencia Cortezon, E., Perez, E., Perrozzi, L., Petrilli, A., Pfeiffer, A., Pierini, M., Pimiä, M., Piparo, D., Polese, G., Quertenmont, L., Racz, A., Reece, W., Rodrigues Antunes, J., Rolandi, G., Rommerskirchen, T., Rovelli, C., Rovere, M., Sakulin, H., Santanastasio, F., Schäfer, C., Schwick, C., Segoni, I., Sekmen, S., Sharma, A., Siegrist, P., Silva, P., Simon, M., Sphicas, P., Spiga, D., Spiropulu, M., Tsirou, A., Veres, G. I., Vlimant, J. R., Wöhri, H. K., Worm, S. D., Zeuner, W. D., Bertl, W., Deiters, K., Erdmann, W., Gabathuler, K., Horisberger, R., Ingram, Q., Kaestli, H. C., König, S., Kotlinski, D., Langenegger, U., Meier, F., Renker, D., Rohe, T., Sibille, J., Bäni, L., Bortignon, P., Buchmann, M. A., Casal, B., Chanon, N., Deisher, A., Dissertori, G., Dittmar, M., Dünser, M., Eugster, J., Freudenreich, K., Grab, C., Hits, D., Lecomte, P., Lustermann, W., Martinez Ruiz del Arbol, P., Mohr, N., Moortgat, F., Nägeli, C., Nef, P., Nessi-Tedaldi, F., Pandolfi, F., Pape, L., Pauss, F., Peruzzi, M., Ronga, F. J., Rossini, M., Sala, L., Sanchez, A. K., Starodumov, A., Stieger, B., Takahashi, M., Tauscher, L., Thea, A., Theofilatos, K., Treille, D., Urscheler, C., Wallny, R., Weber, H. A., Wehrli, L., Aguilo, E., Amsler, C., Chiochia, V., De Visscher, S., Favaro, C., Ivova Rikova, M., Millan Mejias, B., Otiougova, P., Robmann, P., Snoek, H., Tupputi, S., Verzetti, M., Chang, Y. H., Chen, K. H., Kuo, C. M., Li, S. W., Lin, W., Liu, Z. K., Lu, Y. J., Mekterovic, D., Singh, A. P., Volpe, R., Yu, S. S., Bartalini, P., Chang, P., Chang, Y. H., Chang, Y. W., Chao, Y., Chen, K. F., Dietz, C., Grundler, U., Hou, W.-S., Hsiung, Y., Kao, K. Y., Lei, Y. J., Lu, R.-S., Majumder, D., Petrakou, E., Shi, X., Shiu, J. G., Tzeng, Y. M., Wan, X., Wang, M., Adiguzel, A., Bakirci, M. N., Cerci, S., Dozen, C., Dumanoglu, I., Eskut, E., Girgis, S., Gokbulut, G., Gurpinar, E., Hos, I., Kangal, E. E., Karapinar, G., Kayis Topaksu, A., Onengut, G., Ozdemir, K., Ozturk, S., Polatoz, A., Sogut, K., Sunar Cerci, D., Tali, B., Topakli, H., Vergili, L. N., Vergili, M., Akin, I. V., Aliev, T., Bilin, B., Bilmis, S., Deniz, M., Gamsizkan, H., Guler, A. M., Ocalan, K., Ozpineci, A., Serin, M., Sever, R., Surat, U. E., Yalvac, M., Yildirim, E., Zeyrek, M., Gülmez, E., Isildak, B., Kaya, M., Kaya, O., Ozkorucuklu, S., Sonmez, N., Cankocak, K., Levchuk, L., Bostock, F., Brooke, J. J., Clement, E., Cussans, D., Flacher, H., Frazier, R., Goldstein, J., Grimes, M., Heath, G. P., Heath, H. F., Kreczko, L., Metson, S., Newbold, D. M., Nirunpong, K., Poll, A., Senkin, S., Smith, V. J., Williams, T., Basso, L., Bell, K. W., Belyaev, A., Brew, C., Brown, R. M., Cockerill, D. J. A., Coughlan, J. A., Harder, K., Harper, S., Jackson, J., Kennedy, B. W., Olaiya, E., Petyt, D., Radburn-Smith, B. C., Shepherd-Themistocleous, C. H., Tomalin, I. R., Womersley, W. J., Bainbridge, R., Ball, G., Beuselinck, R., Buchmuller, O., Colling, D., Cripps, N., Cutajar, M., Dauncey, P., Davies, G., Della Negra, M., Ferguson, W., Fulcher, J., Futyan, D., Gilbert, A., Guneratne Bryer, A., Hall, G., Hatherell, Z., Hays, J., Iles, G., Jarvis, M., Karapostoli, G., Lyons, L., Magnan, A.-M., Marrouche, J., Mathias, B., Nandi, R., Nash, J., Nikitenko, A., Papageorgiou, A., Pela, J., Pesaresi, M., Petridis, K., Pioppi, M., Raymond, D. M., Rogerson, S., Rose, A., Ryan, M. J., Seez, C., Sharp, P., Sparrow, A., Stoye, M., Tapper, A., Vazquez Acosta, M., Virdee, T., Wakefield, S., Wardle, N., Whyntie, T., Chadwick, M., Cole, J. E., Hobson, P. R., Khan, A., Kyberd, P., Leslie, D., Martin, W., Reid, I. D., Symonds, P., Teodorescu, L., Turner, M., Hatakeyama, K., Liu, H., Scarborough, T., Charaf, O., Henderson, C., Rumerio, P., Avetisyan, A., Bose, T., Fantasia, C., Heiste (2012). Measurement of the pseudorapidity and centrality dependence of the transverse energy density in pb-pb collisions at $\sqrt{s_{\mathrm{NN}}} = 2.76$ TeV. *Phys. Rev. Lett.*, 109:152303. 6, 20

[17] Collaboration, T. A., Aamodt, K., Quintana, A. A., Achenbach, R., Acounis, S., Adamov, D., Adler, C., Aggarwal, M., Agnese, F., Rinella, G. A., Ahammed, Z., Ahmad, A., Ahmad, N., Ahmad, S., Akindinov, A., Akishin, P., Aleksandrov, D., Alessandro, B., Alfaro, R., Alfarone, G., Alici, A., Alme, J., Alt, T., Altinpinar, S., Amend, W., Andrei, C., Andres, Y., Andronic, A., Anelli, G., Anfreville, M., Angelov, V., Anzo, A., Anson, C., Antici, T., Antonenko, V., Antonczyk, D., Antinori, F., Antinori, S., Antonioli, P., Aphecetche, L., Appelshuser, H., Aprodu, V., Arba, M., Arcelli, S., Argentieri, A., Armesto, N., Arnaldi, R., Arefiev, A., Arsene, I., Asryan, A., Augustinus, A., Awes, T. C., ysto, J., Azmi, M. D., Bablock, S., Badal, A., Badyal, S. K., Baechler, J., Bagnasco, S., Bailhache, R., Bala, R., Baldisseri, A., Baldit, A., Bn, J., Barbera, R., Barberis, P.-L., Barbet, J. M., Barnfoldi, G., Barret, V., Bartke, J., Bartos, D., Basile, M., Basmanov, V., Bastid, N., Batigne, G., Batyunya, B., Baudot, J., Baumann, C., Bearden, I., Becker, B., Belikov, J., Bellwied, R., Belmont-Moreno, E., Belogianni, A., Belyaev, S., Benato, A., Beney, J. L., Benhabib, L., Benotto, F., Beol, S., Berceanu, I., Bercuci, A., Berdermann, E., Berdnikov, Y., Bernard, C., Berny, R., Berst, J. D., Bertelsen, H., Betev, L., Bhasin,

A., Baskar, P., Bhati, A., Bianchi, N., Bielik, J., Bielikov, J., Bimbot, L., Blanchard, G., Blanco, F., Blanco, F., Blau, D., Blume, C., Blyth, S., Boccioli, M., Bogdanov, A., Bggild, H., Bogolyubsky, M., Boldizsr, L., Bombara, M., Bombonati, C., Bondila, M., Bonnet, D., Bonvicini, V., Borel, H., Borotto, F., Borshchov, V., Bortoli, Y., Borysov, O., Bose, S., Bosisio, L., Botje, M., Bttger, S., Bourdaud, G., Bourrion, O., Bouvier, S., Braem, A., Braun, M., Braun-Munzinger, P., Bravina, L., Bregant, M., Bruckner, G., Brun, R., Bruna, E., Brunasso, O., Bruno, G. E., Bucher, D., Budilov, V., Budnikov, D., Buesching, H., Buncic, P., Burns, M., Burachas, S., Busch, O., Bushop, J., Cai, X., Caines, H., Calaon, F., Caldogno, M., Cali, I., Camerini, P., Campagnolo, R., Campbell, M., Cao, X., Capitani, G. P., Romeo, G. C., Cardenas-Montes, M., Carduner, H., Carena, F., Carena, W., Cariola, P., Carminati, F., Casado, J., Diaz, A. C., Caselle, M., Castellanos, J. C., Castor, J., Catanescu, V., Cattaruzza, E., Cavazza, D., Cerello, P., Ceresa, S., ern, V., Chambert, V., Chapeland, S., Charpy, A., Charrier, D., Chartoire, M., Charvet, J. L., Chattopadhyay, S., Chattopadhyay, S., Chepurnov, V., Chernenko, S., Cherney, M., Cheshkov, C., Cheynis, B., Chochula, P., Chiavassa, E., Barroso, V. C., Choi, J., Christakoglou, P., Christiansen, P., Christensen, C., Chykalov, O. A., Cicalo, C., Cifarelli-Strolin, L., Ciobanu, M., Cindolo, F., Cirstoiu, C., Clausse, O., Cleymans, J., Cobanoglu, O., Coffin, J.-P., Coli, S., Colla, A., Colledani, C., Combaret, C., Combet, M., Comets, M., Balbastre, G. C., del Valle, Z. C., Contin, G., Contreras, J., Cormier, T., Corsi, F., Cortese, P., Costa, F., Crescio, E., Crochet, P., Cuautle, E., Cussonneau, J., Dahlinger, M., Dainese, A., Dalsgaard, H. H., Daniel, L., Das, I., Das, T., Dash, A., Silva, R. D., Davenport, M., Daues, H., Caro, A. D., de Cataldo, G., Cuveland, J. D., Falco, A. D., de Gaspari, M., de Girolamo, P., de Groot, J., Gruttola, D. D., Haas, A. D., Marco, N. D., Pasquale, S. D., Remigis, P. D., de Vaux, D., Decock, G., Delagrange, H., Franco, M. D., Dellacasa, G., Dell'Olio, C., Dell'Olio, D., Deloff, A., Demanov, V., Dnes, E., D'Erasmo, G., Derkach, D., Devaux, A., Bari, D. D., Bartolomeo, A. D., Giglio, C. D., Liberto, S. D., Mauro, A. D., Nezza, P. D., Dialinas, M., Diaz, L., Valdes, R. D., Dietel, T., Dima, R., Ding, H., Dinca, C., Divi, R., Dobretsov, V., Dobrin, A., Doenigus, B., Dobrowolski, T., Domnguez, I., Dorn, M., Drouet, S., Dubey, A. E., Ducroux, L., Dumitrache, F., Dumonteil, E., Dupieux, P., Duta, V., Majumdar, A. D., Majumdar, M. D., Dyhre, T., Efimov, L., Efremov, A., Elia, D., Emschermann, D., Engster, C., Enokizono, A., Espagnon, B., Estienne, M., Evangelista, A., Evans, D., Evrard, S., Fabjan, C. W., Fabris, D., Faivre, J., Falchieri, D., Fantoni, A., Farano, R., Fearick, R., Fedorov, O., Fekete, V., Felea, D., Feofilov, G., Tllez, A. F., Ferretti, A., Fichera, F., Filchagin, S., Filoni, E., Finck, C., Fini, R., Fiore, E. M., Flierl, D., Floris, M., Fodor, Z., Foka, Y., Fokin, S., Force, P., Formenti, F., Fragiacomo, E., Fragkiadakis, M., Fraissard, D., Franco, A., Franco, M., Frankenfeld, U., Fratino, U., Fresneau, S., Frolov, A., Fuchs, U., Fujita, J., Furget, C., Furini, M., Girard, M. F., Gaardhje, J.-J., Gabrielli, A., Gadrat, S., Gagliardi, M., Gago, A., Gaido, L., Torreira, A. G., Gallio, M., Gandolfi, E., Ganoti, P., Ganti, M., Garabatos, J., Lopez, A. G., Garizzo, L., Gaudichet, L., Gemme, R., Germain, M., Gheata, A., Gheata, M., Ghidini, B., Ghosh, P., Giolu, G., Giraudo, G., Giubellino, P., Glasow, R., Glssel, P., Ferreiro, E. G., Gutierrez, C. G., Gonzales-Trueba, L. H., Gorbunov, S., Gorbunov, Y., Gos, H., Gosset, J., Gotovac, S., Gottschlag, H., Gottschalk, D., Grabski, V., Grassi, T., Gray, H., Grebenyuk, O., Grebieszkow, K., Gregory, C., Grigoras, C., Grion, N., Grigoriev, V., Grigoryan, A., Grigoryan, C., Grigoryan, S., Grishuk, Y., Gros, P., Grosse-Oetringhaus, J., Grossiord, J.-Y., Grosso, R., Grynyov, B., Guarnaccia, C., Guber, F., Guerin, F., Guernane, R., Guerzoni, M., Guichard, A., Guida, M., Guilloux, G., Gulkanyan, H., Gulbrandsen, K., Gunji, T., Gupta, A., Gupta, V., Gustafsson, H.-A., Gutbrod, H., Hadjidakis, C., Haiduc, M., Hamar, G., Hamagaki, H., Hamblen, J., Hansen, J. C., Hardy, P., Hatzifotiadou, D., Harris, J. W., Hartig, M., Harutyunyan, A., Hayrapetyan, A., Hasch, D., Hasegan, D., Hehner, J., Heine, N., Heinz, M., Helstrup, H., Herghelegiu, A., Herlant, S., Corral, G. H., Herrmann, N., Hetland, K., Hille, P., Hinke, H., Hippolyte, B., Hoch, M., Hoebbel, H., Hoedlmoser, H., Horaguchi, T., Horner, M., Hristov, P., Hivnov, I., Hu, S., Guo, C. H., Humanic, T., Hurtado, A., Hwang, D. S., Ianigro, J. C., Idzik, M., Igolkin, S., Ilkaev, R., Ilkiv, I., Imhoff, M., Innocenti, P. G., Ionescu, E., Ippolitov, M., Irfan, M., Insa, C., Inuzuka, M., Ivan, C., Ivanov, A., Ivanov, M., Ivanov, V., Jacobs, P., Jacholkowski, A., Janurov, L., Janik, R., Jasper, M., Jena, C., Jirden, L., Johnson, D. P., Jones, G. T., Jorgensen, C., Jouve, F., Jovanovi, P., Junique, A., Jusko, A., Jung, H., Jung, W., Kadija, K., Kamal, A., Kamermans, R., Kapusta, S., Kaidalov, A., Kakoyan, V., Kalcher, S., Kang, E., Kapitan, J., Kaplin, V., Karadzhev, K.,

Karavichev, O., Karavicheva, T., Karpechev, E., Karpio, K., Kazantsev, A., Kebschull, U., Keidel, R., Khan, M. M., Khanzadeev, A., Kharlov, Y., Kikola, D., Kileng, B., Kim, D., Kim, D. S., Kim, D. W., Kim, H. N., Kim, J. S., Kim, S., Kinson, J. B., Kiprich, S. K., Kisel, I., Kiselev, S., Kisiel, A., Kiss, T., Kiworra, V., Klay, J., Bsing, C. K., Kliemant, M., Klimov, A., Klovning, A., Kluge, A., Kluit, R., Kniege, S., Kolevatov, R., Kollegger, T., Kolojvari, A., Kondratiev, V., Kornas, E., Koshurnikov, E., Kotov, I., Kour, R., Kowalski, M., Kox, S., Kozlov, K., Krlik, I., Kramer, F., Kraus, I., Kravkov, A., Krawutschke, T., Krivda, M., Kryshen, E., Kucheriaev, Y., Kugler, A., Kuhn, C., Kuijer, P., Kumar, L., Kumar, N., Kumpumaeki, P., Kurepin, A., Kurepin, A. N., Kushpil, S., Kushpil, V., Kutovsky, M., Kvaerno, H., Kweon, M., Labb, J.-C., Lackner, F., de Guevara, P. L., Lafage, V., Rocca, P. L., Lamont, M., Lara, C., Larsen, D. T., Laurenti, G., Lazzeroni, C., Bornec, Y. L., Bris, N. L., Gailliard, C. L., Lebedev, V., Lecoq, J., Lee, K. S., Lee, S. C., Lefvre, F., Legrand, I., Lehmann, T., Leistam, L., Lenoir, P., Lenti, V., Leon, H., Monzon, I. L., Lvai, P., Li, Q., Li, X., Librizzi, F., Lietava, R., Lindegaard, N., Lindenstruth, V., Lippmann, C., Lisa, M., Listratenko, O. M., Littel, F., Liu, Y., Lo, J., Lobanov, V., Loginov, V., Noriega, M. L., Lpez-Ramrez, R., Torres, E. L., Lorenzo, P. M., Lvhiden, G., Lu, S., Ludolphs, W., Lunardon, M., Luquin, L., Lusso, S., Lutz, J.-R., Luvisetto, M., Lyapin, V., Maevskaya, A., Magureanu, C., Mahajan, A., Majahan, S., Mahmoud, T., Mairani, A., Mahapatra, D., Makarov, A., Makhlyueva, I., Malek, M., Malkiewicz, T., Mal'Kevich, D., Malzacher, P., Mamonov, A., Manea, C., Mangotra, L. K., Maniero, D., Manko, V., Manso, F., Manzari, V., Mao, Y., Marcel, A., Marchini, S., Mare, J., Margagliotti, G. V., Margotti, A., Marin, A., Marin, J.-C., Marras, D., Martinengo, P., Martnez, M. I., Martinez-Davalos, A., Garcia, G. M., Martini, S., Chiesa, A. M., Marzocca, C., Masciocchi, S., Masera, M., Masetti, M., Maslov, N. I., Masoni, A., Massera, F., Mast, M., Mastroserio, A., Matthews, Z. L., Mayer, B., Mazza, G., Mazzaro, M. D., Mazzoni, A., Meddi, F., Meleshko, E., Menchaca-Rocha, A., Meneghini, S., Meoni, M., Perez, J. M., Mereu, P., Meunier, O., Miake, Y., Michalon, A., Michinelli, R., Miftakhov, N., Mignone, M., Mikhailov, K., Milosevic, J., Minaev, Y., Minafra, F., Mischke, A., Mikowiec, D., Mitsyn, V., Mitu, C., Mohanty, B., Moisa, D., Molnar, L., Mondal, M., Mondal, N., Zetina, L. M., Monteno, M., Morando, M., Morel, M., Moretto, S., Morhardt, T., Morsch,

A., Moukhanova, T., Mucchi, M., Muccifora, V., Mudnic, E., Mller, H., Mller, W., Munoz, J., Mura, D., Musa, L., Muraz, J. F., Musso, A., Nania, R., Nandi, B., Nappi, E., Navach, F., Navin, S., Nayak, T., Nazarenko, S., Nazarov, G., Nellen, L., Nendaz, F., Nianine, A., Nicassio, M., Nielsen, B. S., Nikolaev, S., Nikolic, V., Nikulin, S., Nikulin, V., Nilsen, B., Nitti, M., Noferini, F., Nomokonov, P., Nooren, G., Noto, F., Nouais, D., Nyiri, A., Nystrand, J., Odyniec, G., Oeschler, H., Oinonen, M., Oldenburg, M., Oleks, I., Olsen, E. K., Onuchin, V., Oppedisano, C., Orsini, F., Ortiz-Velzquez, A., Oskamp, C., Oskarsson, A., Osmic, F., sterman, L., Otterlund, I., Ovrebekk, G., Oyama, K., Pachr, M., Pagano, P., Pai, G., Pajares, C., Pal, S., Pal, S., Plla, G., Palmeri, A., Pancaldi, G., Panse, R., Pantaleo, A., Pappalardo, G. S., Pastirk, B., Pastore, C., Patarakin, O., Paticchio, V., Patimo, G., Pavlinov, A., Pawlak, T., Peitzmann, T., Pnichot, Y., Pepato, A., Pereira, H., Peresunko, D., Perez, C., Griffo, J. P., Perini, D., Perrino, D., Peryt, W., Pesci, A., Peskov, V., Pestov, Y., Peters, A. J., Petrek, V., Petridis, A., Petris, M., Petrov, V., Petrov, V., Petrovici, M., Peyr, J., Piano, S., Piccotti, A., Pichot, P., Piemonte, C., Pikna, M., Pilastrini, R., Pillot, P., Pinazza, O., Pini, B., Pinsky, L., Morais, V. P., Pismennaya, V., Piuz, F., Platt, R., Ploskon, M., Plumeri, S., Pluta, J., Pocheptsov, T., Podesta, P., Poggio, F., Poghosyan, M., Poghosyan, T., Polk, K., Polichtchouk, B., Polozov, P., Polyakov, V., Pommeresch, B., Pompei, F., Pop, A., Popescu, S., Posa, F., Pospil, V., Potukuchi, B., Pouthas, J., Prasad, S., Preghenella, R., Prino, F., Prodan, L., Prono, G., Protsenko, M. A., Pruneau, C. A., Przybyla, A., Pshenichnov, I., Puddu, G., Pujahari, P., Pulvirenti, A., Punin, A., Punin, V., Putschke, J., Quartieri, J., Quercigh, E., Rachevskaya, I., Rachevski, A., Rademakers, A., Radomski, S., Radu, A., Rak, J., Ramello, L., Raniwala, R., Raniwala, S., Rasmussen, O. B., Rasson, J., Razin, V., Read, K., Real, J., Redlich, K., Reichling, C., Renard, C., Renault, G., Renfordt, R., Reolon, A. R., Reshetin, A., Revol, J.-P., Reygers, K., Ricaud, H., Riccati, L., Ricci, R. A., Richter, M., Riedler, P., Rigalleau, L. M., Riggi, F., Riegler, W., Rindel, E., Riso, J., Rivetti, A., Rizzi, M., Rizzi, V., Cahuantzi, M. R., Red, K., Rhrich, D., Romn-Lpez, S., Romanato, M., Romita, R., Ronchetti, F., Rosinsky, P., Rosnet, P., Rossegger, S., Rossi, A., Rostchin, V., Rotondo, F., Roukoutakis, F., Rousseau, S., Roy, C., Roy, D., Roy, P., Royer, L., Rubin, G., Rubio, A., Rui, R., Rusanov, I., Russo, G., Ruuskanen, V., Ryabinkin, E., Rybicki, A., Sadovsky, S., afak, K., Sahoo, R., Saini, J., Saiz, P., Salur, S., Sambyal, S., Samsonov, V., ndor, L., Sandoval, A., Sann, H., Santiard, J.-C., Santo, R., Santoro, R., Sargsyan, G., Saturnini, P., Scapparone, E., Scarlassara, F., Schackert, B., Schiaua, C., Schicker, R., Schioler, T., Schippers, J. D., Schmidt, C., Schmidt, H., Schneider, R., Schossmaier, K., Schukraft, J., Schutz, Y., Schwarz, K., Schweda, K., Schyns, E., Scioli, G., Scomparin, E., Snow, H., Sedykh, S., Segato, G., Sellitto, S., Semeria, F., Senyukov, S., Seppnen, H., Serci, S., Serkin, L., Serra, S., Sesselmann, T., Sevcenco, A., Sgura, I., Shabratova, G., Shahoyan, R., Sharkov, E., Sharma, S., Shigaki, K., Shileev, K., Shukla, P., Shurygin, A., Shurygina, M., Sibiriak, Y., Siddi, E., Siemiarczuk, T., Sigward, M. H., Silenzi, A., Silvermyr, D., Silvestri, R., Simili, E., Simion, V., Simon, R., Simonetti, L., Singaraju, R., Singhal, V., Sinha, B., Sinha, T., Siska, M., Sitr, B., Sitta, M., Skaali, B., Skowronski, P., Slodkowski, M., Smirnov, N., Smykov, L., Snellings, R., Snoeys, W., Soegaard, C., Soerensen, J., Sokolov, O., Soldatov, A., Soloviev, A., Soltveit, H., Soltz, R., Sommer, W., Soos, C., Soramel, F., Sorensen, S., Soyk, D., Spyropoulou-Stassinaki, M., Stachel, J., Staley, F., Stan, I., Stavinskiy, A., Steckert, J., Stefanini, G., Stefanek, G., Steinbeck, T., Stelzer, H., Stenlund, E., Stocco, D., Stockmeier, M., Stoicea, G., Stolpovsky, P., Strme, P., Stutzmann, J. S., Su, G., Sugitate, T., umbera, M., Suire, C., Susa, T., Kumar, K. S., Swoboda, D., Symons, J., Szarka, I., Szostak, A., Szuba, M., Szymanski, P., Tadel, M., Tagridis, C., Tan, L., Takaki, D. T., Taureg, H., Tauro, A., Tavlet, M., Munoz, G. T., Thder, J., Tieulent, R., Timmer, P., Tolyhy, T., Topilskaya, N., de Matos, C. T., Torii, H., Toscano, L., Tosello, F., Tournaire, A., Traczyk, T., Trger, G., Tromeur, W., Truesdale, D., Trzaska, W., Tsiledakis, G., Tsilis, E., Tsvetkov, A., Turcato, M., Turrisi, R., Tuveri, M., Tveter, T., Tydesjo, H., Tykarski, L., Tywoniuk, K., Ugolini, E., Ullaland, K., Urbn, J., Urciuoli, G. M., Usai, G. L., Usseglio, M., Vacchi, A., Vala, M., Valiev, F., Vyvre, P. V., Brink, A. V. D., Eijndhoven, N. V., Kolk, N. V. D., van Leeuwen, M., Vannucci, L., Vanzetto, S., Vanuxem, J.-P., Vargas, M. A., Varma, R., Vascotto, A., Vasiliev, A., Vassiliou, M., Vasta, P., Vechernin, V., Venaruzzo, M., Vercellin, E., Vergara, S., Verhoeven, W., Veronese, F., Vetlitskiy, I., Vernet, R., Victorov, V., Vidak, L., Viesti, G., Vikhlyantsev, O., Vilakazi, Z., Baillie, O. V., Vinogradov, A., Vinogradov, L., Vinogradov, Y., Virgili, T., Viyogi, Y., Vodopianov, A., Volpe, G., Vranic, D., Vrlkov, J., Vulpescu, B., Wabnitz, C., Wagner, V., Wallet, L., Wan, R., Wang, Y., Wang, Y., Wheadon, R., Weis, R., Wen, Q., Wessels, J., Westergaard, J., Wiechula, J., Wiesenaecker, A., Wikne, J., Wilk, A., Wilk, G., Williams, C., Willis, N., Windelband, B., Witt, R., Woehri, H., Wyllie, K., Xu, C., Yang, C., Yang, H., Yermia, F., Yin, Z., Yin, Z., Ky, B. Y., Yushmanov, I., Yuting, B., Zabrodin, E., Zagato, S., Zagreev, B., Zaharia, P., Zalite, A., Zampa, G., Zampolli, C., Zanevskiy, Y., Zarochentsev, A., Zaudtke, O., Zvada, P., Zbroszczyk, H., Zepeda, A., Zeter, V., Zgura, I., Zhalov, M., Zhou, D., Zhou, S., Zhu, G., Zichichi, A., Zinchenko, A., Zinovjev, G., Zoccarato, Y., Zubarev, A., Zucchini, A., and Zuffa, M. (2008). The alice experiment at the cern lhc. *Journal of Instrumentation*, 3(08):S08002. 24

[18] Connors, M., Nattrass, C., Reed, R., and Salur, S. (2017). Review of Jet Measurements in Heavy Ion Collisions. vi, 10, 11, 13

[19] Elia, D. and the ALICE Collaboration (2013). Strangeness production in alice. *Journal of Physics: Conference Series*, 455(1):012005. 16

[20] Evans, L. and Bryant, P. (2008). Lhc machine. *Journal of Instrumentation*, 3(08):S08001. 9

[21] Floris, M. (2014). Hadron yields and the phase diagram of strongly interacting matter. *Nuclear Physics A*, 931:103 – 112. QUARK MATTER 2014. 6

[22] Foka, P. and Janik, M. A. (2016). An overview of experimental results from ultra-relativistic heavy-ion collisions at the cern lhc: Bulk properties and dynamical evolution. *Reviews in Physics*, 1:154 – 171. 10

[23] Gyulassy, M. (2004). The QGP discovered at RHIC. In *Structure and dynamics of elementary matter. Proceedings, NATO Advanced Study Institute, Camyuva-Kemer, Turkey, September 22-October 2, 2003*, pages 159–182. 7

[24] Heuser, J. M. (2013). The compressed baryonic matter experiment at fair. *Nuclear Physics A*, 904-905:941c – 944c. The Quark Matter 2012. 5

[25] Hilke, H. J. (2010). Time projection chambers. *Reports on Progress in Physics*, 73(11):116201. 25

[26] Huovinen, P., Kolb, P. F., Heinz, U., Ruuskanen, P. V., and Voloshin, S. A. (2001). Radial and elliptic flow at RHIC: further predictions. *Physics Letters B*, 503:58–64. 14

[27] Jacobs, P. and Wang, X.-N. (2005). Matter in extremis: ultrarelativistic nuclear collisions at RHIC. *Progress in Particle and Nuclear Physics*, 54:443–534. 14

[28] Kapusta, J. I. (1979). Quantum chromodynamics at high temperature. *Nuclear Physics B*, 148(3):461 – 498. 3

[29] Luo, X. (2016). Exploring the qcd phase structure with beam energy scan in heavy-ion collisions. *Nuclear Physics A*, 956:75 – 82. The XXV International Conference on Ultrarelativistic Nucleus-Nucleus Collisions: Quark Matter 2015. 19

[30] Nattrass, C. (2009). System, energy, and flavor dependence of jets through di-hadron correlations in heavy ion collisions. v, 10, 25

[31] Odyniec, G. (2013). The rhic beam energy scan program in star and what's next ... *Journal of Physics: Conference Series*, 455(1):012037. 19

[32] Ozaki, S. and Roser, T. (2015). Relativistic heavy ion collider, its construction and upgrade. *Progress of Theoretical and Experimental Physics*, 2015(3):03A102. vi, 8

[33] Paquet, J.-F., Shen, C., Denicol, G., Luzum, M., Schenke, B., Jeon, S., and Gale, C. (2016). Thermal and prompt photons at rhic and the lhc. *Nuclear Physics A*, 956:409 – 412. The XXV International Conference on Ultrarelativistic Nucleus-Nucleus Collisions: Quark Matter 2015. 15, 16

[34] Patrignani, C. and Group, P. D. (2016). Review of particle physics. *Chinese Physics C*, 40(10):100001. 21

[35] Preghenella, R. (2011). Transverse momentum spectra of identified charged hadrons with the ALICE detector in Pb-Pb collisions at $\sqrt{s_{NN}} = 2.76$ TeV. *PoS*, EPS-HEP2011:118. 23

[36] Satz, H. (2006). Colour deconfinement and quarkonium binding. *Journal of Physics G: Nuclear and Particle Physics*, 32(3):R25. 4, 5

[37] Sazdjian, H. (2017). Introduction to chiral symmetry in QCD. *EPJ Web Conf.*, 137:02001. 17

[38] Schenke, B. (2017). Origins of collectivity in small systems. *Nuclear Physics A*, 967:105 – 112. The 26th International Conference on Ultra-relativistic Nucleus-Nucleus Collisions: Quark Matter 2017. 14

[39] Shao, M., Barannikova, O. Yu., Dong, X., Fisyak, Y., Ruan, L., Sorensen, P., and Xu, Z. (2006). Extensive particle identification with TPC and TOF at the STAR experiment. *Nucl. Instrum. Meth.*, A558:419–429. 25

[40] Shuryak, E. V. (1988). The qcd vacuum and quark-gluon plasma. *Zeitschrift für Physik C Particles and Fields*, 38(1):141–145. 3

[41] Snellings, R. (2011). Elliptic flow: a brief review. *New Journal of Physics*, 13(5):055008. 14

[42] Stock, R. (2004). Ultra-relativistic nucleus-nucleus collisions. Proceedings, 17th International Conference, Quark Matter 2004, Oakland, USA, January 11-17, 2004. *J. Phys.*, G30:S633–S648. 7

[43] Strickland, M. (2014). Anisotropic hydrodynamics: Motivation and methodology. *Nuclear Physics A*, 926:92–101. 14

[44] Stcker, H. (2005). Collective flow signals the quarkgluon plasma. *Nuclear Physics A*, 750(1):121 – 147. Quark-Gluon Plasma. New Discoveries at RHIC: Case for the Strongly Interacting Quark-Gluon Plasma. Contributions from the RBRC Workshop held May 14-15, 2004. vii, 18

[45] Tang, Z., Xu, Y., Ruan, L., van Buren, G., Wang, F., and Xu, Z. (2009). Spectra and radial flow at RHIC with Tsallis statistics in a Blast-Wave description. *Phys. Rev.*, C79:051901. 29

[46] Tripathy, S., Khuntia, A., Tiwari, S. K., and Sahoo, R. (2017). Transverse Momentum Spectra and Nuclear Modification Factor using Boltzmann Transport Equation with Flow in Pb+Pb collisions at $\sqrt{s_{NN}} = 2.76$ TeV. *Eur. Phys. J.*, A53(5):99. 29

[47] Vovchenko, V., Anchishkin, D., and Csernai, L. P. (2014). Time dependence of partition into spectators and participants in relativistic heavy-ion collisions. *Phys. Rev. C*, 90:044907. vi, 12

[48] Wilde, M. (2013). Measurement of Direct Photons in pp and Pb-Pb Collisions with ALICE. *Nucl. Phys.*, A904-905:573c–576c. 16

[49] Wong, C.-Y. (1994). *Introduction to high-energy heavy-ion collisions.* World scientific. vi, 16, 17, 78

Appendices

A Kinematic Variables

The description of the collision physics and the interpretation of its results are aided by the construction of variables that undergo simple transformations under a change of reference frame. Two such variables, rapidity and pseudorapidity, are described in this section.

The rapidity, y, of a particle is defined as:

$$y \equiv \frac{1}{2} \ln \frac{p_0 + p_z}{p_0 - p_z} \tag{1}$$

$$= \frac{1}{2} \ln \frac{E + p_z}{E - p_z}, \tag{2}$$

where p_0 and p_z are the components of its contravariant four-momentum $p = (p_0, p_x, p_y p_z)$ with $p_0 = \frac{E}{c}$, E being the relativistic energy of the particle and c, the speed of light, being equal to 1 in natural units.

The rapidity of a particle is used as a relativistic description of its velocity. Unlike the canonical velocity of a particle, its rapidity transforms simply additively under a Lorentz boost of the frame of reference. For example, suppose a particle has a rapidity y in the laboratory frame. Let y' denote its rapidity as measured in a frame that is Lorentz boosted with a velocity β in the z-direction with respect to the laboratory frame. Then the relationship between the rapidities in the two different frames is simply

$$y' = y - y_\beta \tag{3}$$

Here,

$$y_\beta = \frac{1}{2} \ln \frac{1 + \beta}{1 - \beta} \tag{4}$$

is the rapidity the particle would have in the laboratory frame if it were moving with a velocity β in the z-direction with respect to the laboratory frame, as can be verified from equation 1 with $p_0 = \gamma m$ and $p_z = \gamma \beta m$, γ being the Lorentz factor $\frac{1}{\sqrt{1-\beta^2}}$ [49].

The convenience provided by this construct comes with a cost. As evident from equation 1, the calculation of the rapidity of a particle requires the measurement of two different observables associated with it, such as the energy and the z-direction momentum. However, experimental constraints may sometimes only facilitate the measurement of the direction of the detected particle with respect to the beam axis. What's more convenient in such a case is the use of another variable construct called pseudorapidity, η, defined as:

$$\eta \equiv -\ln \tan \frac{\theta}{2}, \tag{5}$$

where θ is the angle the particle's momentum vector, $\boldsymbol{p}$, makes with the z-direction. The above equation can also be written in terms of the momentum as:

$$\eta = \frac{1}{2} \ln \frac{|\boldsymbol{p}| + p_z}{|\boldsymbol{p}| - p_z} \tag{6}$$

From equations 1 and 6, it is evident that $\eta \approx y$ when $|\boldsymbol{p}| \approx p_0$, i.e., when the momentum is large. The transformation of the particle distribution from the y-space to the η-space is discussed in section 4.3.2.

B Results from BGBW Fits